Aus der
Abteilung für Neuropsychologie und Verhaltensneurobiologie
Zentrum für Kognitionswissenschaften (ZKW)

Temporo-Spatial Characteristics in Working Memory Processes Investigated with Static and Dynamic Complex Stimuli

–

Functional Magnetic Resonance Imaging,
Event-Related Potentials and
fMRI-Constrained Source Analysis

vorgelegt dem Fachbereich 2 (Biologie/Chemie) der
Universität Bremen
als

DISSERTATION
zur Erlangung des akademischen Grades

Doktor der Naturwissenschaften
(Dr. rer. nat.)

von

Dipl.-Psych. Daniela Galashan

Tag des öffentlichen Kolloquiums:	24.11.2008
Gutachter der Dissertation:	Prof. Dr. Dr. Manfred Herrmann
	Prof. Dr. Andreas K. Kreiter

Table of contents

Preface

Working memory bridges perception and action because it provides the possibility to keep information in mind for a short time which is not available in the environment. Furthermore, this information can be processed and manipulated even in the presence of distracting stimuli. There are a lot of studies exploring working memory mechanisms, but nevertheless many aspects of working memory processing still remain unexplained. In the present doctoral thesis, working memory processing is examined from different perspectives, methodological as well as in content.

The experimental studies described in the present thesis were conducted within the framework of a CAI (Center for Advanced Imaging) project at the University of Bremen (second funding period, project # BMBF 01GO0506, 3.1.7, "Characterization of interactions between cortical neuronal ensembles involved in a shape-tracking working memory task with combined studies in macaque monkeys and humans"). Project leaders were Prof. Dr. A. K. Kreiter and Prof. Dr. Dr. M. Herrmann and in their departments, comparable experiments were carried out with macaque monkeys and human participants, respectively, to allow for a comparison between species. In general, this project aimed at an identification of brain structures associated with cognitive processing during different working memory tasks with increasing cognitive load and at a characterization of interactions between these brain areas. The data reported in the present thesis derive from the corresponding experiments with human study participants which were conducted in the Department of Neuropsychology and Behavioral Neurobiology (Prof. Dr. Dr. M. Herrmann).

Abstract

Experiment 1:

In the majority of experiments studying working memory (WM) tasks either delayed match-to-sample (DMTS) or n-back tasks were used to assess WM operations. In n-back tasks, however, a separation of different WM processes is impossible, whereas in DMTS tasks it is usually not required to monitor the WM content.

In Experiment 1, a variant of a DMTS task with continuously morphing stimuli was applied, requiring human participants to continuously monitor and compare the currently presented stimulus to the held-in-mind target shape during the retention period. To asses changes caused by cognitive load two different types of stimuli were employed: Complex curved shapes and a simple circle. Furthermore four different delay durations (3, 6, 9, 12 s) have been applied.

The goal of the present fMRI study was to characterize brain areas responsible for WM maintenance under continuous monitoring conditions in a WM task with morphing shapes. Moreover, the influence of cognitive load on maintenance activity in motion-sensitive area MT+ should be investigated.

Data from 15 study participants are presented. Conjunction analysis including the contrasts complex versus simple shapes over all delay durations revealed activations in a widespread fronto-parietal network, which has been discussed to be involved in WM by a large body of literature. In area MT+ an association with target complexity was shown, resulting in a significant signal enhancement while monitoring complex shapes (compared with the maintenance of simple circle trials).

The present results demonstrate that the level of activation during the maintenance interval might be dependent on target complexity, because complex targets caused a stronger activation than simple circle targets in brain areas associated with WM processes even during similar visual stimulation.

Experiment 2:

So far, WM retrieval has been investigated only in a few studies. In Experiment 2, a DMTS task using static stimuli was applied to examine differences in the processing of different probe types (targets, non-targets) during the retrieval epoch. Probe stimuli were presented at different positions in the trial (trial position A, B, and C), resulting in parametrically increasing delay durations (3, 7, and 11 seconds) before probe presentation.

Twenty individuals completed a similar WM task in an fMRI session as well as in an EEG session. The objective of the present study was to characterize differences in the cognitive processing of target probes and non-target probes by using different methodological approaches (behavioral, fMRI, EEG, and SA data) and to examine the influence of delay duration (cognitive load) on these differences.

P3b mean amplitudes showed higher values for target trials compared with non-target trials at electrode position Cz, corroborating old/new effects reported from long-term memory research. The majority of brain regions which showed activation in fMRI in the probe epoch regardless of probe type (probe epoch versus fixation) did also show activation when contrasting target trials with non-target trials. This indicated a specific involvement of these brain areas in the processing of target stimuli. Altogether, behavioral, fMRI and EEG data indicated probe type-related processing differences, which might have been influenced by the ratio of target stimuli to non-target stimuli and also by the presence of distracting probe stimuli during longer delay periods (7, 11 s).

The source analysis revealed a sequence of source activities during probe type processing starting with activity in occipital and temporal brain regions. This was presumably linked to the visual processing of stimulus features, followed by a simultaneous involvement of parietal and frontal brain regions and later processing in superior frontal gyrus (pre-SMA). Differences in source activity between targets and non-targets indicated a specific involvement of left fusiform gyrus in the non-target condition, probably associated with the mental imagination of the target stimulus during non-target probe processing. Furthermore, source activities showed specific engagements in target processing for the regional source in anterior cingulate cortex (ACC) before response execution and also for the regional source in superior frontal gyrus (SFG) before and simultaneously to response execution. These findings might be an indicator for the involvement of both regions in different stages of conflict managing operations because target trials had a lower stimulus frequency compared with non-target trials (at trial positions A and B).

Summarized, different WM processes (maintenance, retrieval) were investigated in both experiments, and different methodological approaches were applied. In the general discussion, findings from both experiments are linked to each other, considering brain regions which were involved in the processing of both tasks.

Key words: Working memory, cognitive load, maintenance, retrieval, fMRI, EEG, source analysis

German abstract / Deutsche Zusammenfassung

Experiment 1:

Bei den meisten Arbeitsgedächtnis-Experimenten wurden bisher entweder „delayed match-to-sample“- (DMTS) oder „n-back“-Aufgaben verwendet, um Arbeitsgedächtnisprozesse zu untersuchen. Bei der Verwendung von n-back-Aufgaben ist eine separate Untersuchung unterschiedlicher Arbeitsgedächtnisprozesse nicht möglich, während bei DMTS-Aufgaben üblicherweise keine Überwachung des Arbeitsgedächtnisinhalts erforderlich ist.

In Experiment 1 wurde eine Variante einer DMTS-Aufgabe mit kontinuierlich morphenden Stimuli verwendet, dabei mussten menschliche Probanden den sich verändernden aktuell präsentierten Stimulus kontinuierlich überwachen und mit dem im Gedächtnis gehaltenen Zielreiz vergleichen. Um Veränderungen durch kognitive Beanspruchung bestimmen zu können, wurden zwei unterschiedliche Arten von Stimuli verwendet: komplexe kurvige Figuren und ein einfacher Kreis. Außerdem wurden vier unterschiedlich lange Aufrechterhaltungs-Zeiträume (3, 6, 9, 12 s, zwischen Enkodierung und Abruf) verwendet.

Das Ziel dieser Kernspin-Studie war es, Hirnareale zu charakterisieren, die zuständig sind für die Aufrechterhaltung im Arbeitsgedächtnis wenn ein Objekt kontinuierlich überwacht werden muss in einer Arbeitsgedächtnis-Aufgabe mit morphenden Figuren. Ferner sollte während der gedanklichen Aufrechterhaltung im Arbeitsgedächtnis der Einfluss kognitiver Beanspruchung auf die Aktivität im bewegungssensitiven Hirnareal MT+ untersucht werden.

Es werden Daten von 15 Probanden präsentiert. Konjunktions-Analysen, die die Kontraste von komplexen im Vergleich zu simplen Figuren zusammengenommen über alle Aufrechterhaltungs-Zeiträume beinhalten, zeigten Aktivierungen in einem weit verteilten fronto-parietalen Netzwerk, das in der Literatur als an Arbeitsgedächtnis-Prozessen beteiligt beschrieben wird. Im Areal MT+ zeigte sich eine Modulation durch Zielreiz-Komplexität, die sich in einem signifikanten Signalanstieg während der gedanklichen Aufrechterhaltung komplexer Figuren (im Vergleich zum Kreis) äußerte.

Die hier präsentierten Ergebnisse zeigen, dass der Aktivierungslevel während des Aufrechterhaltungs-Intervalls von der Zielreiz-Komplexität abhängen könnte, weil die gedankliche Aufrechterhaltung von komplexen Zielreizen in Hirnarealen, die an Arbeitsgedächtnis-Prozessen beteiligt sind, eine stärkere Aktivierung hervorrief als die Aufrechterhaltung einfacher Kreise, obwohl die visuelle Stimulation in beiden Fällen identisch war.

Experiment 2:

Bisher wurde der Abruf aus dem Arbeitsgedächtnis nur in wenigen Studien erforscht. In Experiment 2 wurde eine DMTS-Aufgabe mit statischen Stimuli verwendet, um Unterschiede in der Verarbeitung unterschiedlicher Teststimuli (Zielreize, Distraktoren) während der Abruf-Epoche zu untersuchen. Die Teststimuli wurden an unterschiedlichen Positionen im Durchgang (Position A, B und C) präsentiert, daraus ergaben sich parametrisch ansteigende Aufrechterhaltungs-Zeiträume (3, 7 und 11 Sekunden) vor der Präsentation der Teststimuli. Zwanzig Probanden absolvierten eine vergleichbare Arbeitsgedächtnis-Aufgabe sowohl in einer Kernspin- als auch in einer EEG-Sitzung.

Das Ziel dieser Studie war es, die Unterschiede in der kognitiven Verarbeitung von Zielreizen und Distraktoren mit Hilfe unterschiedlicher methodischer Ansätze (Verhaltensdaten, Kernspin-, EEG-Daten und Quellenanalyse) zu charakterisieren und den Einfluss der Aufrechterhaltungs-Dauer (kognitive Beanspruchung) auf diese Unterschiede zu untersuchen.

Mittlere P3b-Amplituden zeigten höhere Werte für Zielreize im Vergleich zu Distraktoren an Elektrodenposition Cz, in Übereinstimmung mit alt/neu-Effekten, die in der Langzeitgedächtnis-Forschung berichtet werden.

Die meisten Hirnregionen, die während der Präsentation der Teststimuli unabhängig vom Teststimulus-Typ (Teststimulus im Vergleich zum Fixationsintervall) Aktivierung im Kernspin zeigten, zeigten auch Aktivierung beim Kontrast der Zielreize mit den Distraktoren. Dies deutete auf eine besondere Beteiligung dieser Areale bei der Verarbeitung von Zielreizen hin.

Zusammengenommen deuten Verhaltens-, fMRI- und EEG-Daten auf Teststimulus-spezifische Verarbeitungs-Unterschiede hin, die durch das Verhältnis von Zielreizen zu Distraktoren beeinflusst worden sein könnten und auch durch die Präsenz ablenkender Stimuli während längerer Aufrechterhaltungs-Perioden (7, 11 Sekunden).

Die Quellenanalyse ergab eine Abfolge an Quellen-Aktivierungen während der Teststimulus-Verarbeitung beginnend mit Aktivierungen in okzipitalen und temporalen Hirnregionen. Dies war vermutlich verbunden mit der visuellen Verarbeitung von Stimulus-Eigenschaften, gefolgt von einer gleichzeitigen Beteiligung parietaler und frontaler Hirnregionen und späterer Verarbeitung im Gyrus frontalis superior (pre-SMA).

Unterschiede in der Quellenaktivität zwischen Zielreizen und Distraktoren wiesen auf eine spezifische Beteiligung des linken Gyrus fusiformis in der Distraktor-Bedingung hin, eventuell in Zusammenhang mit der mentalen Imagination des Zielreiz-Stimulus während der Distraktor-Verarbeitung.

Außerdem zeigten die Quellenaktivitäten spezifische Beteiligungen an der Zielreiz-Verarbeitung für die regionale Quelle im anterioren cingulären Kortex (ACC) vor der Antwort-Ausführung und auch für die regionale Quelle im Gyrus frontalis superior (SFG) vor und während der Antwort-Ausführung. Da Zielreize eine geringere Auftretens-Wahrscheinlichkeit hatten im Vergleich zu Distraktoren (an den Positionen A und B), könnten diese Ergebnisse darauf hinweisen, dass beide Regionen an unterschiedlichen Stufen von konflikt-verarbeitenden Operationen beteiligt sein könnten.

Zusammengefasst wurden in beiden Experimenten unterschiedliche Arbeitsgedächtnis-Prozesse (Aufrechterhaltung, Abruf) untersucht, und unterschiedliche methodische Ansätze wurden verwendet. In der generellen Diskussion ("general discussion") wurden die Ergebnisse beider Experimente zueinander in Beziehung gesetzt, unter anderem in Bezug auf Hirnregionen, die an der Verarbeitung beider Aufgaben beteiligt waren.

Schlagworte: Arbeitsgedächtnis, kognitive Beteiligung, Aufrechterhaltung, Abruf, Kernspin, EEG, Quellenanalyse

Abbreviations

*	p<.05
**	p<.01
µV	microvolt
ACC	anterior cingulate cortex
ANOVA	analysis of variance
BA	Brodmann area
DLPFC	dorsolateral prefrontal cortex
DMTS	delayed match-to-sample
EEG	electroencephalography, electroencephalogram
ERP(s)	event-related potential(s)
fMRI	functional magnetic resonance imaging
IFG	inferior frontal gyrus
IOG	inferior occipital gyrus
IPS	intraparietal sulcus
LTM	long-term memory
MFG	middle frontal gyrus
mm	millimeter(s)
MOG	middle occipital gyrus
ms	millisecond(s)
N vs. fix	conjunction of non-target trials versus fixation epoch over all delay durations
nAM	nanoamperemeter
PFC	prefrontal cortex
PSC	percent signal change
RCZp	posterior portion of the rostral cingulate zone
RS(s)	regional source(s)
s	second(s)
SA	source analysis
SD	standard deviation
SEM	standard error of the mean
SFG	superior frontal gyrus
SMA	supplementary motor area

T vs. fix	conjunction of target trials versus fixation epoch over all delay durations
T vs. N	contrast of target trials versus non-target trials
VLPFC	ventrolateral prefrontal cortex
vs.	versus
WM	working memory

1 General introduction – Working memory

This chapter provides a short overview of the theoretical concept of working memory (WM), including a definition and a survey of different possibilities to look at WM (process-based, content-based) and a brief outline of common WM models. Furthermore, the concept of cognitive load in WM tasks is described because both WM experiments involve a manipulation of cognitive demand, and common WM tasks are characterized with their usually applied load manipulations. At the end of this chapter, an overview of the structure of the present thesis is provided.

1.1 Definitions of working memory

William James (1890) used the term „primary memory“ to describe memory representations which were temporarily maintained, whereas long-term permanent representations were described as belonging to „secondary memory“. In the „modal model“ (Atkinson & Shiffrin, 1968; 1971), memory was also subdivided according to the time of memory storage into a brief sensory memory store, a short-term memory and a long-term memory (LTM) store. The term “working memory” was introduced by G. A. Miller, Galanter and Pribram (1960, p. 65) and Baddeley and Hitch (1974) used this term in their influential multiple-component model to describe a cognitive processing system capable to hold information over short time periods and to operate on these maintained representations. This proposal led from the former rather static view of a short-term memory buffer (Atkinson & Shiffrin, 1968; 1971) to a more dynamic concept of a multiple-component processing system equipped with executive control mechanisms.

The following definition summarizes what most WM researchers understand by “working memory”:

> Working memory is those mechanisms or processes that are involved in the control, regulation, and active maintenance of task-relevant information in the service of complex cognition, including novel as well as familiar, skilled tasks. It consists of a set of processes and mechanisms and is not a fixed “place” or “box” in the cognitive architecture. It is not a completely unitary system in the sense that it involves multiple representational codes and/or different subsystems. Its capacity limits reflect multiple factors and may even be an emergent property of the multiple processes and mechanisms involved. Working memory is closely linked to LTM [long-term

> memory; note from the author], and its contents consist primarily of currently activated LTM representations, but can also extend to LTM memory representations that are closely linked to activated retrieval cues and, hence, can be quickly reactivated (Miyake & Shah, 1999, p. 450).

This definition highlights different fundamental aspects of WM: The execution of heterogeneous control and regulation operations, the contribution to high-level cognitive functions, the fact that WM encompasses many different sub-processes and types of representational codes, the capacity limitation and the close connection to LTM.

Most daily activities would not be possible without cognitive processing mechanisms capable to hold information online for the short-term and to process this information in order to react adequately to a dynamic environment. Thus, WM enables us to accomplish complex cognitive functions such as reasoning, mental calculation, planning etc. Therefore, WM has been considered to be „perhaps the most significant achievement of human mental evolution“ (Goldman-Rakic, 1992, p. 111).

1.2 Organization principles in working memory

WM can be looked at from different perspectives. For example, WM processing can be subdivided into different types of processing mechanisms, namely the encoding of information, its temporary retention and finally the retrieval of this information (Baddeley & Hitch, 1974). Another perspective focuses on the differentiation of WM processing by the type of the WM content (object, spatial, verbal).

The prefrontal cortex (PFC) plays a special role in WM research. Therefore, dissociations found in PFC processing in electrophysiological studies with non-human primates and in neuroimaging studies with human participants led to specific proposals concerning WM organization on a neuronal level. It was suggested that dorsolateral and ventrolateral parts of the PFC might be dissociable according to the type of representation maintained in WM (domain-specific) or according to the type of cognitive operation supported during task processing (process-specific). In the domain-specific model of PFC functional organization (Goldman-Rakic, 1995; 1996), it was proposed that visual spatial representations are processed in dorsolateral prefrontal cortex (DLPFC) whereas visual non-spatial representations are processed in ventrolateral prefrontal cortex (VLPFC) during WM tasks. In contrast, the process-specific model (Owen et al., 1999; Petrides, Alivisatos, Evans, & Meyer, 1993) assumes that manipulation and monitoring processes in WM engage the DLPFC

whereas the VLPFC is linked to pure WM maintenance processing without manipulation requirements. Some reviews and meta-analyses point to a PFC organization by process type rather than by material type when summarizing imaging studies with human individuals (Cabeza & Nyberg, 2000b; D'Esposito et al., 1998; Wager & Smith, 2003).

According to the most well-known multiple-component model (Baddeley & Hitch, 1974; Baddeley, 2003; Repovs & Baddeley, 2006), WM can be fractionated into a phonological loop, a visuo-spatial sketchpad and a central executive. Later on, the episodic buffer was added to the model as a separate component (Baddeley, 2000). A sketch of the model is shown in Figure 1. Each of the two slave systems mentioned first is equipped with a passive storage buffer (phonological store; visual cache) and an active reactivation process (rehearsal process; inner scribe).

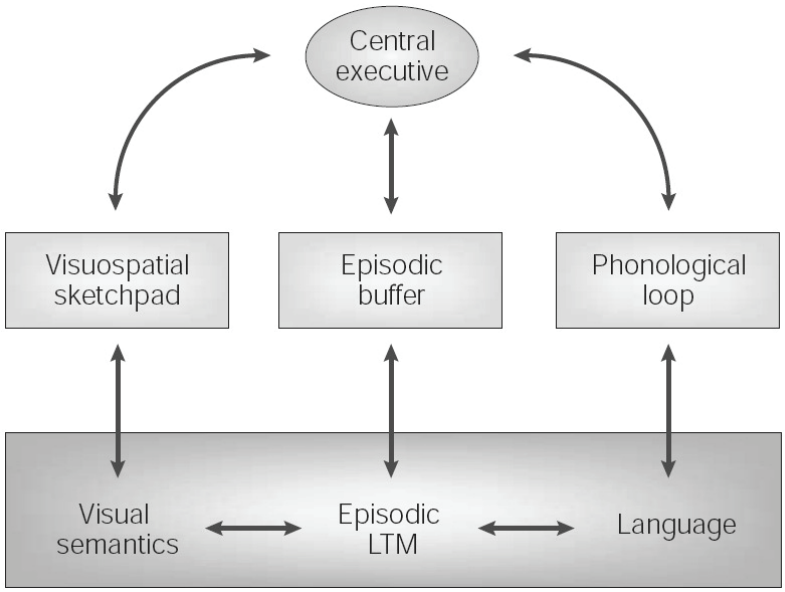

Figure 1: The multiple-component model by Baddeley (2003, p. 835, Figure 5). The three subsystems located in the middle illustrate „fluid“ capacities, which do not change with learning. „Crystallized“ systems are depicted below and they are capable to accumulate long-term knowledge.

The phonological loop is used to maintain verbal material and is thought to rely on left-hemispheric temporo-parietal cortex and Broca's area. In contrast, the visuo-spatial sketchpad is concerned with the processing of visual and spatial material and assumed to involve occipital, (right) inferior parietal and inferior frontal cortex. In the episodic buffer, multi-modal representations are integrated by the use of a common multi-dimensional code and

linked to LTM. The central executive operates on the subsystems and accomplishes several control and regularization processes. These processes are thought to rely on prefrontal brain areas (Baddeley, 2003).

In the embedded-process model of WM (Cowan, 1988, 1995, 1999) a hierarchical arrangement linking mnemonic and attentional mechanisms is proposed in contrast to the multiple-component model. According to the view proposed by the embedded-process model of WM, the subset of the long-term store which is currently activated, is called „activated memory“ (short-term store). These activated mental representations also contain another subset of representations which are currently in the focus of attention and awareness. A central executive is used to control the focus of attention voluntarily and an attentional orienting system provides involuntary control over the focus of attention. In this model, the central executive is thought to be located in PFC and the focus of attention is linked to the parietal lobes (Cowan, 1999).

The PBWM model (prefrontal cortex, basal ganglia working memory model) by O'Reilly and colleagues (Hazy, Frank, & O'Reilly, 2006, 2007; O'Reilly & Frank, 2006) was developed from a computational framework (O'Reilly, 1998) and integrates biological and computational principles. In this model, the PFC/basal ganglia system performs active maintenance (PFC) and dynamic updating (basal ganglia), the hippocampus is concerned with rapid learning and posterior perceptual and motor cortices are involved in inference processing. In contrast to most other WM models (e.g., Baddeley & Logie, 1999; Cowan, 1999), controlled processing is thought to emerge from interactions between all systems (especially from the two first-mentioned systems) and not to be based on a central executive housed in PFC.

Some other models examining WM processing are derived from cognitive architectures which are based on production systems, e.g., the ACT-R (Lovett, Reder, & Lebiere, 1999) or EPIC architectures (Kieras, Meyer, Mueller, & Seymour, 1999). These computational models describe different components of the cognitive information processing system and their interactions and aim at comparisons between simulated and experimental data from complex WM tasks.

1.3 The impact of cognitive load on working memory processing

Due to the capacity limitation in WM (see G. A. Miller, 1956), it is possible to investigate the handling of increasing demand (load) in WM tasks and its influence on WM processing

mechanisms. In WM studies, increasing demands on task processing are sometimes subsumed under the term „cognitive load“ and sometimes labeled „WM load“. There is no straightforward distinction between both types of load and it is difficult to confidently determine if a manipulation exclusively influences WM processing mechanisms. Therefore, in the present thesis the term „cognitive load“ is preferred to describe a higher level of cognitive demand in a WM task.

To examine human visual WM two types of tasks were usually used: Firstly, the n-back task (see Owen, McMillan, Laird, & Bullmore, 2005), and secondly, the so called Sternberg Item Recognition task (SIRT, Sternberg, 1966). The SIRT is equal to the delayed match-to-sample task (DMTS task) frequently used in non-human primate research. In the n-back task, stimuli are presented consecutively with blank periods in between. Participants are asked to give a manual response if the current stimulus is identical with the stimulus presented „n“ trials before. Therefore, the cognitive load is mostly defined through the number „n“ in n-back tasks.

The structure of the n-back task permits no isolation of maintenance or retrieval processes because encoding, maintenance and retrieval processes related to different stimuli occur simultaneously.

In contrast, in a traditional DMTS task individuals are asked to keep one stimulus or a set of stimuli in mind over a short (blank) delay period and are further asked to indicate with a button press if a subsequently presented probe stimulus matches the target stimulus or not.

Accordingly, the DMTS task primarily involves maintenance functions, whereas the solution of the n-back task also requires monitoring, updating and manipulation of the WM content.

The cognitive load is varied in most DMTS tasks either by manipulating the number of items to be held in WM (item set size, e.g., Linden et al., 2003), or altering the length of the retention interval (e.g., Barch et al., 1997). Defining cognitive load through item set size as usually done in DMTS tasks leads to a confound of visual stimulus processing with cognitive demands because more demanding task conditions involve the visual processing of an increasing number of stimuli.

When examining cognitive load in WM tasks, a widespread network of brain areas is usually reported. This load-sensitive network includes activations in inferior frontal gyrus (IFG), middle frontal gyrus (MFG) and superior frontal gyrus (SFG), posterior parietal cortex, anterior cingulate cortex (ACC), insula, and basal ganglia (Braver et al., 1997; Bunge, Ochsner, Desmond, Glover, & Gabrieli, 2001; Cairo, Liddle, Woodward, & Ngan, 2004;

Callicott et al., 1999; Leung, Seelig, & Gore, 2004; Linden et al., 2003; Rypma, Prabhakaran, Desmond, Glover, & Gabrieli, 1999).

In electrophysiological data, cognitive load is expressed heterogeneously in task-specific variations of event-related potential (ERP) amplitudes, latencies and scalp topographies.

Therefore, a survey of task-specific ERP load effects is given in the introduction to Experiment 2 (Chapter 2, page 16).

1.4 Structure and scope of the present thesis

The present thesis is composed of the description of two experimental WM studies, using slightly differing experimental designs to focus on different WM processing mechanisms. In both tasks comparable complex shape stimuli are chosen to minimize the use of verbalization strategies by the study participants. In each experiment another WM processing stage is focused on. In the first experiment which uses dynamically morphing stimuli during the WM delay, the focus is laid on this maintenance period when information is actively held in WM. In the second experiment which applies a WM task with serially presented stimuli, where target and non-target stimuli are presented at different positions in the trial, the retrieval period is in the focus of investigation.

In both experiments different methodological approaches are used: The first experiment was conducted in functional magnetic resonance imaging (fMRI) to permit new insights through the good spatial resolution of maintenance processes and the opportunity to focus on one particular region of interest. In the second experiment, individuals participated in an fMRI as well as an electroencephalography (EEG) session. This provides the possibility to combine a good resolution in both, spatial and temporal domains, and to examine the interplay of brain regions involved in WM retrieval in detail.

To maximize the specificity of the results, parametric designs were adopted in both experiments (see Hartley & Speer, 2000). These designs have already been used successfully in former WM studies by other authors (e.g., Braver et al., 1997; Cairo et al., 2004).

The experiment including dynamic stimuli is described first (Experiment 1), followed by the description of the experiment including static stimuli (Experiment 2). For both study descriptions, at the beginning a survey of the relevant literature is given to provide a background for the study and a possibility to deduce the study goals. This is followed by a detailed description of the applied methods and the obtained results. Finally, the obtained results are discussed with reference to the literature.

Conclusively, Chapter 4 (General Discussion) presents the integration of findings from both experiments and potential prospects for future research.

2 Experiment 1: A shape-tracking working memory task

2.1 Introduction

In the present experiment, the maintenance epoch of a dynamic shape-tracking WM task is investigated with functional magnetic resonance imaging (fMRI). A particular focus is laid on the brain region MT+, a brain region which is usually reported to be involved in motion processing (Zeki et al., 1991). In the following sections, a short description of WM maintenance processing in general is given, as well as an overview of brain areas involved in maintenance processing. At the end of the introduction a short survey of the study design and the study goals are presented.

2.1.1 Maintenance processing in working memory – General

Maintenance in WM is the process of temporarily holding information available for fast access and/or manipulation of the representation held-in-mind. This process is discussed to rely on either reactivated information from long-term memory (LTM) or information derived from an external input. Usually, in WM tasks where maintenance processes are investigated, as in the DMTS task, the maintenance process occurs in a distinct, distractor-free interval using a blank screen only covered with a fixation point. However, this situation of „pure“ maintenance without any visual or auditory stimulation is artificial because maintenance situations in everyday life usually occur with concurrent physical stimulation. In other WM tasks, e.g., the n-back task, different WM processes are merged and cannot be separated.

Electrophysiological studies on macaque monkeys showed increased neuronal activity throughout the maintenance period of simple WM tasks in different brain areas as in, e.g., frontal (Funahashi, Bruce, & Goldman-Rakic, 1989; Fuster & Alexander, 1971), posterior parietal (Chafee & Goldman-Rakic, 1998), and (inferior) temporal cortices (Miyashita & Chang, 1988). This increased activity was interpreted to support and underlie the retention process. Furthermore, activity in these brain regions produced different behavior when the maintenance period was disrupted by distractor stimuli. In particular, regions in prefrontal cortex (PFC) exhibited persistent maintenance activity despite distraction, whereas continuous maintenance activity in inferior temporal (IT) cortex (E. K. Miller, Li, & Desimone, 1993; E. K. Miller, Erickson, & Desimone, 1996) and in posterior parietal cortex (PPC) was

interrupted by intervening stimuli (Constantinidis & Steinmetz, 1996; Postle, Druzgal, & D'Esposito, 2003). Several authors suggested that brain regions showing persistent activity during the presentation of distracting stimuli might actively contribute to the maintenance of the stimulus representation (Funahashi, Bruce, & Goldman-Rakic, 1989; E. K. Miller & Cohen, 2001), even if the proper representation is held somewhere else in the brain (D'Esposito, Postle, & Rypma, 2000; Fuster, 2001).

2.1.2 Maintenance processing – Evidence from fMRI studies

Functional imaging studies in human individuals also showed that WM tasks activate a complex network of brain areas including parietal, mid- and inferior frontal regions, premotor, and supplementary motor areas (SMA), and also inferior temporal regions, especially when using objects as stimulus material (Wager & Smith, 2003).

Most WM studies examining the maintenance period focused on the prefrontal cortex (PFC) because this brain region is supposed to be involved in processing mechanisms crucial for the successful completion of WM tasks. This assumption is indicated by the observation that sustained activity was preserved in PFC neurons during the maintenance period even when distracting stimuli were presented (E. K. Miller et al., 1996).

A few years ago, a preliminary and unpublished pilot study using a comparable shape-tracking task was conducted in the Department of Neuropsychology and Behavioral Neurobiology (University of Bremen) where the author of the present thesis was working throughout the accomplishment of her thesis. In this former pilot study, activations in Brodmann area (BA) 6, MT+ and the intraparietal sulcus (IPS) were found when contrasting the morph periods (4, 8, 12 s) with the encoding periods of simple triangles and complex polygons. Furthermore, percent signal change (PSC) values indicated that variations in delay duration modulated activations in area MT+.

The abbreviation “MT+” is often used as an identifier when referring to the medial temporal complex, which comprises the area defined as MT (medial temporal area) per se and another motion-sensitive region, area MST (medial superior temporal cortex). The abbreviations stem from the topological positions of these regions in monkeys (Allman & Kaas, 1971; see Van Essen, Maunsell, & Bixby, 1981).

It has been shown that neuronal responses in area MT+ are modulated by attention, in non-human primates (Treue & Maunsell, 1996), as well as in humans (Chawla, Rees, & Friston, 1999; O'Craven, Rosen, Kwong, Treisman, & Savoy, 1997).

As fMRI measurements were used in the present experiment basic principles of fMRI are outlined in Text box 1.

Text box 1: Digression on basic principles of fMRI

FMRI: In the MR scanner, participants lie in a strong magnetic field and therefore (inter alia) a fraction of the hydrogen nuclei in their body (which spin around their axis) are oriented in the direction of the magnetic field. This alignment is perturbed by a brief radiofrequency impulse which causes the hydrogen nuclei to tip. Afterwards they return to their prior orientation while emitting energy (relaxation). This decaying signal is influenced by field inhomogeneities. A high concentration of paramagnetic deoxyhaemoglobin produces inhomogeneities in the magnetic field. This leads to a decrease in the (T2*-weighted) MR signal, whereas a high level of oxygen-rich blood results in an increase in the MR signal. Local neuronal activity is followed by an initial increase in deoxyhaemoglobin concentration (decreased MR signal) due to a rising oxygen consumption and then by a subsequent increase in oxygenation level (increased MR signal) until the MR signal returns to baseline (Heeger & Ress, 2002; Hopfinger, Khoe, & Song, 2005). Thus, fMRI is typically used to measure changes in blood oxygenation level (Kwong et al., 1992; Ogawa et al., 1992).

2.1.3 Survey of the present study and study goals

Here, a variant of a DMTS task was applied in which participants were asked to encode a static shape which began to change its contours and participants had to indicate with a button press when the initial shape reappeared after different delay durations (see Schmiedt, Meistrowitz, Schwendemann, Herrmann, & Basar-Eroglu, 2005; Taylor, Mandon, Freiwald, & Kreiter, 2005). This type of WM task required not only the maintenance of the initial shape but also the continuous comparison of the dynamic changing shapes with the initial target shape. This task emphasized the more natural situation, where the maintained memory representation had to be robust against new incoming sensory information.

Cognitive load was modulated both by complexity of target shapes (complex shapes vs. simple circle) and by a parametrical variation of the delay duration (3, 6, 9, and 12 s).

Since the pilot study mentioned before pointed towards a modulation of MT+ activity with cognitive load, it was expected that MT+ would be especially engaged in the present task variant using dynamic morphing stimuli. To enable a more detailed examination of this brain region of interest, a functional localizer task was used to localize this brain region in each individual study participant.

Study goals:

Following the aspects mentioned before, brain areas specific for WM maintenance were expected to show activation in the present task because the distracting stimuli would necessitate a more focused task processing in order to enable successful task completion.

Furthermore, a cognitive load-dependent variation in area MT+ was to be expected.

Visual stimulation during the delay was identical in all conditions; they only differed with regard to the retention duration and with regard to the complexity of the WM content (complex or simple shape).

2.2 Methods

In the following section, all information relevant to the present study is provided. Study participants are characterized and ethical issues concerning the treatment of participants and their data are described. Furthermore, descriptions of the stimulus material, task procedure, trial sequence and data recording and analysis parameters for behavioral as well as fMRI measurements are given.

2.2.1 Study participants

Nineteen healthy students (9 male; 20-30 years; mean age = 24.8; SD = 3.0) who were naïve to the hypotheses and had normal or corrected-to-normal vision completed the task. All participants were right-handed (laterality quotient of 80-100 percent) according to a modified Edinburgh Handedness Inventory (Oldfield, 1971). Participants did not report any contraindications for MR measurement, history of neurological and/or psychiatric disorders, medication affecting the central nervous system or substance abuse. Four data sets (3 female) had to be excluded due to technical problems, misunderstanding of the instructions, or motion artifacts in the fMRI data.

In two data sets of the MT+ localizer scan no segregation of area MT+ was possible and the data of another participant resulted only in a right-hemispheric MT+ activation. Therefore, these three data sets were excluded from further region of interest analyses addressing the region MT+.

2.2.2 Ethical guidelines and data privacy procedures

The study protocol was designed and performed according to the Helsinki Declaration of the World Medical Association (Rickham, 1964) and approved by the local ethics committee. All study participants gave informed and written consent prior to participation in the study (see Appendix A) and afterwards they were paid 10€.

All items mentioned in the declaration of consent were discussed with the participants prior to handing over of the declaration form. Individuals were informed about their right to quit the experiment at any time without giving reasons, about the study procedure and the anonymized usage of their data sets and questionnaires. They were also informed about the risks of the fMRI measurement (see Appendix B (2)) and it was checked that they did not meet the

exclusion criteria for fMRI measurements (see Appendix C; Appendix D). Participants were naïve to the stimulus material and the hypotheses of the present study.

2.2.3 Experimental design: Stimuli and task presentation

The stimulation software „Presentation 9.90“ (Build 10.21.05) was used to display the stimuli with a JVC video projector onto a rear projection screen via a mirror attached to the head coil. A set of eleven shapes was used for the present DMTS task (see Figure 2). The outline of these shapes was defined by 16 points connected through a smooth Bezier curve. Continuous morphing was implemented by moving the points from one shape configuration on a linear trajectory into the position of the following shape (see Taylor et al., 2005). The radius and angle of these points were randomly jittered using a normal distribution in order to create the complex shapes. The circle as a simple baseline condition was also defined by 16 points. All stimuli consisted of gray outlines and covered 3.3-4.9° angle of vision. Complex curved shapes and the simple circle were chosen to avoid easy identification through salient features such as rough edges. Altogether, 120 complex shape trials and 80 circle trials were used.

Figure 2: Set of shapes used for the morphing delayed match-to-sample task. Complex shapes: (S) 1 to 10; simple shape (S) 11.

In the simple task condition, only circle trials were used as target stimulus, whereas for the complex conditions, ten different shapes were introduced that were randomly generated and selected as hardly to be verbalized. For both, simple and complex trials, only the complex shapes alternately acted as morphing shapes during the delay periods. The morphing shapes were randomly distributed within a trial but without repetitions of a given shape within a trial. All complex shapes were used with the same amount as target stimulus for each delay stage (see Figure 3 for illustration of the trial sequence).

For a given complex target shape, it was avoided that a particular other complex shape was shown more than once as first morphing shape after the encoding epoch in order to avoid an association of a target shape with a particular morphing shape. Moreover, each complex shape

acted equally often as first morphing stimulus during the maintenance period and as last shape before target-reappearance to prevent that some shapes were shown more often at these important positions in the trial.

The stimuli were presented in four separate runs with run order counterbalanced over all study participants. Each run was composed of 30 complex shape trials and 20 simple circle trials. To ensure comparable conditions in all runs, each target was presented at least twice and not more than four times per delay condition in each run. Furthermore, there were at maximum four consecutive trials where the circle acted as target in a given run, and no complex shape acted more than twice consecutively as target in each run. The number of trials with simple and complex shapes and the number of trials within each delay duration were comparable across all runs. All participants were instructed outside the scanner and performed a practice run prior to the scanner session which consisted of six trials (four complex and two simple circle trials).

After the scanning session, all study participants completed a questionnaire concerning their subjective judgment of task difficulty, based on a ten point scale (1 = very easy; 10 = very difficult) and concerning their encoding strategies for the different target shapes (e.g., verbalization, memorizing the number or direction of bulges, memorizing a characteristic feature of the target or the entire gestalt, see Appendix E for an example page of the questionnaire and Appendix F for the post-test evaluation questions (subjective task difficulty etc.).

The trial sequence is depicted in Figure 3. During the encoding epoch, the static target shape was presented for 2.4 seconds and subsequently started to continuously morph into other shapes. Every 1.5 seconds during this morphing process, a new shape configuration from the predefined set of ten shapes was presented completely and the participants were instructed to press a button with the right index finger as soon as the shape configuration was morphing through the target shape. The morphing period (i.e. the time between encoding epoch and complete reappearance of the target) lasted 3, 6, 9, or 12 seconds, which corresponded with the complete presentation of 1, 3, 5 or 7 predefined shape configurations, respectively. After complete reappearance of the target shape the morphing period continued for another 1.5 seconds in order to prevent trials ending with the target shape. Thereafter, a fixation point was displayed for 2 ± 0.3 seconds (jittered intertrial interval).

Six of the remaining individuals were presented the run order 1, 2, 3, 4 and nine were presented the reverse run order.

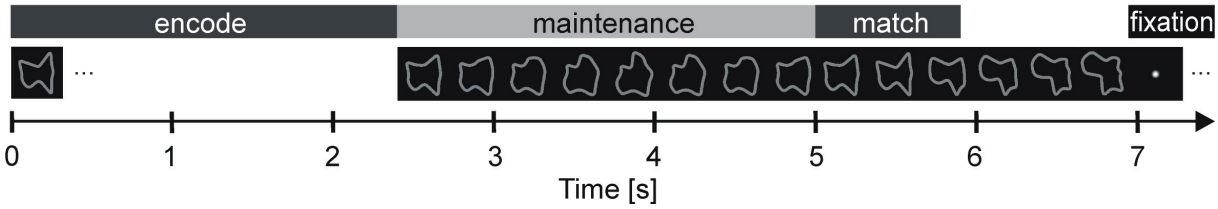

Figure 3: Trial sequence: During the encoding period, a static target shape was presented for 2.4 s. Thereafter, the target stimulus started to continuously change its contours and morphed with a smooth motion into another of the predefined shapes. After a delay period of continuously morphing shape configurations of 3, 6, 9 or 12 s, respectively, the target shape reappeared and the participants were asked for a rapid button response. After complete presentation of the target shape configuration, the sequence morphed into one other shape in order to prevent trial termination with the target.

2.2.4 Data recording and data analysis

2.2.4.1 Behavioral data – Data analysis

Only trials in which the participants responded within a time interval 400 ms prior to 500 ms after the complete reappearance of the target shapes were considered for the analysis of reaction times (RTs). Erroneous trials (including misses) were excluded from RT analysis. An alpha level of 0.05 was applied in all behavioral data analyses. RTs were analyzed with a repeated-measures three-way ANOVA including the within-subjects factors *stimulus type* (complex, simple) and *delay* (3, 6, 9, 12 s) and the between-subjects factor *run order* (order 1, 2, 3, 4 / order 4, 3, 2, 1). Differences between RTs to different target shapes were analyzed with a one-way repeated-measure ANOVA and post-hoc t-tests with Bonferroni correction to avoid an accumulation of Type I error because ten different shapes were compared with each other.

Percent error rates were analyzed with Friedman tests separately for complex and for simple trials with the four delay durations as different conditions and separately for trials with erroneous responses and with misses. The reported percentage values for trials with errors and misses relate to the quantity of all trials considered together. Wilcoxon tests were used for subsequent post-hoc comparisons between the error rates of the different delay durations and between simple and complex trials.

The encoding questionnaire data were parameterized as follows: To summarize the encoding strategies of all participants each participant was given ten scores per target shape for each of

the ten complex target shapes. Some participants marked either two or three strategies for one target. In these cases, the ten scores were divided up between the specified strategies. Finally, percent frequencies for each strategy were computed.

2.2.4.2 fMRI – Data acquisition and data analysis

Functional and anatomical magnetic resonance imaging data were obtained using a 3 T Allegra® scanner (Siemens, Erlangen, Germany) equipped with a standard quadrature head coil. Participants lay on a scanner couch in a dimly lit scanner room and wore foam earplugs. Functional images were acquired using an echo-planar imaging (EPI) sequence optimized for blood oxygenation level-dependent (BOLD) contrasting procedures (TR = 2.06 s, TE = 30 ms, flip angle = 80°, 64 x 64 matrix, FOV 192 x 192, 3 mm³ voxels, interleaved slice acquisition, 38 slices). During each experimental run (12 min each with a 1-5 min break in-between) 343 volumes were obtained. The MT+ localizer run consisted of 202 volumes (i.e. around 7 min scan time).

T1-weighted anatomical images were obtained using an MPRAGE sequence (TR = 2.3 s, TE = 4.38 ms, flip angle = 8°, TI = 900 ms, FOV 256 x 256, 1 mm³ voxels, 160 slices, duration ~10 min). Behavioral data (reaction times and error rates) were recorded using an fMRI compatible button device with a button each for the index finger and the middle finger of the right hand.

The MT+ localizer consisted of three conditions: 1. a static field with 500 gray squares (2 percent luminance) of variable size on a black background, 2. a moving flowfield where the gray squares moved towards the borders of the screen with a motion velocity of 150 cm/s, and 3. a rest condition with a blank screen. All three conditions contained a red fixation point (size: 12 arcmin) at the center of the screen and participants were instructed to maintain fixation on this point during the whole MT+ localizer run.

First-level analysis of the functional MR data was conducted using the software package „Statistical Parametric Mapping“ (SPM, Friston, Frith, Turner, & Frackowiak, 1995), version SPM2 (Wellcome Department of Cognitive Neurology, University College, London, http://www.fil.ion.ucl.ac.uk/spm/software/). All other SPM analyses (localizer task and 2nd-level analysis of the functional MR data) were carried out using version SPM5. Pre-processing of functional data included motion correction (realigned to the 10th volume of each run using six parameter rigid-body transformations; realign and unwarp algorithm), slice timing correction and normalization to the MNI standard space including SPM default

resampling to 2 mm³ isotropic voxels. Data were spatially smoothed applying a 6 mm full width at half maximum (FWHM) Gaussian kernel. For all functional data sets, serial autocorrelations were corrected by an AR(1) model and a high-pass filter of 128 Hz was enabled to remove low frequency drifts.

For the analysis of the WM task functional data, each event (encoding, delay, retrieval) was modeled with a box-car function convolved with the "SPM-canonical" hemodynamic response function (Della-Maggiore, Chau, Peres-Neto, & McIntosh, 2002; Friston, Holmes, & Worsley, 1999; Friston, Holmes, Price, Büchel, & Worsley, 1999). The resulting design matrix contained regressors for the maintenance period and for the retrieval period separately for complex shape trials and for simple circle trials and for the four different delay stages. The encoding condition was separately modeled for complex and simple trials irrespective of the different delay stages. Maintenance duration was defined as the time interval starting with the morphing process and ending when the pre-target shape configuration started morphing into the target shape in order to ensure that retrieval processes were modeled apart from the maintenance condition and that the complex and simple conditions only differed concerning the complexity of the stored material. Within these time periods, all visual stimulation was comparable among both conditions.

In the design matrix, all responses were modeled together. Errors and misses were pooled, but specified separately for each delay duration. The resulting five regressors (responses and pooled errors and misses per delay stage) were not considered in further contrasting procedures. The six realignment parameters (x, y, z translation, and three rotation angles) were included as regressors of no interest in order to handle movement-related artifacts (see Johnstone et al., 2006).

Voxel-wise fixed-effects contrasts were accomplished on a single-subject level and individual contrasts were utilized for multi-subject random effects analyses (Holmes & Friston, 1998) to allow for a generalization to the population and to account for inter-individual variance. Maintenance periods for the complex shape trials were contrasted with the maintenance periods for the simple circle trials, separately for each delay stage.

A conjunction analysis (conjunction null according to Nichols, Brett, Andersson, Wager, & Poline, 2005) was conducted for the contrasts of the complex shape maintenance epochs with the simple circle maintenance epochs over all delay stages. The conjunction null approach was chosen in order to examine only those effects which were present in all four delay durations to allow the conclusion that the obtained regions are involved in each individual delay duration condition. For inferences, the false-discovery-rate (FDR) approach was used,

correcting for multiple comparisons (Benjamini & Hochberg, 1995; Genovese, Lazar, & Nichols, 2002). Statistical threshold for contrasting procedures was fixed at a significance level of $p<.001$. Significant clusters had to exceed an extent threshold of 20 contiguous voxels ($k>20$) to be considered for further discussion.

EPI volumes of the MT+ localizer run were pre-processed in the same way as the WM data except for a co-registration of the individual T1 images to the tenth volume of the functional data and a segmentation of the individual T1 image into cerebro-spinal fluid, gray and white matter. The resulting segmentation parameter file was used to normalize the functional data which were subsequently smoothed with an 8 mm FWHM Gaussian filter.

The MT+ localizer data comprised three conditions: Motion, static and rest. To extract area MT+ the motion condition was contrasted with the static condition on a single-subject level applying t-test statistics. Different thresholds had to be applied on single-subject level to permit an individual identification of area MT+. Using the Marsbar toolbox (www.marsbar.sourceforge.net), PSC values were computed for individual MT+ clusters separately for all delay periods of complex and simple trials. Only the data of 12 participants who showed bilateral MT+ activation for the localizer contrasts were included in the PSC analysis. PSC values from MT+ were analyzed with regard to delay duration differences by using non-parametric Friedman tests separately for complex shape and simple circle trials. Post-hoc comparisons were conducted using non-parametric Wilcoxon tests. Since it was hypothesized in the present study that PSC values from MT+ might be higher for complex shape trials compared with simple circle trials, this hypothesis was tested with Wilcoxon tests separately for each delay stage.

Peak coordinates of brain regions activated in the WM task as well as in the localizer task were converted from MNI to Talairach space (using the MATLAB script „mni2tal.m“, http://imaging.mrc-cbu.cam.ac.uk/imaging/MniTalairach).

Anatomical locations were determined using the „Talairach Daemon Client“ software (http://ric.uthscsa.edu/projects/talairachdaemon.html) and the Talairach Atlas (Talairach & Tournoux, 1988).

2.3 Results

In the results section, behavioral data (reaction times, error rates, individual evaluation of task parameters) are described, followed by a characterization of suprathreshold fMRI clusters and results of the PSC analysis in area MT+.

2.3.1 Behavioral data

In the present WM task, RTs have to be interpreted with the reservation that there is obviously no zero point; i.e. due to the morphing process, identification of the target stimulus may have started before the target shape configuration was completely presented. Depending on the preceding shape and the respective target shape, some shapes could be recognized a little earlier or later during the morphing process. Thus, more valid behavioral information is assumed to be obtained by the analysis of error rates. Trials with misses were analyzed separately from committed errors (when participants responded outside the predefined time window too early or too late). Reaction times and error rates are shown in Figure 4. A three-way ANOVA including within-subjects factors *stimulus type* (complex, simple) and *delay* (3, 6, 9, 12 s) and between-subjects factor *run order* (order 1, 2, 3, 4 / order 4, 3, 2, 1) yielded a significant main effect of *stimulus type* ($F_{[1,13]}$= 22.5; p<.001). This indicated that RTs in response to simple circle trials were significantly faster compared with complex shapes (mean ± S.E.M: 37.2±30.7 vs. 102.9±19.1 ms).

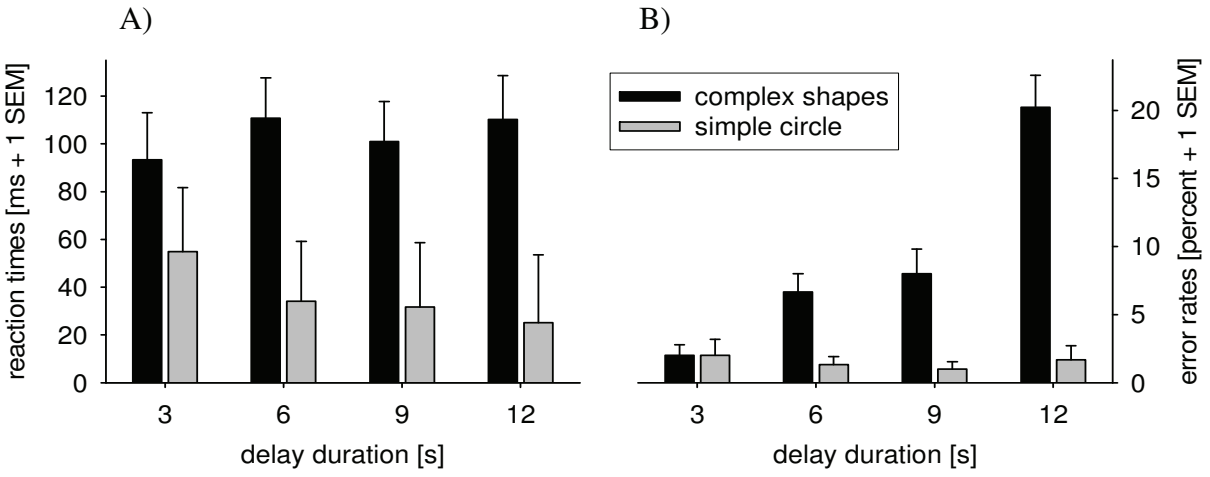

Figure 4: Reaction times (A) and percent error rates (B) for complex shape trials (black) and simple circle trials (gray). Error bars show 1 SEM.

Friedman tests for the error rates (excluding missing trials) yielded significant differences between the four delay stages only for complex shape trials ($\chi^2_{[df = 3]} = 23.9$, $p<.001$) and no delay differences for simple circle trials ($\chi^2_{[df = 3]} = .3$, $p = .97$). Post-hoc Wilcoxon tests revealed higher error rates with increasing delay duration (see also Figure 4), significantly differing between delay periods, except for the 9 seconds versus 6 seconds delay (see Table 1). Wilcoxon tests comparing error rates of simple and complex trials within each delay period yielded higher error rates for complex shapes than for simple circle trials for all but the three seconds delay period (see Table 1). The number of misses did not differ significantly between delay durations.

Table 1: Left side: Wilcoxon tests comparing different delay durations for percent error rates of complex shape trials. Right side: Wilcoxon tests comparing simple and complex trials for percent error rates within each delay duration condition. Significant results are indicated with asterisks (* p<.05, ** p<.01).

Complex shape trials: Delay duration differences			**Simple vs. complex trials at different delay durations**		
	Z-value	**p-value**		**Z-value**	**p-value**
6 s versus 3 s	-2.4	=.02 *	**3 s delay**	-0.1	=.944
9 s versus 3 s	-2.4	=.02 *	**6 s delay**	-2.8	=.005 **
12 s versus 3 s	-3.4	=.001 **	**9 s delay**	-2.7	=.007 **
9 s versus 6 s	-0.5	=.647	**12 s delay**	-3.4	=.001 **
12 s versus 6 s	-3.2	=.002 **			
12 s versus 9 s	-3.0	=.003 **			

The evaluation of individual task difficulty using a ten point scale (1 = very easy; 10 = very difficult) ranged between 2 and 8 (mean 5.1±SD 1.9). The most often applied encoding strategy was verbalization (mean 38.2±13.4 percent), followed by memorizing a characteristic feature of the target shape (26.9±11.8), encoding the entire gestalt of the target shape (19.7±8.4), memorizing the direction of characteristic bulges (12.3±7.4), and counting the number of bulges of a target (2.9±3.6). Some participants also reported a combined strategy, mostly the „entire gestalt“ strategy, in combination with another strategy. Each participant verbalized the simple stimulus as „circle“.

2.3.2 fMRI data

2.3.2.1 Neuronal correlates of WM maintenance

Contrasting maintenance periods of complex trials with those of simple trials separately for all delay durations revealed a fairly comparable activation pattern, but partially differing peak activations (see Figure 5; glass brains with the corresponding activation patterns are shown in

Appendix G). For example, the most prominent occipito-parieto-temporal activation was agglomerated to one cluster covering both hemispheres for the 6, 9 and 12 seconds delay conditions but split into one right-hemispheric and one left-hemispheric cluster in the three seconds delay condition.

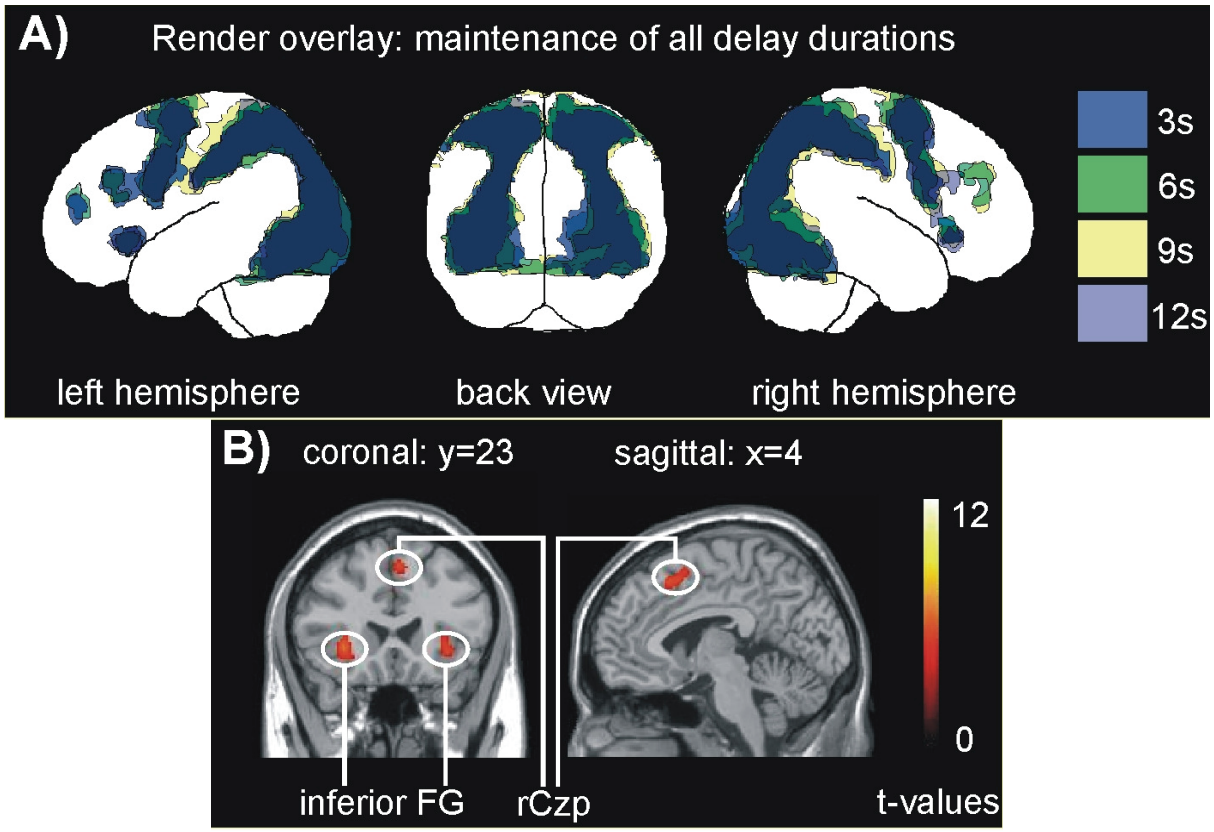

Figure 5: A) Rendered brain statistics superimposing all delay durations (maintenance of complex shape trials vs. maintenance of simple circle trials, each with FDR-correction; p<.001, k>20). B) Activated clusters in inferior frontal gyrus and medial frontal gyrus including the posterior portion of the rostral cingulate zone (RCzp), derived from a conjunction analysis contrasting maintenance periods for complex shape trials versus maintenance periods for simple circle trials across all four delay durations (conjunction null; FDR-corrected; p<.001). Abbreviations: FG = frontal gyrus; rCZp = posterior portion of the rostral cingulate zone.

Conjunction analysis over all delay durations (conjunction null; complex vs. simple) revealed two widespread activation clusters extending bilaterally from inferior and middle occipital gyri (MOG) to middle and inferior temporal gyri and spreading to inferior and superior parietal areas with two activation peaks in the right hemisphere in superior parietal lobule and one sub-gyral near inferior parietal lobule) and in the left hemisphere in inferior parietal sulcus, precuneus and MOG. Further suprathreshold voxels were located in middle frontal

gyri (MFG) bilaterally. The left-hemispheric middle frontal cluster showed one peak activation in MFG and two in inferior frontal gyrus (IFG). In the right-hemisphere, the middle frontal activations consisted of two smaller clusters in MFG. Further activation patterns were located in medial frontal gyrus (peak coordinates in the posterior portion of the rostral cingulate zone „RCZp", see Figure 5 of Picard and Strick, 1996) with two activation peaks, one in each hemisphere. This cluster comprised medial frontal as well as cingulate (BA 32) voxels. Additional activation patterns were found bilaterally in IFG, extending into the anterior insulae, and in right IFG, left medial globus pallidus, in the right-hemispheric head of the caudate nucleus and two activation clusters in right cerebellum. Talairach coordinates of the activation patterns mentioned above are listed in Table 2.

Table 2: Talairach coordinates of activation peaks revealed by a conjunction analysis of the maintenance period of complex trials versus maintenance period of simple circle trials conjunct over all four delay durations (FDR-corrected, p<.001; k>20). Anatomical labels of peak activations are listed in boldface and significant sub-peaks are listed without boldface. Abbreviations: g. = gyrus; BA = Brodmann area; r = range of nearest gray matter in mm; R = right hemisphere; L = left hemisphere.

Anatomical region (BA, r)	side	cluster size	t-value	peak coordinate (Talairach)		
				x	y	z
Superior parietal lobule (BA 7, r = 5)	R	4899	11.59	18	-65	55
Superior parietal lobule (BA 7, r = 3)			9.75	26	-58	53
Inferior parietal lobule (BA 40, r = 5)			9.72	40	-33	46
Inferior parietal lobule (BA 40)	L	5585	9.70	-36	-44	48
Precuneus (BA 7, r = 3)			9.22	-18	-69	51
Middle occipital g. (BA19)			9.21	-46	-74	-5
Middle frontal g. (BA 6, r = 3)	L	1146	9.69	-28	-1	55
Inferior frontal g. (BA 9)			6.05	-57	9	27
Inferior frontal g. (BA 9, r = 5)			6.02	-50	9	24
Middle frontal g. (BA 6, r = 3)	R	827	9.61	30	1	57
Inferior frontal g. (BA 47, r = 5)	L	155	6.56	-32	21	-3
Medial frontal g. (BA 6, r = 3 /BA32)	L	330	6.47	-4	14	47
Medial frontal g. (BA 6)			6.19	6	16	45
Inferior frontal g. (BA 47, r = 7)	R	109	6.36	32	25	-5
Lentiform nucleus	L	39	5.29	-12	2	0
Middle frontal g. (BA 8, r = 3)	R	54	4.93	48	8	42
Middle frontal g. (BA 6, r = 3)			4.78	42	4	38
Cerebellum culmen	R	22	4.92	36	-53	-21
Caudate head (r = 3)	R	33	4.87	12	8	1
Inferior frontal g. (BA 44, r = 5)	R	42	4.77	50	11	22
Inferior frontal g. (BA 44, r = 3)			4.40	51	12	12
Inferior frontal g. (BA 45, r = 5)			4.24	57	15	21
Cerebellum declive	R	49	4.67	28	-75	-16

2.3.2.2 Percent signal change in MT+

Wilcoxon tests demonstrated significantly higher PSC values for complex compared with simple trials at each delay stage (3 s: p=.012; 6 s: p=.001; 9 s: p=.002; 12 s: p=.002).

Friedman tests for PSC data revealed significant differences between the four delay stages for complex shape trials ($\chi^2_{[df = 3]} = 29.5$, p<.001) as well as for simple circle trials ($\chi^2_{[df = 3]} = 23.2$, p<.001). Post-hoc Wilcoxon tests yielded increasing PSC values with increasing delay duration for complex as well as for simple trials (see Figure 6), except for the comparison of the 9 seconds versus 12 seconds delay of complex shape trials (see Table 3).

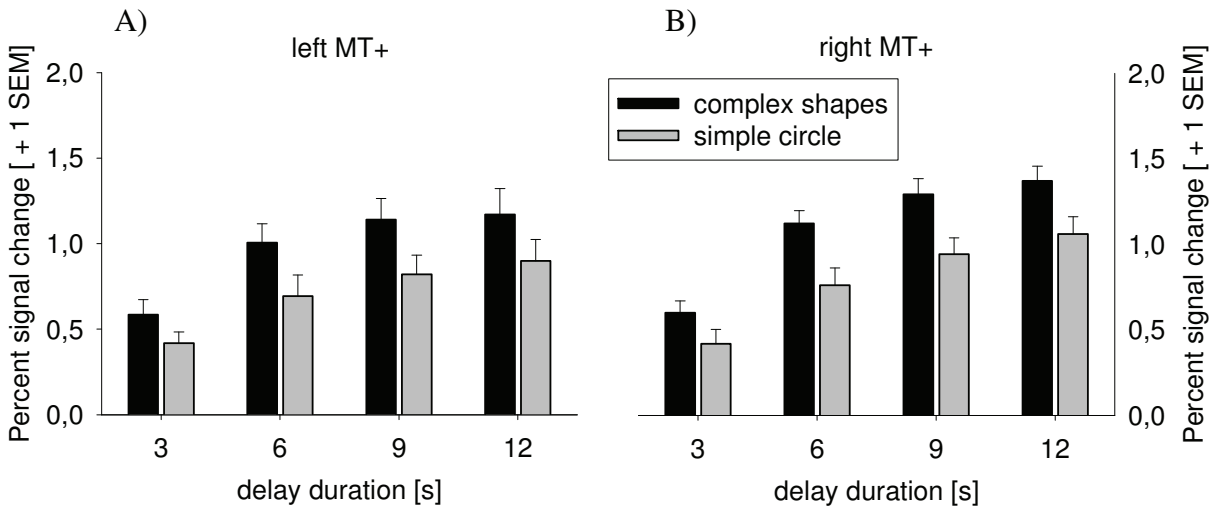

Figure 6: Percent signal change values in area MT+ for the maintenance period of complex shape trials (black) and simple circle trials (gray): A) left hemisphere B) right hemisphere. Error bars show 1 SEM.

Table 3: Wilcoxon tests comparing different delay durations for percent signal change values from brain region MT+. Left side: Data for complex shape trials. Right side: Data for simple circle trials. Significant results are indicated with asterisks (* p<.05, ** p<.01).

Complex shape trials: Delay duration differences			**Simple circle trials: Delay duration differences**		
	Z-value	**p-value**		**Z-value**	**p-value**
6 s versus 3 s	-3.1	=.002 **	**6 s versus 3 s**	-2.6	=.010 *
9 s versus 3 s	-3.1	=.002 **	**9 s versus 3 s**	-3.0	=.003 **
12 s versus 3 s	-3.1	=.002 **	**12 s versus 3 s**	-3.0	=.003 **
9 s versus 6 s	-2.9	=.004 **	**9 s versus 6 s**	-2.5	=.012 *
12 s versus 6 s	-2.9	=.004 **	**12 s versus 6 s**	-3.0	=.003 **
12 s versus 9 s	-1.4	=.16	**12 s versus 9 s**	-2.4	=.015 *

2.4 Discussion

In the discussion section, results from behavioral data are discussed first, followed by a discussion of the neuronal correlates involved in WM maintenance processing. Then, implications of the signal modulation in area MT+ and also influences of task difficulty and cognitive load on the present results are discussed.

2.4.1 Behavioral data

Behavioral data analysis based on RTs and error rates showed a significantly better performance for simple circle trials compared with complex shape trials. Indeed, RTs might just reflect that the simple circle could be identified earlier than complex shapes during the morphing process. However, this would not explain the difference in the error rates. The prolonged delay period was associated with significantly more errors in the complex compared with the simple task condition. Altogether, only few errors occurred on circle trials, hence, the circle was probably so easy to maintain that the duration of the retention interval did not affect behavioral performance in the simple condition. These data show that both stimulus complexity and increasing maintenance periods lead to more demanding task conditions and increasing cognitive load in the present WM task variant. However, contrary to classic DMTS tasks which mainly focus on retention and retrieval processes, the present WM task requires additional and more complex mental sub-processes such as continuously monitoring the morphing stimuli, inhibiting erroneous responses to the irrelevant morphing shape configurations, and continuously matching each shape during the retention period with the target shape. In particular, inhibition is one of the most prominent features of the present task as each of the ten complex stimuli could act as either a target stimulus or as a distractor the sequence was morphing through. According to several studies (D'Esposito, Postle, Jonides, & Smith, 1999; Stern, Sherman, Kirchhoff, & Hasselmo, 2001), familiar probe stimuli were discussed to evoke conflict processing mechanisms, a fact which prompted some researchers to use non-repetitive stimulus sequences (Postle et al., 2003) in WM tasks. In the present task, ten different complex shapes were used both, as targets and as distractors, but the distractors were at no time relevant for the current trial (in contrast to the study of Yoon, Curtis, & D'Esposito, 2006). The stimulus repetition during the course of the experiment emphasized WM processing mechanisms because participants could not come to the correct decision (“this is the matching target shape”) when their judgment relied on an impression of

familiarity. Indeed, sometimes the current distractor shape had been presented as the target shape in the previous trial or it could act as the target in the following trial. Nevertheless, to ensure identical conditions for maintenance epochs of complex and simple trials, the circle never acted as distractor during the delay. Thus, the examined maintenance period for complex and simple trials was identical with regard to stimulus familiarity.

In DMTS tasks, the different task periods (encoding, maintenance, and retrieval) cannot be randomized and, therefore, contrasts between the different task periods have to be treated with caution. In the present experimental design, this problem was avoided by applying a low-level baseline, which posed identical demands on visual and motor processing, but lower demands on WM. Therefore, the only difference between the maintenance periods for complex and for simple trials was the memorized object (complex shape versus simple circle).

2.4.2 fMRI data

2.4.2.1 Neural correlates of WM maintenance in a shape-tracking task

In the present study, a remarkably consistent fronto-parietal activation pattern during WM maintenance processing was found across all four applied delay durations. This network corresponds well to the activation patterns reported for WM tasks, in particular for the so-called n-back task (see Owen et al., 2005). It is important to consider that these widespread activation patterns obtained for different delay durations each resulted from contrasts of two conditions (complex, simple), which were strictly identical, apart from the target representation held-in-mind (complex shape or simple circle).

One prominent peak activation in WM processing was localized in bilateral IFG, thus replicating the data of de Zubicaray and colleagues (2001), which showed an inferior frontal signal increase during the retention period in a delayed nonmatching-to-sample task. The location of the present activation also fits well with bilateral activations in mid-ventrolateral frontal regions, which were also reported in a meta-analytical approach which integrated information of a large body of literature on the n-back task (see Owen et al., 2005). The requirement to continuously track and monitor the changing stimuli in the present experiment (instead of simply holding the target in mind) is more similar to the cognitive demand in n-back tasks than to the requirements of classical DMTS tasks. As similar IFG activations were also present in Experiment 2, these activations are discussed in the General Discussion section (beginning on page 98).

Parietal activation clusters in WM tasks were often attributed to WM storage processes (Paulesu, Frith, & Frackowiak, 1993; Smith & Jonides, 1997). Otherwise, parietal activations were frequently reported when attentional load or WM load were involved (Culham, Cavanagh, & Kanwisher, 2001; Jaeggi et al., 2003; Jovicich et al., 2001). The present bilateral parietal activation pattern is in line with both of these hypotheses. Furthermore, there is evidence that WM processes and visuospatial attention overlap in parietal and especially IPS regions (LaBar, Gitelman, Parrish, & Mesulam, 1999; Mayer et al., 2007; Naghavi & Nyberg, 2005).

The rostral cingulate zone has been mostly characterized as part of the anterior cingulate cortex (ACC), and was sub-divided on the basis of functional imaging (positron emission tomography, PET) studies into an anterior and a posterior portion (Picard & Strick, 1996; Picard & Strick, 2001). The present data showed a medial frontal cluster of activation, which corresponds to the RCZp (see Figure 5 of Picard & Strick, 1996), a region that has been linked to the following: Response selection (Picard & Strick, 2001), especially during the processing of competing information streams (Fan, Hof, Guise, Fossella, & Posner, 2008; Wittfoth, Buck, Fahle, & Herrmann, 2006), conflict monitoring and decision uncertainty (Botvinick, Cohen, & Carter, 2004; Ridderinkhof, Ullsperger, Crone, & Nieuwenhuis, 2004), and WM processes (Petit, Courtney, Ungerleider, & Haxby, 1998). Petit and colleagues (1998) reported sustained activity during WM maintenance in rostral anterior cingulate (RCZp) as well as in pre-SMA (pre-supplementary motor area). The present peak activation in medial frontal gyrus was located at the border between these two areas and a second sub-peak was located more inferior in the RCZp (see Petit et al., 1998, Figure 4). Thus, for the present task, this activation pattern might be ascribed to several mechanisms: Firstly, it may reflect WM-related processes, which were more demanding in the complex compared to the simple condition. Secondly, the complex shape condition might have resulted in a more demanding discrimination process between morphing distractors and targets, which in turn may have led to a higher degree of decision uncertainty and distractor interference during these trials. Thirdly, several authors (de Fockert, Rees, Frith, & Lavie, 2001; Lavie, Hirst, de Fockert, & Viding, 2004; Olivers, Meijer, & Theeuwes, 2006) reported that the impact of distractor interference is higher under conditions of high WM load whereas distractors were less interfering under conditions of higher perceptual load (Lavie, 1995). Accordingly, there should be higher distractor interference in the complex condition resulting in an increase in

conflict monitoring and conflict resolution demands during these trials. For further interpretations of RCZp activation see the General Discussion section (integration of results, beginning on page 99).

2.4.2.2 MT+ modulation and its impact on WM processing during continuous shape-monitoring

In an fMRI study, de Fockert and colleagues (2001) demonstrated a larger susceptibility to distractor interference and larger activations in face processing areas in response to distractor faces in the higher-load condition of a task requiring concurrent WM and attentional resources. The authors concluded that distractor faces were processed more extensively under higher WM demands. Similarly, in the present experimental design, the higher cognitive load in complex shape trials and with increasing delay duration might have caused an enhanced interference susceptibility and an increased activity in regions specifically associated with the processing of inherent task demands. In the present WM task, variant distraction was presumably generated by the morphing process through the presentation of different distractor shapes. Thus, an association of increasing MT+ activation with higher cognitive load seems to be a plausible finding in the present experimental context. An alternative explanation for enhanced MT+ activation in longer delay durations and in complex trials might be attributed to the fact that the task conditions required different amounts of attentional resources. With increasing delay duration it was probably more demanding to focus attentional resources on the morphing process, in particular during the complex shape condition. Furthermore, during maintenance of complex shapes, it might have been necessary to pay more attention to the morphing process because the discrimination between the different complex shapes was more difficult than between the complex shapes and the simple circle. Thus, the recruitment of more attentional resources might have resulted in an increased activation in area MT+.

2.4.2.3 Task difficulty and cognitive load

There is evidence for confounding effects of general task difficulty and cognitive load in the present WM task variant. Both concepts might relate to each other, e.g., Paus and colleagues (1998) reported a positive correlation between WM load and task difficulty in ACC activation. Furthermore, Duncan and Owen (2000) identified several frontal brain regions (middorsolateral PFC, midventrolateral PFC, extending to the anterior insula and dorsal anterior cingulate), which were recruited task- and stimulus-independent during different levels of task difficulty (response conflict, novelty, number of elements in WM, WM delay,

perceptual difficulty). The activation patterns in the present study corroborate this finding. Bilateral IFG activation patterns might reflect differences in task difficulty (associated with the retention of complex and simple shapes) and not exclusively in WM load. Nevertheless, an fMRI study by Barch and colleagues (1997), in which the authors separately investigated the influence of task difficulty and of long and short delay durations, led to the conclusion that WM is involved when the delay duration is manipulated. Therefore, it can be assumed that both, the delay duration and the stimulus complexity manipulations, involved cognitive load drawing on WM processing mechanisms.

2.4.3 Critical reflections

The results of the present study should be cautiously discussed in relation to data of former studies on the topic. The present WM task based on continuously morphing stimuli remarkably differs from traditional DMTS task designs. Here, a baseline with low-level demands on WM processing was used and WM performance was contrasted for different delay periods. This approach differs from experimental designs utilizing a baseline without WM processing (e.g., the intertrial interval).

Can it be possible that higher activation during the encoding epoch of complex trials might have affected the maintenance activity (due to the lag of the hemodynamic response and the fact that each maintenance phase is preceded by an encoding epoch in DMTS tasks)? This might serve as an explanation for the differences in activation between complex and simple trials. Nevertheless, if encoding activity would have determined the differences between both conditions, then, less pronounced differences should be found for longer delay durations (because of a decreasing influence of encoding activity with increasing duration). The finding of a widespread activation pattern, which was remarkably stable over different delay durations might rule out a possible influence of encoding activity on the reported activations.

Indeed, there is yet another factor to be considered when interpreting the results: The influence of the delay duration manipulation on both stimulus complexity conditions. It might be possible that increasing cognitive load caused by increasing delay duration might have affected processing mechanisms similarly in the complex as well as in the simple condition. Thus, this kind of cognitive load effect might have been cancelled out in the present data, potentially leading to the observed stable activation pattern for each delay duration.

The maintenance period of the present experiment might furthermore involve retrieval mechanisms due to the dynamic stimulation during the delay and the requirement to compare the current morphing shape with the target shape.

In the present experiment, eye movements were not recorded during the fMRI session. Although dynamic stimuli were used, each stimulus was presented centrally and only the outline of the stimulus morphed into another shape while the overall position of each shape remained constant in the center of the screen. This might led to the assumption that the present results were not influenced by large saccadic eye movements, but it is possible that small eye movements in order to track the moving outline of the shapes have been performed during the maintenance period.

2.4.4 Preliminary conclusions

The task used in the present study comprised two manipulations of cognitive load thought to produce higher WM demands, namely different delay durations and different stimulus complexity.

A large fronto-parietal network of regions usually associated with WM processing was found. This network of activations was consistently shown to be involved in WM maintenance, even when different delay durations were used. The activation patterns remained consistent over different delay durations and did not expand with increasing delay duration when contrasted against a baseline with low-level WM requirements.

For area MT+, a PSC modulation by stimulus complexity as well as by delay duration was found. PSC values were higher for complex compared to simple targets and increased with longer retention periods. This finding indicates that the distracting morphing process resulted in a specific engagement of a motion-specialized region under conditions of higher demand.

3 Experiment 2: Serial delayed match-to-sample (DMTS) task

3.1 Introduction

In the second experiment, WM retrieval processing is brought into the focus of investigation. The probe epoch of a WM task using static stimuli is examined with fMRI and EEG. Collecting data from one sample of study participants with these two different methodological approaches using the same WM task permits an integration of both methods by using an fMRI-constrained source analysis (SA) approach.

In the following, a short description of WM retrieval processing in general is given, as well as an overview of evidences from fMRI, EEG and SA. Then, the fMRI-constrained SA approach is described and at the end of the introduction, a short survey of the study design along with the presentation of the study goals is given.

3.1.1 Retrieval processing

Compared with WM *maintenance*, a process that can be maintained persistently over a few seconds, *retrieval* from WM is a rather transient mechanism. Until now, the majority of WM studies has laid their focus on the maintenance period or have used tasks which did not enable a differential investigation of WM retrieval (as the n-back task).

Some studies investigated the influence of cognitive load on WM retrieval (e.g., Gould, Brown, Owen, Ffytche, & Howard, 2003; Linden et al., 2003), but so far, cognitive processing during the retrieval period per se and especially comparisons between different probe types (targets, non-targets) when retrieving information from WM and comparing the held-in-mind representation to the probe stimulus have not been studied very well in WM tasks.

E. K. Miller and colleagues (1996) conducted a single-unit study in non-human primates and detected prefrontal neurons showing stronger responses when target probes were presented, compared with the presentation of non-target probes („match enhancement“).

The term “retrieval” is used in WM research but it is assumed that the representation currently maintained in WM is available quite immediately (see Jonides et al., 2008). Therefore, in WM tasks, in contrast to long-term memory (LTM) retrieval, no demanding retrieval operation is necessary. Instead, it is thought that a rather direct comparison of the held-in-mind

representation with the presented stimulus takes place, at least in tasks where only one stimulus is currently held in WM.

In the following, evidence from studies using fMRI, EEG and source analysis (SA) is aggregated to provide a short overview of neuronal processing during WM retrieval. Particular emphasis is laid on the comparison of retrieval mechanisms elicited by target stimuli, which match the held-in-mind representation (also called positive probes or matching stimuli in other studies) and non-target stimuli, which do not match the held-in-mind representation (negative probes, non-matching stimuli).

3.1.1.1 Evidence from fMRI studies

When contrasting WM retrieval with a low-level baseline (e.g., the intertrial interval), a widespread network of activated regions is reported. Most prominent ones are several frontal and parietal activations (Bledowski et al., 2006; Cairo et al., 2004; de Zubicaray et al., 2001; Narayanan et al., 2005; Rowe, Toni, Josephs, Frackowiak, & Passingham, 2000), but activations in temporal and occipital regions are also evident (Bledowski et al., 2006; Cairo et al., 2004; de Zubicaray et al., 2001). Furthermore, activations related to the processing of probe stimuli seem to be located in the insular cortex (Bledowski et al., 2006; Cairo et al., 2004; Narayanan et al., 2005).

There are only a few WM studies in humans where differences between probe types (target, non-target probes) are investigated with fMRI, and these studies report heterogeneous effects. For example, neither Leung and colleagues (2005), nor Wolf and colleagues (2006) found any supra-threshold activation for the contrast „target versus non-target trials“ in their WM tasks. Indeed, in the latter study, target and non-target trials were not contrasted directly, but each load condition was initially contrasted against a control condition and therefore, these findings have to be treated with caution. In contrast to these results, Druzgal and D'Esposito (2001) reported activation clusters in left middle frontal gyrus (MFG), left precentral gyrus, left fusiform gyrus, left superior temporal gyrus, bilateral middle occipital gyri (MOG), left hippocampus and left thalamus when contrasting target versus non-target trials in a face WM task. Furthermore, Jiang and colleagues (2000) reported an involvement of bilateral inferior frontal gyri (IFG), left insula, bilateral superior temporal gyrus, bilateral fusiform gyrus and supplementary motor area (SMA) when contrasting target trials and non-repeated distractors. Indeed, the distractors were not behaviorally relevant during their face WM task.

Retrieval from LTM is – compared with WM retrieval – associated with more anterior frontopolar prefrontal cortex (PFC) activations (Buckner & Koutstaal, 1998; Cabeza &

Nyberg, 2000a), although there is some evidence for overlapping activations in LTM and WM retrieval (Cabeza, Dolcos, Graham, & Nyberg, 2002; Ranganath, Johnson, & D'Esposito, 2003).

3.1.1.2 Evidence from EEG studies

Most electrophysiological studies on WM focused on variations of the Sternberg task and examined the influence of cognitive load (primarily item set size) on event-related potentials (ERPs) or on oscillatory brain activity during encoding, maintenance and retrieval epochs. Many studies investigated effects on the late positive (P3) complex, therefore, a characterization of P3 sub-components and influencing factors are given in Text box 2 (on page 41) and background from electrophysiological WM research is restricted to this ERP potential.

In WM tasks, decreasing P3b amplitude values are observed with increasing WM load (Gevins et al., 1996; Kotchoubey, Jordan, Grozinger, Westphal, & Kornhuber, 1996; Looren de Jong, Kok, & van Rooy, 1988; McEvoy, Smith, & Gevins, 1998; Mecklinger, Kramer, & Strayer, 1992; Wijers, Mulder, Okita, & Mulder, 1989). P3b amplitude is also modulated by task complexity, with reduced amplitude values for more demanding conditions (Johnson, 1986).

In LTM research, usually a series of items has to be learned in a study phase and in a later recognition test the learned old items are intermixed with new items. Participants have to decide whether the current item is old (previously learned) or new. This decision process resembles the decision process in WM studies when a presented stimulus has to be recognized as target or rejected as non-target stimulus. In these studies, it is frequently observed that ERPs to accurately recognized old stimuli show a more positive-going course than ERPs to correctly rejected new stimuli (Friedman & Johnson, 2000; Mecklinger & Meinshausen, 1998; Rugg, 1995; Rugg & Curran, 2007). Different old/new effects are visible when comparing ERPs for learned old items with ERPs for new items in LTM tasks. The so-called parietal old/new effect is expressed in higher amplitudes in the P3b time window in response to old (target) stimuli compared with new (non-target) stimuli (Friedman & Johnson, 2000; Gomarus, Althaus, Wijers, & Minderaa, 2006; Rugg & Curran, 2007) and is reported to be present also in WM tasks (Guo, Lawson, Zhang, & Jiang, 2008).

Text box 2: Digression on P300 – characterization, nomenclature, interpretation and inconsistencies

The relative positivity, which can be observed about 300-800ms post-stimulus primarily over midline electrode sites (Rugg & Coles, 1997), was described for the first time by Sutton and colleagues (Sutton, Braren, Zubin, & John, 1965). This component is evoked by infrequent stimuli and by target stimuli (Kok, 2001; Polich, 2004), and is classified as endogenous EEG component because its characteristics are relatively unaffected by physical stimulus properties (see Bashore, 1990).

Squires and colleagues (1975) made the first suggestion to distinguish different components of this positive deflection: the P3a component, showing a fronto-central scalp voltage distribution, and the "late-positive complex" consisting of the P3b component and a subsequent positive slow wave, each with a centro-parietal voltage distribution. Further studies confirmed the existence of at least two different sub-components (Dien, Spencer, & Donchin, 2004; Falkenstein, Hohnsbein, & Hoormann, 1994; Falkenstein, Koshlykova, Kiroj, Hoormann, & Hohnsbein, 1995; Verleger, 1997), but due to differing scalp distributions and the existence of two consecutive positive peaks at central or parietal electrode sites various different labels were assigned to these sub-components. Therefore, in different contexts, the P3a component is sometimes described as „Novelty P3“, „No-Go P3“ or „P-SR“ ("positivity–simple response" according to Hohnsbein, Falkenstein, Hoormann, & Blanke, 1991), whereas the P3b component is labeled „P300“, „P3“ or „P-CR“ ("positivity–choice response" according to Hohnsbein et al., 1991). In the present work, the terms P3a and P3b are selected to describe both sub-components with corresponding fronto-central and centro-parietal distributions. The P3a is evoked by infrequent task-irrelevant stimuli which deviate from task-relevant stimuli (Goldstein, Spencer, & Donchin, 2002). Thus, this component is not expected to show up in the current study.

Donchin and Coles (1988) supposed that the P3b reflects context updating processes which are active when the internal representation of the external environment in WM has to be modified. Therefore, increases in P3b amplitude are often interpreted as reflecting increasing perceptual/central resources (Donchin, 1981; Pritchard, 1981). This assumption conflicts with the finding of reduced P3b amplitudes with increasing task or WM demands (as described previously). In more recent publications, P3b is assumed to reflect event categorization processing mechanisms which contribute to target identification (Kok, 2001). A direct relationship between the P3b component and memory operations is currently under debate (see Polich, 2007; Verleger, 2008). It is assumed that the P3b is mainly generated in temporal and parietal cortex (see Bledowski et al., 2004; Menon, Ford, Lim, Glover, & Pfefferbaum, 1997; Polich, 2007; Verleger, 2008). Apart from the problem that the P3 is not a unitary phenomenon, another problem arises from the existence of two separate peaks even for the P3b component (Rösler, 1988; Verleger, 1997), sometimes labeled P300 and P500. Until now, no agreement exists concerning the specification of all subcomponents of the late positive complex and concerning their underlying processing mechanisms.

3.1.1.3 Evidence from source analyses

Until now, there is only one study examining WM retrieval using an fMRI-constrained SA approach (Bledowski et al., 2006). In this study, SA revealed the mental chronometry of

regions associated with perceptual evaluation processes (inferior temporal areas), operations on the WM storage buffer (posterior parietal), retrieval processing (ventrolateral prefrontal cortex, VLPFC) and response selection (premotor and medial frontal cortex). Serial as well as parallel processing mechanisms were reported during WM retrieval.

Reinvang and colleagues (1998) used a SA approach constrained by anatomical assumptions to analyze the test stimulus epoch of a delayed spatial frequency discrimination task. Since study participants had to decide if the first grating (encoding stimulus) or the test stimulus (after 10 s delay) had the highest spatial frequency, no pure recognition was involved in the test phase. Four sources (occipital, parietal, left and right temporal) were used to model activity from 200 to 600 ms post-stimulus. The authors concluded that early activities in the occipital and temporal sources might be related to perceptual encoding mechanisms whereas later parietal source activity might reflect retrieval from perceptual memory.

3.1.2 Methodological approach: fMRI-constrained source analysis

By using the different methodological approaches „functional magnetic resonance imaging“ (fMRI) and „electroencephalography“ (EEG), scientists pursue the same objective – to gain insight into brain processing mechanisms. Basic principles of EEG are outlined in Text box 3 (basic principles of fMRI: see Text box 1 on page 18).

Text box 3: Digression on basic principles of EEG

EEG: For EEG measurement, electrodes are attached to the scalp surface of the participants to measure voltage differences. The measured signal is mainly determined by postsynaptic potentials: e.g., the release of an excitatory neurotransmitter at the apical dendrites of a pyramidal cell will result in a net negativity around the apical dendrites outside the cell. In contrast, the current flow leaving the cell body and basal dendrites will result in a net positivity around cell body and basal dendrites. Consequently, a minuscule dipole ensues. If many neurons with a similar orientation receive the same type of input (excitatory or inhibitory), their dipoles sum up and generate a measurable voltage distribution at the scalp. These conditions are fulfilled most likely in pyramidal cells of the cortex because of their alignment perpendicular to the cortex surface. Event-related potentials (ERPs) are composed of time windows with EEG activity which are time-locked to certain external or internal events and averaged over several epochs (Luck, 2005a).

As fMRI provides a rather indirect measure of neuronal activity (Huettel, Song, & McCarthy, 2004), its temporal resolution (5-8 s, see Horwitz, Friston, & Taylor, 2000) is limited by the

lag of the hemodynamic response. Nevertheless, fMRI has a spatial resolution on the order of one to three millimeters (see Arthurs & Boniface, 2002), whereas EEG measurements provide a millisecond temporal resolution combined with a low spatial resolution depending on the depth of the underlying neuronal signature.

The activities of many tiny dipoles sum up in EEG measurements. Therefore, it is possible to approximate the signal recorded at the scalp by using only a few „equivalent current dipoles", which are determined by a given position and orientation. If the underlying source configuration is known, it is possible to compute the scalp distribution of electric activity (forward solution). However, a given distribution of electric activity measured at the scalp can be generated by an infinite number of current source configurations within the brain (ill-posed inverse problem, Helmholtz, 1853). Therefore, SA approaches have to rely on the forward solution to approximate a solution to the inverse problem.

In short, there are two main SA techniques: On the one hand the distributed source approach and on the other hand the equivalent current dipoles approach (Dale & Halgren, 2001; Luck, 2005b; Slotnick, 2005). In the distributed source approach, the brain is subdivided into small voxels each containing an equivalent current dipole. Weighted estimates are continuously estimated for each equivalent current dipole. In contrast, in the equivalent current dipoles approach as implemented in the BESA® software (MEGIS Software GmbH), only a few equivalent current dipoles are used to iteratively approach a final source configuration which accounts best for the electric fields measured on the scalp. The match between the observed scalp distribution and the scalp distribution from the model is calculated as percentage of variance in the measured scalp distribution explained by the current dipole configuration (Hopfinger et al., 2005).
To obtain a stable configuration of possible neuronal sources, either iterative procedures or additional constraints are required. The good spatial resolution of fMRI data can be used to receive possible locations of brain areas involved in the present task. With the fMRI-constrained SA approach, electrophysiological and magnetic resonance imaging data are linked to reveal the chronometry of activation sequences in brain regions which are involved in task processing (see Bledowski et al., 2006). Several steps are necessary for fMRI-constrained SA: Spatial positions of brain activation clusters are obtained with fMRI whereas the temporal information about the activation sequence is obtained with EEG. Both data sets are matched by co-registration into a common coordinate system (like the Talairach space).

Activation foci from fMRI are used as „seeds“ for the SA, and the SA approach offers the source activities in these seeded foci (Bledowski, Linden, & Wibral, 2007).

Hopfinger and colleagues (Hopfinger et al., 2005, beginning on page 352) specified four „frames of reference“, which should be considered when conducting a combined study using different methodologies like fMRI and EEG. The first „experimental“ frame of reference includes the application of identical experimental designs inducing identical task requirements and expectations in both sessions and the second „sensory“ frame of reference comprises the necessity to use identical sensory stimulation in both sessions. The third „biological“ frame of reference refers to the participation of the same individuals in both measurement sessions, whereas the fourth „spatial“ frame of reference comprises the requirement to use a common spatial reference space (e.g., the Talairach space) in order to establish a close match between data from both modalities.

3.1.3 Survey of the present study and study goals

As it was intended to integrate EEG and fMRI data to permit a detailed analysis of the mental chronometry of WM retrieval, the present experiment was designed to meet the afore-mentioned four frames of reference. The same individuals participated in both measurement sessions and accomplished the same DMTS task with comparable stimulus material. Stimuli for the EEG session and for the fMRI session were randomly selected from the same pool of stimuli, i.e., stimuli were comparable but not identical in both sessions in order to prevent learning effects. Measurement order was counterbalanced across all participants and the Talairach space was used as common reference space for both data sets.

Retention length was varied by using trials with different delay durations (3, 7 and 11 s). In all trials, after the encoding epoch, a blank delay epoch was presented, followed by up to three probe stimuli each with blank delay epochs in between. If a probe stimulus matched the target stimulus, the trial was completed. The sequence of trial events is depicted in Figure 7 on page 48.

Summarized, experimental manipulations consisted of the use of different probe types (target, non-target) and the use of different temporal positions in the trial when probe stimuli were presented (trial position A, B, and C).

The present design allowed for a detailed investigation of probe stimulus processing – either when a target shape was accurately recognized (correct recognition), or when a non-target

shape was correctly identified as non-matching shape (correct rejection). This combination provided insights into the chronological sequence of activation of brain regions involved in probe stimulus processing. Furthermore, a comparison between target recognition and non-target identification was possible, allowing for a characterization of differences and similarities between both mental processes.

Study goals:

Differences in cognitive processing of different probe types (targets, non-targets) should be investigated using different methodological approaches.

The influence of probe type and trial position on P3b mean amplitudes was to be examined. Higher P3b mean amplitudes were expected for the target condition compared with the non-target condition, in line with parietal old/new effects. Increasing cognitive load with increasing delay duration should be expressed in decreasing P3b mean amplitudes with increasing delay duration.

Contrasting targets and non-targets (separately) against the fixation period should result in activation in brain regions usually associated with WM retrieval regardless of probe type.

These activation foci should be reduced according to a priori determined rules to obtain a reasonable number of regional source positions for SA.

The SA should reveal the chronological sequence of source activity in these selected regions.

Subsequent bootstrap analyses should indicate which brain regions show a differential processing for different probe types (targets, non-targets) and trial positions.

3.2 Methods

In the Methods section, relevant information concerning the present study is described. At the beginning, a characterization of the study participants and a description of the treatment of participants and there data are given. Thereafter, stimulus material, task procedure and trial sequence are described. Furthermore, data recording and data analysis parameters for behavioral, fMRI and EEG measurements as well as the analysis procedure for SA are specified.

3.2.1 Study participants

Data were recorded from 20 healthy study participants (10 male; mean age: 25.85 years ± SD 3.76; range: 20-33 years). All participants were right-handed with a mean laterality quotient of 95 percent (SD: 8.89, range: 80-100 percent) according to The Edinburgh Inventory by Oldfield (1971) and had normal or corrected-to-normal vision.

None of the study participants reported former or current psychiatric or neurological disorders, medication affecting the central nervous system or substance abuse. Furthermore, there were no deviations in SFT scores (six factors test), a self report scale by Von Zerssen (1994) to examine higher order personality factors.

All participants took part in both experimental sessions (fMRI measurement and recording of electrophysiological data) and were paid 15€ for their participation. For all individuals, there was a minimum of one day and a maximum of eight days between the two measurement sessions.

3.2.2 Ethical guidelines and data privacy procedures

As for Experiment 1, the study protocol was designed and performed according to the Helsinki Declaration of the World Medical Association (Rickham, 1964) and approved by the local ethics committee. All study participants gave informed and written consent to participate in both measurement sessions prior to the first measurement session (see Appendix A)

All items mentioned in the declaration of consent were discussed with the participants prior to handing over of the declaration form. Individuals were informed about their right to quit the experiment at any time without giving reasons, about the study procedure and the anonymized usage of their data sets and questionnaires. They were also informed about the measurement

methods (fMRI, see Appendix B (1); EEG, see Appendix H) and the risks of the fMRI measurement and it was checked that they did not meet the exclusion criteria for fMRI measurements (see Appendix C and Appendix D) prior to the first measurement session, even if their first session was the EEG session. Participants were naïve to the stimulus material and the hypotheses of the present study.

3.2.3 Experimental design: Stimuli and task presentation

The study was conducted in an fMRI- and in an EEG-version. The only differences between both versions were the length of the intertrial interval (longer in fMRI session) and the overall number of trials (more trials in EEG session to provide enough trials for the averaging procedure). To control for learning effects, half of the experimental group (five male, five female) started with the fMRI measurement and the other half started with the EEG session. A modified DMTS task with complex curved shapes was applied.

A detailed instruction was given to the participants before the experimental measurement. They were asked to respond as fast and as accurately as possible, to hold fixation at the center of the screen, to move little und to blink rarely. A test run was performed right before the experiment (outside the scanner) to confirm that the participants had understood the instructions. The entire experiment consisted of 220 trials (EEG, 52 min) as well as 120 trials (fMRI, 39 min), presented in four (EEG) and three (fMRI) runs, containing 55 (EEG) and accordingly 40 (fMRI) trials. Run order was balanced across participants. Participants had the opportunity to take a short break (1-5 min) between the runs.

All stimuli consisted of gray shapes presented against a black background. They were generated with a custom-made program in MATLAB (version 6.5.1; with the following parameters: number of points: 14, variation of the angle for each point: 0.7°, variation of radius: 0.3°, xy-ratio: 1, rotation of the whole shape: theta: 0) and selected to be difficult to verbalize.

The stimuli were presented with Presentation® (Version 11.0) on a monitor located 45 cm (EEG)/ 43 cm (fMRI, with a JVC video projector onto a screen, visible through a mirror, attached to the head coil) from the participants. They covered 2.54 to 4.19° (EEG) and (fMRI) 3.06 to 4.79° visual angle. Altogether, 55 (EEG) and 30 (fMRI) different shape stimuli were used. Each shape acted as target and also as non-target probe stimulus during the experiment. The shapes were pseudo-randomly distributed within trials and runs and each shape was used

equally often as target for each run and each trial type. One shape was used as target stimulus at maximum one time per run and at maximum twice per run as non-target probe stimulus. The timeline within a trial and all possible types of trials are illustrated in Figure 7.

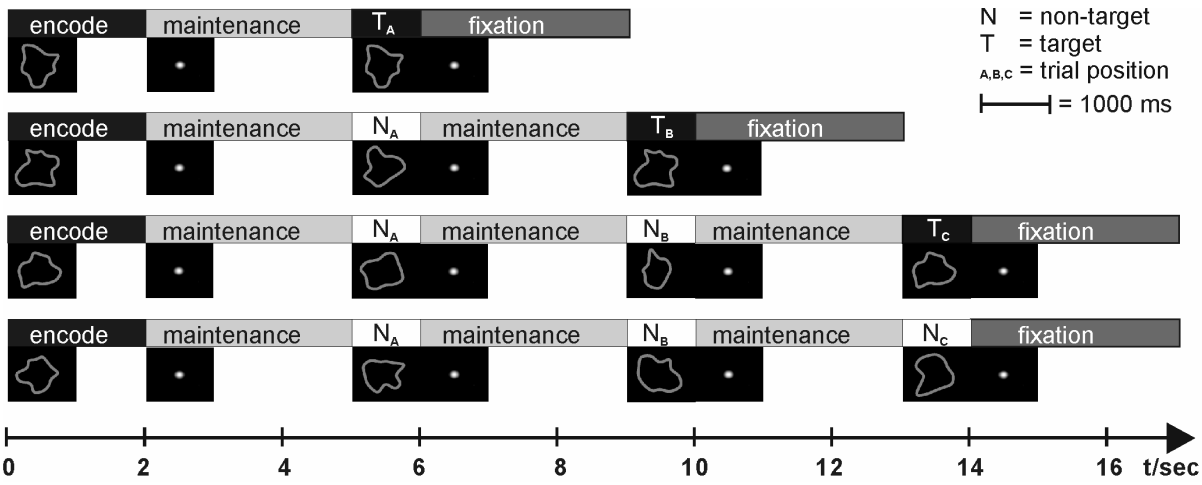

Figure 7: Overall, there were four different types of trials: Trials where the target stimulus was presented either 3, 7 or 11 seconds after offset of the encoding stimulus (see rows 1-3 of the Figure), and trials, which ended without presentation of the target stimulus (see bottom row). Trial sequence: A target stimulus was presented for 2 seconds. Thereafter, a fixation point was presented for 3 seconds, followed by a probe stimulus, which could either be the target (target at trial position A, see 1st row) or a non-target stimulus (non-target at trial position A, see all other rows). If a non-target probe stimulus was shown, the fixation point was presented again for 3 seconds, again followed by a probe stimulus (either target at trial position B, see 2nd row / or non-target ~, see 3rd and 4th row). If the second probe stimulus was again a non-target, another 3 seconds delay was presented, followed by another probe stimulus (either target at trial position C, see 3rd row / or non-target ~, see 4th row). A trial ended with presentation of the word "ENDE" whenever a target probe had been presented, and also when the third probe stimulus had been a non-target.

At the beginning of each trial the participants were instructed by the message „new shape" (duration: 500 ms) on the screen to memorize the subsequently presented shape. The first encoding stimulus (target) was presented for 2000 ms in the center of the screen, followed by a delay interval (3 s) with a small smoothed fixation point (diameter: 0.51° visual angle in EEG, 0.53° in fMRI). Then, either the target shape or a non-target probe stimulus was presented (1 s). Participants had to decide if the stimulus matched the target and indicated their decision by pressing the left („yes") or right („no") mouse button (with their index finger and middle finger, respectively). In case of a match, the current trial ended. This held true for all trials and was clarified by the screen message „ENDE" („end" in English, 300 ms). In case

of a non-match, a second shape was presented after a further maintenance period, followed by the same decision procedure as described previously. In case of another non-match, this sequence (another maintenance period and probe stimulus) was repeated. To avoid building up the expectation that the third item was always the target, half of the long trials ended with a non-target probe. In these cases the subsequent screen message „ENDE“ (300 ms) also indicated the end of the trial. Each maintenance period lasted for three seconds and each probe type was presented for one second.

Summarizing, target as well as non-target stimuli were presented at three different temporal positions in the trial (trial position A: 3 s after offset of the encode stimulus; position B: 7 s after encode offset; position C: 11 s after encode offset). Hence, the resulting trials had delay durations of either 3, 7 or 11 seconds. To prevent a fixed timing between the trials, fixation periods (intertrial intervals), with presentation of a smoothed fixation point, were randomly jittered (fMRI: 6000-9000 ms; EEG: 2700-3300 ms). Following the first experimental session, participants were asked to fill in a personality questionnaire (Sechs-Faktoren-Test, Von Zerssen, 1994) and a questionnaire on the applied encoding strategies like verbalization, specific attributes of the shape etc. (in Appendix I all stimuli used in the EEG session are shown and in Appendix J all stimuli used in the fMRI session).

3.2.4 Data recording and data analysis

3.2.4.1 Behavioral data – Data analysis

Behavioral data were analyzed using SPSS (Version 10.0.5, SPSS Inc.). Erroneous trials were analyzed separately as percentages of the corresponding condition and excluded from the analyses. An alpha level of 0.05 was applied for all statistical tests unless specified otherwise. Repeated-measurement ANOVAs were conducted on RTs using *Method* (EEG, fMRI), *Probe Type* (target, non-target) and *Trial Position* (A, B, C) as within-factors. Dependent t-tests were used for post-hoc comparisons. Only trials with a correct response occurring within probe presentation (1000 ms) were used for RT analysis and trials with erroneous, delayed, or missed reactions were excluded. Nonparametric Friedman tests were applied for the percent error rates separately for the fMRI- and the EEG session and for post-hoc comparisons Wilcoxon-tests were completed. Post-hoc tests (t-tests as well as Wilcoxon tests) included

nine different comparisons. Therefore, p-values were adjusted according to Bonferroni to avoid an accumulation of the type I error.

For behavioral data analysis, the non-target trials at trial position A of the 7 seconds and the 11 seconds delay trials as well as the non-target trials at trial position B for the two conditions (targets and non-targets) of the 11 seconds delay trials, were pooled together, because the participants were not able to anticipate the following events of the trials and therefore it is assumed that these trials were processed identically.

Information from the encoding questionnaire was categorized in different encoding strategies: Spatial encoding, verbal encoding, all other mentioned strategies, a mixed verbal and spatial strategy, any other combination of two different strategies and a category indicating that the applied strategy for this target was forgotten. Frequencies were computed for each participant over all targets and then means and standard deviations (SDs) of the different categories were computed over all participants. This was done separately for the EEG and for the fMRI session.

3.2.4.2 fMRI – Data acquisition and data analysis

A Siemens Allegra® 3T scanner (Siemens, Erlangen, Germany) equipped with a standard quadrature head coil was used for image acquisition. Participants lay on a scanner couch in the dimly lit scanner room and wore foam earplugs. Functional data were acquired with a gradient echo-planar imaging (EPI) sequence (TR= 2 s/volume, TE 29 ms, flip-angle: 80°, voxel size: 3 mm^3, 38 slices, interleaved acquisition, 396-411 volumes per run).

A T1-weighted structural image was acquired (MPRAGE; 176 slices; TR: 2.3 s/volume, TE: 4.38 ms; voxel size: 1 mm^3; flip angle: 8°).

The data were converted from DICOM (Digital Imaging and Communications in Medicine) into NifTI format. The first four images of each scanning run were discarded because of magnetic saturation effects. Statistical analyses (pre-processing, first- and second-level analysis) were performed with SPM5 (Wellcome Department of Imaging Neuroscience, 2005; http://www.fil.ion.ucl.ac.uk/spm/software/spm5/) running on Matlab 6.5.1.

For the pre-processing, the fMRI data were slice-time corrected and realigned to the 6^{th} functional volume of each run using six parameter rigid-body transformations (estimate and reslice). T1 images were co-registered to the mean image and segmented into cerebro-spinal fluid, gray and white matter. The resultant parameters were used to normalize the functional data to the implemented EPI template in MNI (Montreal Neurological Institute) space

including SPM5 default resampling to 2 mm³ isotropic voxels and smoothed spatially with an 8mm Gaussian filter (full-width; half-maximum; FWHM). Serial autocorrelations were corrected by an AR(1) model and a high-pass filter of 128 Hz was enabled to remove low frequency drifts.

Functional data were obtained by modeling the delay epochs with a box-car function convolved with the SPM canonical HRF and all other stimulus onsets as events (Della-Maggiore et al., 2002; Friston, Holmes, Price et al., 1999).

The Design matrix contained regressors for the encoding epoch, for the maintenance periods and for the retrieval periods separately for each position in the trial (A, B, C, apart from the encoding condition where all trials were pooled together). The jittered intertrial intervals were pooled together. Trials with erroneous or missing responses were treated together and the six realign-motion-parameters were modeled separately (Johnstone et al., 2006). These last-mentioned conditions (errors, misses, motion-parameters) were not utilized for further contrasts.

Voxel-wise fixed-effects contrasts were accomplished on single-subject level: Maintenance and probe epochs were treated separately for the different positions in the trial and probe epochs were treated separately for target and non-target stimuli.

Individual contrasts were utilized for multi-subject random effects analyses (Holmes & Friston, 1998) to allow for a generalization to the population and to account for inter-subject variance. Probe epochs were contrasted with fixation (intertrial interval), separately for target and non-target trials and for each position in the trial. A contrast of target versus non-target trials was conducted separately for each trial position to provide a direct comparison of both probe types.

All fMRI contrasts (including conjunction analyses) of Experiment 2 were carried out with a false-discovery rate (FDR) correction for multiple comparisons using a threshold of $p<.05$ and a voxel threshold exceeding 20 contiguous voxels ($k>20$), if not specified differently. Peak coordinates of activated brain regions were converted from MNI to Talairach space (using the MATLAB script „mni2tal.m“, http://imaging.mrc-cbu.cam.ac.uk/imaging/MniTalairach). Anatomical locations were determined using the „Talairach Daemon Client“ software (http://ric.uthscsa.edu/projects/talairachdaemon.html) and the Talairach Atlas (Talairach & Tournoux, 1988).

3.2.4.3 EEG – Data acquisition and data analysis

Participants sat in a comfortable chair in a dimly lit room. EEG data were recorded from 64 channels using a recording cap (EASYCAP, www.easycap.de) equipped with Ag-AgCl sintered ring electrodes (electrode positions are shown in Figure 8), placed according to the extended internationally standardized 10/20-system (American Electroencephalographic Society). EEG signal was amplified with a REFA multi-channel system (TMS international, www.tmsi.com) and digitized with a sampling rate of 512 Hz (unfiltered, average referenced). For electrooculography (EOG), four additional Ag/AgCl surface electrodes were placed infra- and supraorbitally to the right eye and on the left and right canthi of both eyes to measure vertical and horizontal eye movements. Impedance was kept below 15 kΩ for all participants. Electrode locations were digitized with an ultrasonic Motion Analyser System (CMS20; Zebris Medical GmbH).

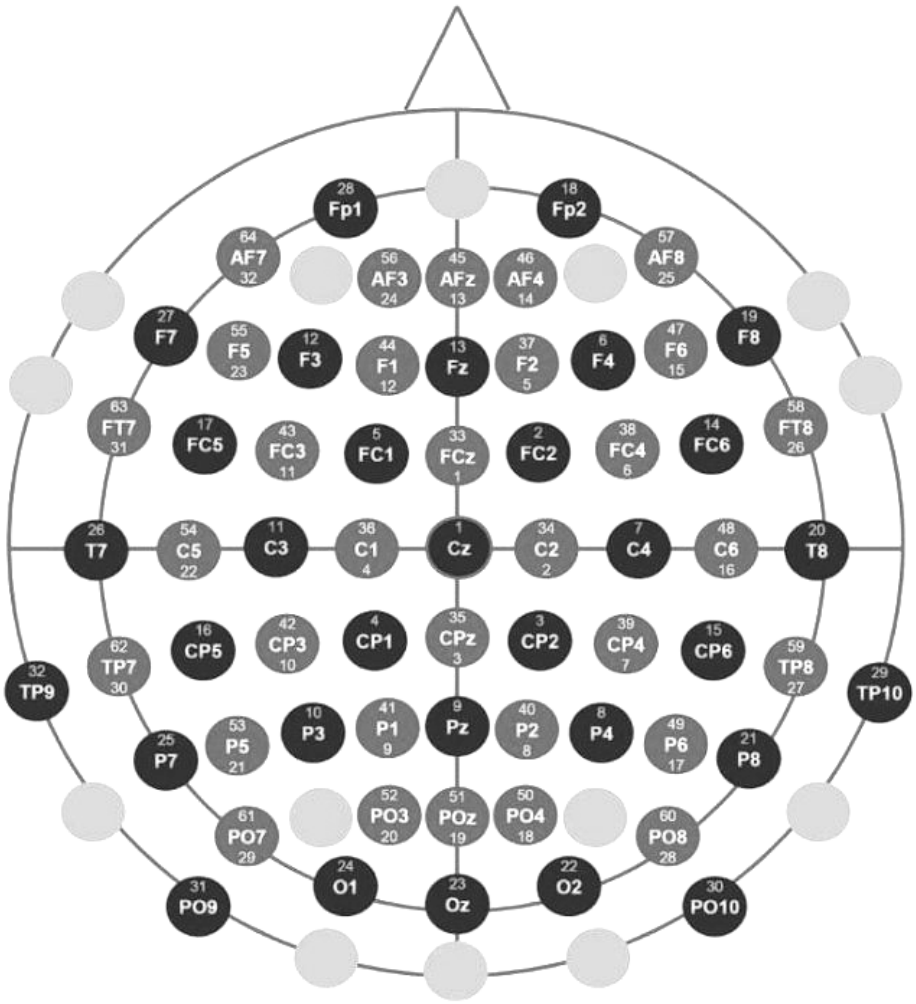

Figure 8: Schematic diagram of 64 electrode positions applied in the present study. Standard electrode positions are shown in black and additional electrode positions are shaded in gray.

ERP data were analyzed with BESA® 5.1.8.10 (Brain Electrical Source Analysis; www.besa.de; MEGIS Software GmbH, 2006). At maximum four channels were interpolated (spherical spline interpolation) for each participant. The number and location of interpolated channels are listed in Appendix K. To generate task-related ERPs, nearly 40 correct trials from each condition were agglomerated from each individual participant for the probe periods of target trials and of non-target trials, separately for the different positions in the trial (position A, B, C; number of sweeps correspondingly for target trials ± SD: 38.7 ±2.5 / 38.9 ±2.1 / 38.5 ±2.5 and for non-target trials: 39.2 ±1.8 / 39.0 ±2.0 / 38.2 ±3.1). For the averaging procedure, a time window between 200 ms pre-stimulus and 1000 ms post-stimulus was set. Trials with artifact-contamination exceeding 100µV and erroneous trials were excluded from further EEG analysis. Due to the fact that some conditions (non-targets at trial positions A and B) contained more trials than the other conditions, the trials, which were accumulated for the averages, were selected uniformly distributed throughout the whole EEG data set for each participant. This was done to ensure that all averages contained a roughly comparable number of sweeps from each of the four experimental runs. This avoids that the averages of some conditions contained more trials from the beginning of the experimental session where all shapes appeared new to the participants.

Data were filtered with a low-cutoff filter of 0.03 Hz (forward) and a high-cutoff filter of 15 Hz (zero-phase). Blinks of each participant were averaged using a template-based method (Ille, Berg, & Scherg, 2002) to generate an individual artifact topography as well as a group artifact topography (resulting from the averaged blink epochs over all study participants). Both artifact topographies were used as spatial components of the blink topographies in SA, respectively for single individual and average-based analyses.

EEG data were averaged for target and non-target stimuli separately at each trial position and furthermore grand average ERPs were computed for all target stimuli together and separately for all non-target stimuli. A grand average ERP combining all (target and non-target) conditions was also generated. Difference waves were computed for target versus non-target trials pooled over all trial positions and also separately for target minus non-target trials at each trial position.

For the analysis of the P3b component, mean amplitudes were computed over a time window ranging between 300 and 700 ms post-stimulus. Since the P3b component showed two distinct peaks, mean amplitude values were determined for overall P3b amplitude in the specified interval. Electrode positions Pz and Cz were selected because the P3b component

reaches its maximum amplitude at these electrode sites. Mean amplitudes were analyzed for each ERP component with a 3-way repeated-measurement ANOVA including the factors *Electrode* (Pz, Cz), *Probe Type* (targets, non-targets) and *Trial Position* (A, B, C). Post-hoc comparisons were conducted with paired t-tests.

3.2.4.4 Source analysis procedure – Integration of fMRI and EEG data

For the SA, all individual ERP waves (64 electrodes) were interpolated using spherical spline interpolation to an 81 electrode configuration on a standard head matching the 10-20 and 10-10 international systems (BESA® software). The resulting electrode montage was co-registered with the Talairach-transformed MNI template using the Brain Voyager/BESA® software interface to ensure matching fMRI and EEG coordinate systems. For this purpose, the spherical coordinates of the standard 81 electrode locations and three fiducial landmarks (nasion, right and left preauricular points) were fitted to the respective landmarks on the Talairach-transformed MNI template head surface (see Figure 9).

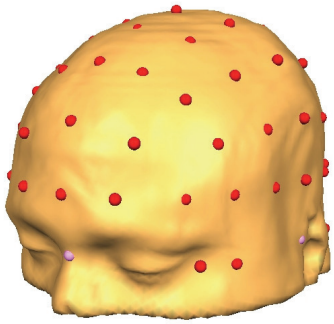

Figure 9: Smoothed reconstructed head surface of the Talairach-transformed MNI brain, co-registered with the standard 81 electrode montage from BESA®.

The SA approach used in the present study based mainly on the procedure used by Bledowski and colleagues (see Bledowski et al., 2006). In order to obtain regional sources (RSs) as "seeds" for the fMRI-constrained SA, fMRI data were entered into conjunction analyses over all trial positions for the contrasts *targets versus fixation* (fixation = intertrial interval; target probes at trial positions A, B and C versus fixation; "*T vs. fix*") and separately for *non-targets versus fixation* (conjunction over non-target probes at all trial positions versus fixation; "*N vs. fix*"). Altogether, this procedure resulted in 26 activation peaks, 13 for each contrast (see Table 9, on page 65). These contrasts were chosen because areas activated for target probes as well as areas activated in the non-target probe conditions were required for SA. Increasing the

number of RSs in a SA model also increases the mutual interaction between these RSs. Therefore, a reduction of the number of RSs was performed (see Bledowski et al., 2006). Distances between the resulting peak coordinates (Talairach space) obtained by both conjunction analyses were computed and peak coordinates were averaged using a nearest neighbor approach. To minimize interactions between different RSs, a minimum distance of 2.5 cm between each RS pair was defined. Each original peak activation (derived from fMRI) should be less than 2.0 cm away from its respective (averaged) RS to ensure relatively homogeneous clusters. Three activation peaks were not transferred to RSs and were not used for further SA. Two of them were located in the Midbrain and one in the Cerebellum. These sources were excluded, because in SA, the activity of a deeply situated source is vulnerable to activities of other brain regions which are not correctly modeled and therefore, deeply located sources are frequently excluded. Furthermore, the cerebellar source fell below the minimum distance criterion because it had a distance of 2.3 cm to the parahippocampal RS.

The calculated RS coordinates were used to define a SA model including 12 RSs applied on individual grand average ERPs (over all six conditions) using a standard four shell spherical head model (four shells with different conductance characteristics: brain, cerebro-spinal fluid, bone, skin) and a regularization constant of 1 percent for the inverse operator (to reduce the interaction between sources). An epoch of -1 ms pre-stimulus to 999 ms post-stimulus was defined as SA time window. To control for residuals of eye artifacts, a spatial topography of each individual blink pattern was included in the model. This approach allowed for a separation of the blink artifact time course from the event-related source activity.

A RS is composed of three orthogonally oriented equivalent current dipoles at the same location (Scherg & Von Cramon, 1986; Scherg & Berg, 1996). The first dipole vector component of each RS was oriented at the maximum amplitude of source activity over the whole examined time interval for each participant to adjust the orientation of the dipoles. This was to account for differing orientations of active cortex regions caused by their individual brain regional anatomy (gyration patterns). This orientation procedure resulted in an alignment of the first component of each RS into the direction of the current flow. The second component was then automatically adjusted to be orthogonal to the first and to explain the residual activity and the third component is orthogonal to both other components.

These stable individual orientations obtained on grand average data were used for further SA of individual difference waves (targets minus non-targets pooled over all trial positions and targets minus non-targets separately for trial positions A, B, C), because grand average data have a higher signal-to-noise ratio and in SA it is more crucial to obtain stable orientations

than to have stable RS locations (in case of deviations of 1-2 cm, see Scherg & Von Cramon, 1986).

The source model on individual grand average data explained on average 98.9 percent (SD: 0.6) of the scalp ERP potential variance. Goodness of fit (= 1 minus residual variance) and global field power (= "sum of squares of the activity over all channels of the current data set", see BESA® manual) of the grand average source model are depicted in Figure 10.

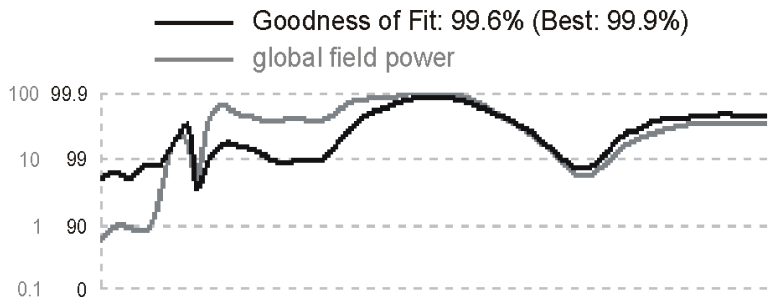

Figure 10: Goodness of Fit and global field power of the grand average source model for the probe presentation epoch (0-999 ms). Both lines represent percentage values in logarithmic scaling. The mean Goodness of Fit value over the whole time epoch is given above, "best" indicates the maximum Goodness of Fit value.

Variance explanation in percent was also averaged over all participants separately for the target and for the non-target conditions in order to confirm that the selected SA model permitted an explanation of both probe type conditions (explained variance for targets: mean ± SD: 98.9 percent, ± 0.6; for non-targets: 98.6, ± 0.8).

Spherical spline topological voltage maps of source activities were computed at peak latencies of the corresponding source waveforms (see Figure 16).

The source waveforms resulting from the source model application to individual difference ERP waves were used to test for differences in source activity between target and non-target conditions with the bootstrap bias-corrected and adjusted (BCa) method (Efron & Tibshirani, 1993). The BCa bootstrap method is non-parametric and therefore does not require distribution assumptions. With 1000 bootstrap samples, a 95%-confidence interval was determined for each source waveform (combining data from all participants). Differences between target and non-target conditions were considered significant when the confidence interval of the difference wave did not include zero.

To evaluate the sensitivity of the determined RSs in the current source model to activity in other brain areas, source sensitivity images were computed for all RSs. Source sensitivity is

defined as „the fraction of power at the scanned brain location that is mapped onto the selected source“ (BESA® manual). Determinants of the source sensitivity are: The selected source model, sensor configuration, head model and regularization constant, whereas the recorded sensor signals do not influence on source sensitivity. Source sensitivity images are depicted in Appendix L.

3.3 Results

In the results section, behavioral data (reaction times, error rates, individual evaluation of task parameters) are described, followed by a description of fMRI results (contrasts of target versus non-target trials, conjunction of targets versus fixation over all trial positions and accordingly of non-targets versus fixation over all trial positions). Then the EEG results are characterized (grand average, P3b mean amplitudes, qualitative ERP differences between probe types and trial positions). Finally, findings from SA are presented (chronological sequence of source activities, differences between source waveforms for the target and non-target conditions and differences between source waveforms separately for each trial position).

3.3.1 Behavioral data

For reaction time (RT) analyses, a repeated measurement ANOVA was conducted with the factors *method* (EEG, fMRI), *probe type* (target, non-target) and *trial position* (A, B, C). A significant main-effect of *method* ($F_{[1;19]} = 6.3$; $p = .021$) was found. RTs were higher in the fMRI- compared with the EEG session. A main-effect of *trial position* revealed differences between the three positions ($F_{[2;38]} = 10.3$; $p < .001$). RTs were shortest at trial position A and RTs were longest at position B.

Furthermore, an interaction effect *method x probe type* ($F_{[1;19]} = 13.7$; $p = .002$) was observed. In the EEG session, RTs were longer to targets compared with non-targets. This was not the case for the fMRI session.

In addition, there was an *method x trial position* interaction ($F_{[2;38]} = 4.9$; $p = .013$). In both experimental sessions (EEG and fMRI), RTs were longest at trial position B. In the EEG session, RTs in response to all stimuli at trial position C were longer than to stimuli at position A, whereas in the fMRI session, RTs were comparable at trial positions C and A.

The *probe type x trial position* interaction also yielded significant results ($F_{[2;38]} = 17.5$; $p < .001$). RTs were increasing for non-target probes with increasing trial position, whereas for target trials RTs were longest at trial position B and shortest at trial position C. To examine the interaction effects, post-hoc t-tests were performed separately for data from both measurement sessions (see Table 4 and Table 5). For target trials, RTs were higher at trial position B compared with position C in both measurement sessions and also higher for position B compared with position A in the EEG session. Non-target trials of the EEG session

yielded significant differences between all positions with highest RTs at position C and lowest at position A. There were no trial position differences for non-target trials in the fMRI session. The direct comparison between target and non-target trials in the EEG session revealed higher RTs for the target condition at trial positions A and B. RTs and error rates are depicted in Figure 11 and Figure 12, for the EEG and for the fMRI session, respectively.

Table 4: T-tests comparing different trial positions for RTs of the EEG session (left) and fMRI session (right), separately for target and non-target trials. A, B and C represent different trial positions. P-values are adjusted according to Bonferroni. Significant results are indicated with asterisks (* p<.05, ** p<.01).

EEG session			**fMRI session**		
	t-value	**p-value**		**t-value**	**p-value**
targets: A versus B	-6.0	<.005 **	**targets: A versus B**	-1.8	.765
targets: A versus C	0.3	1.0	**targets: A versus C**	2.1	.405
targets: B versus C	4.3	<.005 **	**targets: B versus C**	5.5	<.005 **
non-targets: A versus B	-4.1	=.009 **	**non-targets: A versus B**	-0.4	1.0
non-targets: A versus C	-5.6	<.005 **	**non-targets: A versus C**	-1.9	.684
non-targets: B versus C	-3.9	=.009 **	**non-targets: B versus C**	-1.7	1.0

Table 5: T-tests comparing target and non-target conditions for RTs of the EEG session (left) and fMRI session (right), separately for the different trial positions. A, B and C represent different trial positions. P-values are adjusted according to Bonferroni. Significant results are indicated with asterisks (* p<.05, ** p<.01).

targets versus non-targets EEG session			**targets versus non-targets fMRI session**		
	t-value	**p-value**		**t-value**	**p-value**
position A	4.7	<.005 **	**position A**	-1.0	1.0
position B	4.3	<.005 **	**position B**	0.8	1.0
position C	-1.5	1.0	**position C**	-3.1	.054

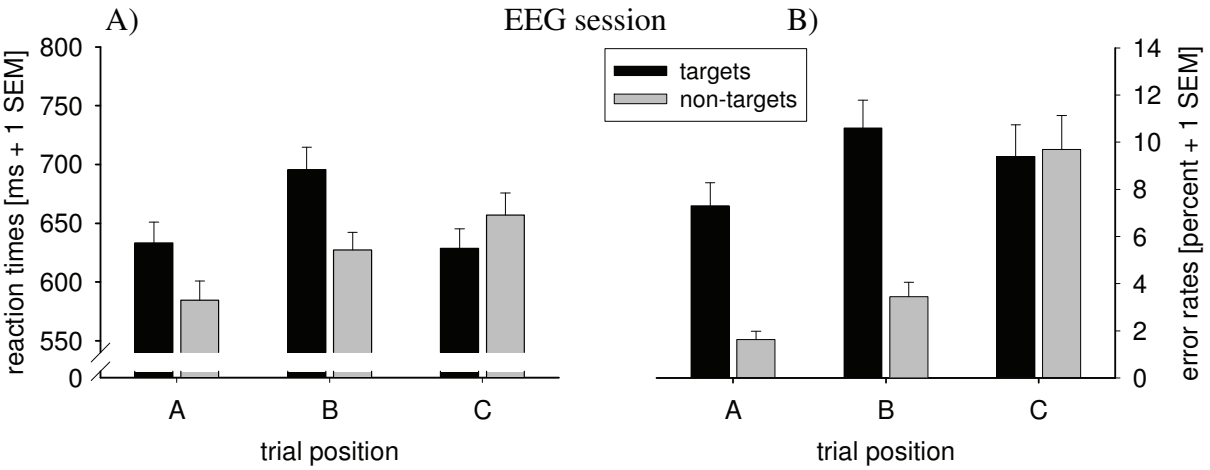

Figure 11: Reaction times (A) and percent error rates (B) measured during the EEG session for target trials (black) and non-target trials (gray). A, B and C represent different positions in the trial. Error bars show 1 SEM.

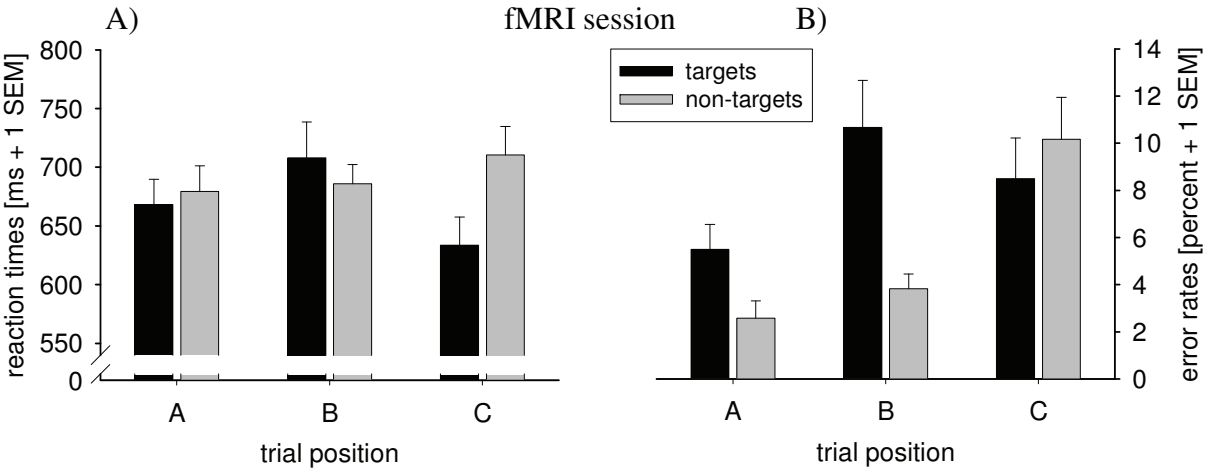

Figure 12: Reaction times (A) and percent error rates (B) measured during the fMRI session for target trials (black) and non-target trials (gray). A, B and C represent different positions in the trial. Error bars show 1 SEM.

A Friedman test for percent error rates yielded significant differences between all probe conditions for the EEG session ($Chi^2 = 61.5$; $p < .001$), as well as for the fMRI session ($Chi^2 = 33.4$; $p < .001$). For both measurement sessions, error rates increased with increasing trial position for non-targets, but for target trials error rates were highest at trial position B and lowest at trial position A (see Figure 11 for EEG data and Figure 12 for fMRI data).

For the EEG session, post-hoc comparisons with Wilcoxon tests for the non-target conditions indicated significant differences between all trial positions (C>B>A; see Table 6). The

comparison between target and non-target trials separately at each trial position revealed higher error rates for target trials at positions A and B (see Table 7).

Table 6: Wilcoxon tests comparing different trial positions for percent error rates of the EEG session (left) and fMRI session (right), separately for target and non-target trials. A, B and C represent different trial positions. P-values are adjusted according to Bonferroni. Significant results are indicated with asterisks (* p<.05, ** p<.01).

EEG session			**fMRI session**		
	z-value	**p-value**		**z-value**	**p-value**
targets: A vs. B	2.5	=.126	**targets: A vs. B**	2.7	=.063
targets: A vs. C	1.8	=.666	**targets: A vs. C**	2.0	=.396
targets: B vs. C	1.0	=1.0	**targets: B vs. C**	1.4	=1.0
non-targets: A vs. B	3.3	=.009 **	**non-targets: A vs. B**	1.7	=.747
non-targets: A vs. C	3.9	<.005 **	**non-targets: A vs. C**	3.7	<.005 **
non-targets: B vs. C	3.8	<.005 **	**non-targets: B vs. C**	3.3	=.009 **

For non-target trials of the fMRI session, post-hoc comparisons with Wilcoxon tests yielded higher error rates at trial position C compared to positions A and B. For target trials, there was only a trend towards higher error rates at trial position B compared to position A (see Table 6). The direct comparison of target and non-target trials revealed higher error rates for target trials at trial position B and a trend towards higher error rates for targets at trial position A (see Table 7). There were no differences between error rates obtained in the fMRI and in the EEG session (Wilcoxon tests, see Appendix M).

Table 7: Wilcoxon tests comparing target and non-target conditions for percent error rates of the EEG session (left) and fMRI session (right), separately for different trial positions. A, B and C represent different trial positions. P-values are adjusted according to Bonferroni. Significant results are indicated with asterisks (* p<.05, ** p<.01).

targets vs. non-targets EEG session			**targets vs. non-targets fMRI session**		
	z-value	p-value		z-value	p-value
position A	-3.7	<.005 **	**position A**	-2.6	=.09
position B	-3.7	<.005 **	**position B**	-3.2	=.009 **
position C	-0.04	=1.0	**position C**	-0.9	=1.0

Task difficulty was evaluated using a ten point scale (1 = very easy; 10 = very difficult) and the study participants stated a difficulty range in the EEG session between 2 and 7 (mean±SD: 4.3±1.8) and in the fMRI session between 1 and 7 (4.2±2). Verbalization was the encoding strategy mostly used in both sessions (EEG: 53.7±14.5 percent; fMRI: 54.3±21.1 percent). Spatial oriented strategies of memorization were subsumed under the strategy to „memorize

either a characteristic feature of the target shape, the number or the direction of characteristic bulges“ (EEG: 32.6±10.5; fMRI: 34.5±13.4). In a few cases, individuals specified an individual encoding strategy (EEG: 0.9±1.6; fMRI: 1.5±2.8) or indicated that they could not remember the encoding strategy for the correspondent target stimulus (EEG: 11±9.8; fMRI: 5.8±3.4). In this regard, it is important to note that the overall number of stimuli was higher in the EEG- (55 stimuli) than in the fMRI session (30 stimuli). Some study participants specified a combined strategy, mostly the verbalization strategy in combination with another strategy (EEG: 1.3±3.4; fMRI: 3.2±7.7), and in some cases a combination of other strategies (EEG: 0.2±0.8; fMRI: 0.2±0.8). In a few cases, participants overlooked some target stimuli in the questionnaire and produced missing values (EEG: 0.3±0.9; fMRI: 0.5±1.2).

3.3.2 FMRI data

Target and non-target trials were directly contrasted at each trial position (targets versus non-targets: “*T vs. N*”). Activated clusters are depicted in Figure 13 and the glass brains with the corresponding activation patterns are shown in Appendix N. Detailed specifications and coordinates of suprathreshold clusters at trial positions A and B are listed in Table 8 on page 63.

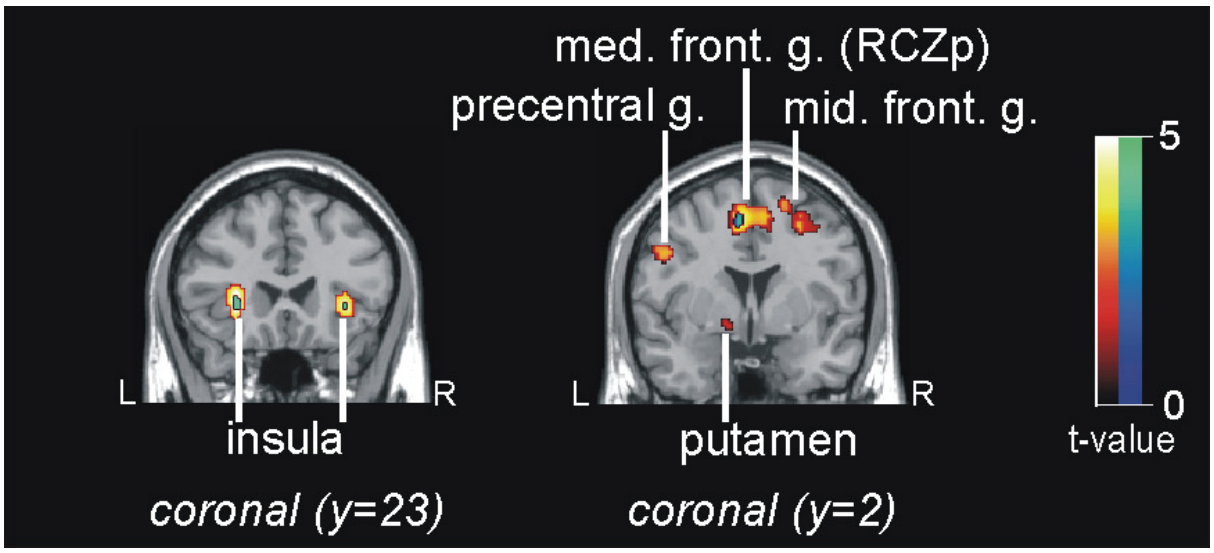

Figure 13: Overlay of activated clusters derived from the contrasts of target probes versus non-target probes at trial position A (colored in blue-green) and at trial position B (colored in red-yellow), both FDR-corrected, p<.05; k>20 voxels. Abbreviations: g. = gyrus; med. front. = medial frontal; RCZp = posterior portion of the rostral cingulate zone; mid. front. = middle frontal; R = right hemisphere; L = left hemisphere.

At trial position A, six clusters passed the threshold: One cluster was located in the midbrain, bilateral clusters were located in lingual gyri and one cluster in medial frontal cortex, including activation in the posterior portion of the rostral cingulate zone (RCZp). Further activated clusters were located in right IFG and in the left claustrum (nearest gray matter at a range of 3mm). The latter two clusters showed nearly comparable Talairach coordinates and might therefore be regarded as corresponding bilateral activations.

Table 8: Talairach coordinates of significant activation peaks derived from the contrasts of target trials versus non-target trials separately at trial position A (shown in the middle) and trial position B (shown on the right side; both FDR-corrected, p<.05; k>20 voxels). Anatomical labels of peak activations are listed in boldface and significant sub-peaks are listed without boldface. In all cases where two values for the range of nearest gray matter are denoted (left column), the first value belongs to trial position A and the second to trial position B. Abbreviations: g. = gyrus; r = range of nearest gray matter in mm; R = right hemisphere; L = left hemisphere.

	Trial position A: Targets vs. non-targets						**Trial position B: Targets vs. non-targets**					
Anatomical region (BA, r)	**side**	**cluster size**	**t-value**	**peak coordinate (Talairach)**			**side**	**cluster size**	**t-value**	**peak coordinate (Talairach)**		
Midbrain, (red nucleus, r=3)	R	243	5.95	4	-22	-7	R	723	5.98	4	-22	-7
Midbrain, (thalamus, r=3)										6	-12	-1
Midbrain, (red nucleus, r=3)										-4	-24	-7
Lingual g. (BA 17, r=9 / r=5)	R	169	5.94	18	-84	-1	R	291	6.06	18	-83	1
Sub-gyral occipital (BA 19, r=9)				30	-72	-1				30	-72	-1
Lingual g. (BA 17, r=9)	L	141	5.45	-18	-86	-2	L	273	5.68	-18	-86	-2
Inferior frontal g. (BA 47, r=7/ r=3)	R	65	5.35	34	25	-3	R	199	6.12	32	27	-3
Sub-lobar (claustrum, r=3/ insula, BA 13, r=3)	L	21	4.5	-28	23	-1	L	215	6.02	-30	23	-1
Medial frontal g. (BA 6, r=5/r=3)	L	131	4.58	-8	2	48	L	958	6.09	-6	0	48
Medial frontal g. (BA 6, r=3)			4.57	8	8	49			4.89	8	8	49
Medial frontal g. (BA 32, r=3)			4.11	-4	10	46			5.46	-4	10	46
Middle frontal g. (BA 6)							R	241	5.44	28	-2	46
Sub-gyral frontal (BA 6, r=5)									3.69	18	5	57
Precentral g. (BA 6)							L	323	4.63	-32	-11	58
Precentral g. (BA 6, r=5)									4.38	-30	-11	50
Postcentral g. (BA 3, r=3)									3.92	-34	-19	45
Lentiform nucleus / putamen							L	24	4.50	-14	4	-7
Precentral g. (BA 6, r=3)							L	61	4.14	-50	3	29
Precentral g. (BA 6, r=5)							L	48	4.12	-38	-4	41
Sub-gyral temporal (BA 31, r=7)							L	48	4.10	-28	-73	24
Sub-gyral parietal (BA 7, r=3)							L	45	3.98	-26	-46	47
Sub-gyral occipital (BA 19, r=7)							L	29	3.97	-28	-68	-3
Inferior frontal g. (BA 9)							R	24	3.58	48	5	31
Sub-gyral frontal (BA 9, r=5)									3.42	42	9	24

The same contrast at trial position B revealed 15 supra-threshold activations. All six clusters described previously for the contrast at trial position A also showed supra-threshold activations at trial position B, with peak coordinates differing only slightly from the peak

coordinates found at trial position A (see Table 8). Additional activations at trial position B were located in right middle frontal gyrus (MFG), right IFG, lentiform nucleus and three clusters in left precentral gyrus. Further activations were found in the left hemisphere, one of them in the temporal lobe (precuneus at a range of 7mm), one in the parietal lobe (precuneus at a range of 3mm) and another in the occipital lobe (lingual gyrus at a range of 7mm).

Contrasting target and non-target trials at trial position C revealed no supra-threshold voxels at all. Even the use of a more liberal threshold without correction for multiple comparisons and without a restriction with regard to the number of contiguous voxels (uncorrected, $p<.001$; k=0 voxels) resulted in only four left-hemispheric clusters with very small voxel sizes (6, 2, 2, 1 voxels).

Retrieval processing per se was examined using single contrasts for target trials versus fixation and for non-target trials versus fixation, each separately for each trial position. Then a conjunction analysis (conjunction null; FDR-corrected, $p<.05$) was computed for target trials versus fixation over all trial positions (*T vs. fix*), and another conjunction for non-target trials versus fixation over all trial positions (*N vs. fix*). Corresponding activated clusters are listed in Table 9 on page 65 and shown in Figure 14 on page 66. Glass brains with the corresponding activation patterns are shown in Appendix O.

Activated clusters for the target condition (versus fixation) were located in left IFG, bilateral MFG and precentral gyri, superior frontal gyrus (SFG), bilateral insulae, left precuneus, right occipital lobe, left lingual gyrus, right cerebellum and a right sub-lobar region including activated voxels in putamen.
Activations for the non-target condition (*N vs. fix*) were found in right superior and medial frontal gyri, left anterior cingulate cortex (ACC), bilateral posterior cingulate, bilateral fusiform gyri, bilateral middle occipital gyri (MOG), right lentiform nucleus and bilateral thalami. Generally, the activation pattern of the target condition appeared to be more widespread than the activation pattern of the non-target condition (see Figure 14, and glass brains with the corresponding activation patterns in Appendix O).

Table 9: Left side: Talairach coordinates of significant activation clusters when contrasting the retrieval epoch against fixation baseline, separately for targets and non-targets, but conjunct over all three trial positions (T = conjunction of target trials vs. fixation over all trial positions; N = conjunction of non-target trials vs. fixation over all trial positions; both FDR-corrected, p<.05; k>20 voxels). Right side: Regional sources and their locations, obtained by an averaging procedure of the corresponding peak coordinates shown on the left side. Abbreviations: con = applied contrast; g. = gyrus; BA = Brodmann area; r = range of nearest gray matter in mm; R = right hemisphere; L = left hemisphere.

con	anatomical region (BA; r)	side	cluster size	t-value	peak coordinate (Talairach)			regional sources	side	coordinate (Talairach)		
					x	y	z			x	y	z
T	Inferior frontal g. (BA 9)	L	551	4.4	-51	5	26	Inferior frontal g. (BA 9)	L	-51	5	26
T	Middle frontal g. (BA9)	R	179	3.68	51	6	35	Inferior frontal g. (BA 9; r=7)	R	51	6	23
T	Precentral g. (BA 44; r=7)	R	21	3.06	51	6	11					
T	Middle frontal g. (BA 6)	L	30	3.66	-20	-9	58	Middle frontal g. (BA 6)	L	-30	-8	58
T	Precentral g. (BA 6)	L	593	4.11	-40	-7	57					
N	Superior frontal g. (BA 6)	R	42	4.05	12	7	62	Superior frontal g. (BA 6)	R	3	5	54
N	Medial frontal g. (BA 6)	R	29	3.45	2	-1	50					
T	Superior frontal g. (BA 6)	L	2351	5.71	-4	8	49					
N	Cingulate g. (BA 24; r=3)	L	63	4.08	-10	15	32	Cingulate g. (BA 24; r=3)	L	-10	15	32
N	Posterior cingulate (BA 18; r=3)	L	268	4.57	-12	-67	14	Precuneus (BA 31; r=3)	L	-13	-66	22
T	Precuneus (BA 7; r=3)	L	99	3.49	-14	-65	29					
N	Fusiform g. (BA 20; r=7)	R	1351	5.55	36	-44	-18	Parahippocampal g. (BA 19; r=7)	R	29	-56	-4
T	Sub-gyral occipital (BA 19; r=9)	R	4713	7.11	30	-62	-5					
N	Posterior cingulate (BA 30; r=3)	R	148	3.99	20	-62	10					
N	Fusiform g. (BA 19; r=7)	L	309	4.47	-30	-53	-9	Fusiform g. (BA 19; r=7)	L	-30	-53	-9
T	Lingual g. (BA 18; r=7)	L	2436	6.49	-20	-84	-4	Inferior occipital g. (BA 18; r=3)	L	-33	-80	-4
N	Middle occipital g. (BA 19; r=7)	L	39	3.56	-46	-78	2					
N	Middle occipital g. (BA 19; r=3)	L	39	4.10	-32	-78	-10					
N	Middle occipital g. (BA 19; r=3)	R	197	5.11	32	-85	17	Middle occipital g. (BA 19; r=3)	R	32	-85	17
T	Insula	L	285	5.79	-30	18	6	Insula	L	-30	18	6
N	Lentiform nucleus (putamen)	R	37	4.08	24	6	0	Lentiform nucleus (putamen)	R	21	11	-3
T	Sub-lobar	R	138	3.77	8	3	-9					
T	Insula (BA 13)	R	285	4.78	32	23	1					
T	Cerebellum declive	R	21	3.52	10	-61	-17					
N	Midbrain (thalamus; r=5)	R	42	4.02	6	-27	1					
N	Midbrain (thalamus; r=3)	L	27	4.01	-12	-29	-2					

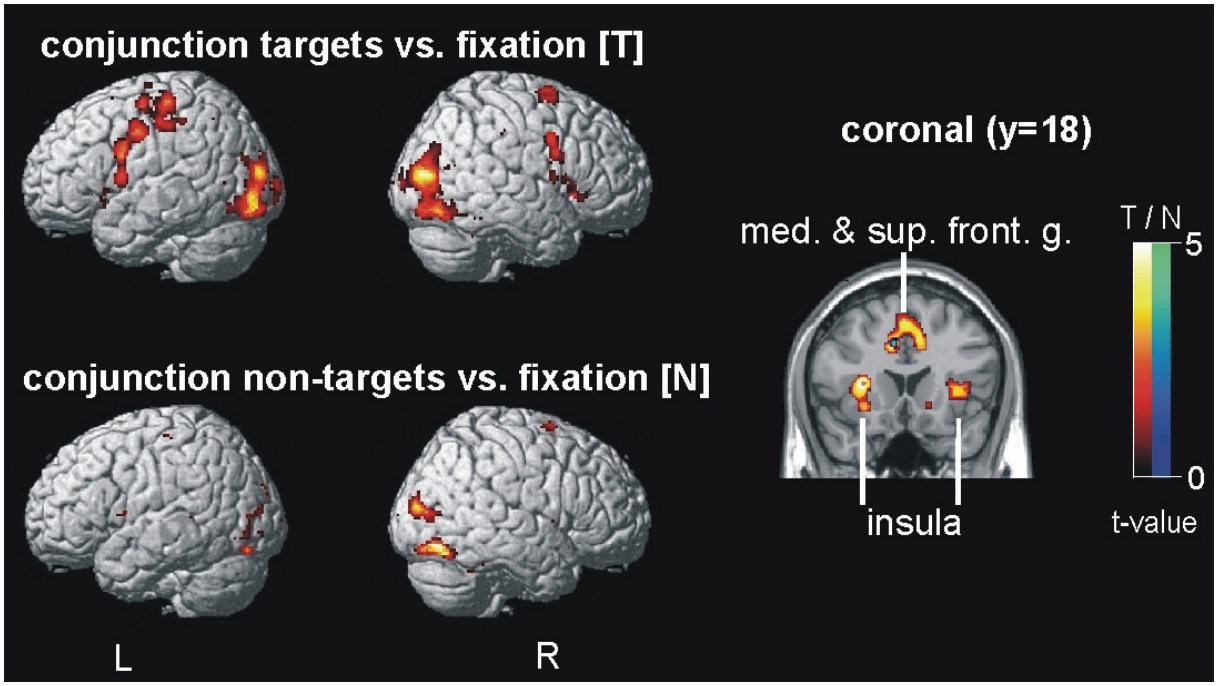

Figure 14: Four rendered brain images are displayed on the left. A conjunction of target trials versus fixation over all trial positions is shown above and a conjunction of non-target trials versus fixation over all trial positions is shown below (conjunction null, each FDR-corrected; p<.05). On the right, activation clusters are overlaid from both conjunctions and show activations in bilateral insulae, medial and superior frontal gyri (=med. & sup. front. g.). Here, clusters from the targets vs. fixation conjunction are colored in yellow-red, and clusters from the non-targets vs. fixation conjunction are colored in blue-green.

3.3.3 EEG data

3.3.3.1 Event-related potentials – Grand average

ERPs show deflections of positive (P) and negative (N) voltage. Usually, they are labeled either according to their occurrence in the ERP (P1, N1, P2, N2, P3 etc.) or some common ERP components are labeled with their polarity and a well-established time specification (like N100, P200, P300, N400 etc.).

In the following, the ERP deflections are labeled according to their polarity and their peak latency (in ms) in the grand average over all probe trials. This nomenclature is chosen to provide an orientation for the reader, because it is easier to distinguish between deflections found in the present experiment and common ERP components. Nevertheless, wherever possible, the ERP deflections observed in the present experiment are linked to well-known components, at least in the discussion section.

The grand average ERP showed bilateral positive deflections with a maximum at electrode sites PO8 and PO7 at 111 ms after stimulus-onset (P111). About 140 ms post-stimulus, a negative deflection started at posterior electrode positions bilaterally and showed a maximum amplitude at electrode positions PO8 and PO7 at 170 ms post-stimulus (N170). Starting approximately 250 ms after stimlus-onset, a negative deflection was visible over fronto-central brain regions, reaching a peak at 303 ms at electrode position FCz (N303). In the same time window, a positive deflection was visible at parietal midline electrodes, showing a scalp voltage distribution comparable to the scalp distribution of the well-known P3b component. This deflection showed two different peaks at parietal electrode sites. The first peak was maximal at electrode position Pz at 367 ms (P367). The scalp distribution of this positive component moved from the first to the second positive peak in an anterior direction from electrode sites over parietal brain regions to central electrode sites. Therefore, the maximum amplitude value of the second peak was located more anterior than the first peak, at electrode position CPz (520 ms; P520). The maximum amplitude value for the second peak at Pz was visible at 484 ms (with lower amplitude values than CPz at 520ms). Between 300 and 700 ms there was a negative deflection over fronto-lateral regions with maximal amplitude values at electrode sites FP1, AF7, FP2 and AF8 (at 510, 512, 502 and 482 ms; N510). The grand average ERP potential and the corresponding scalp voltage maps are shown in Figure 15.

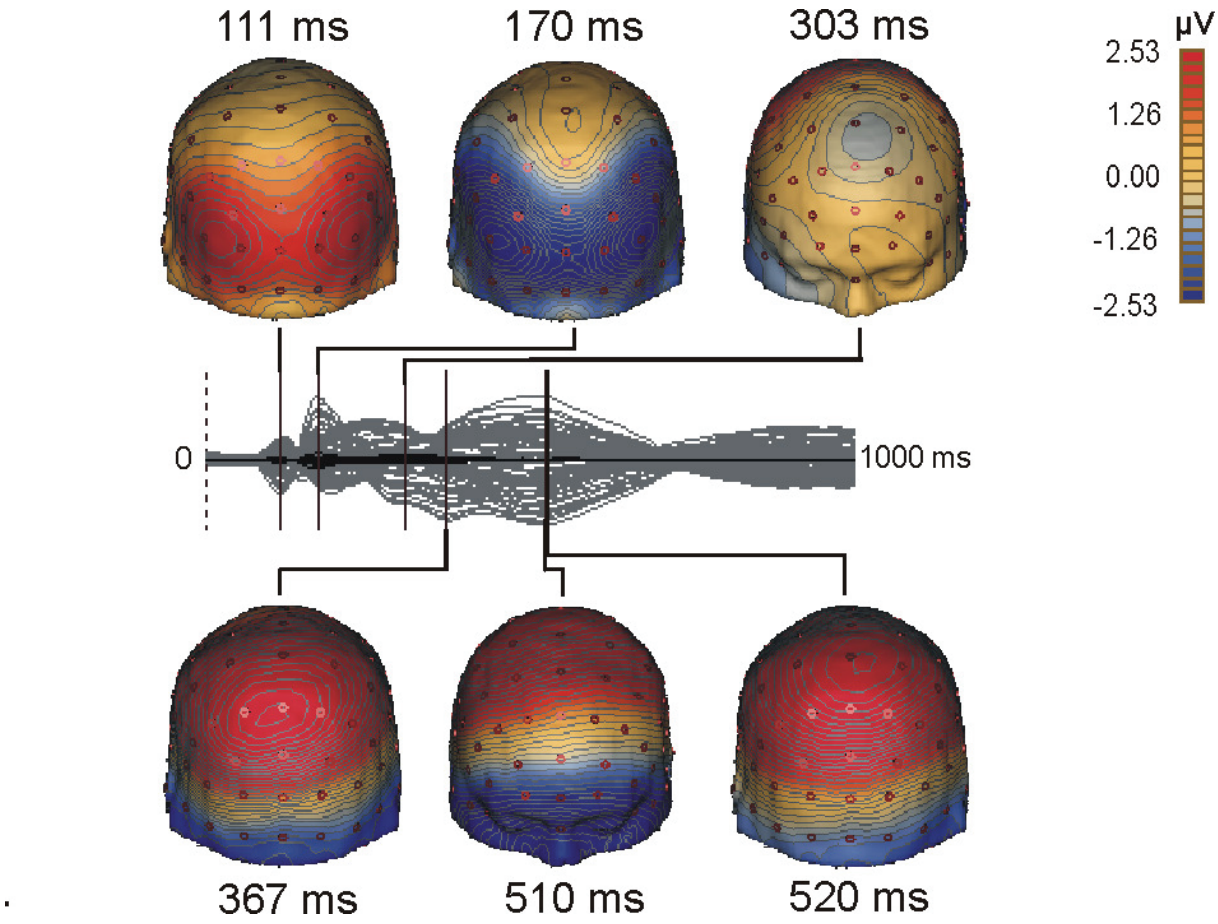

Figure 15: Grand average ERP waveform over all probe types and trial positions for probe presentation (0-999 ms) is shown in the middle. Above and below: Spline-interpolated scalp voltage maps at time points where peak amplitudes were visible in the grand average ERP (over all conditions: P111, N170, N303, P367, N510, P520).

3.3.3.2 Mean amplitudes of the P3b component

One of the previously mentioned ERP components (P3b) was selected to examine effects of probe type or trial position on mean amplitude values. Mean amplitudes between 300 and 700 ms post-stimulus were analyzed with a 3-way ANOVA including the factors *electrode* (Pz, Cz), *probe type* (target, non-target) and *trial position* (A, B, C).

A main effect of *electrode* ($F[1;19]= 12.3$, $p=.002$) can be explained by higher positive mean amplitudes at electrode position Pz compared to Cz. A *probe type* main effect ($F[1;19]= 22.5$, $p<.001$) was observed. Higher positive mean amplitude values were found for the target condition compared with the non-target condition. A main effect of *trial position* was found ($F[2;38]= 5.7$, $p=.007$). Mean amplitude values were highest at trial position C and comparable with each other at positions A and B. There was an *electrode x trial position* interaction ($F[2;38]= 3.9$, $p=.029$).

Post-hoc t-tests examining the *electrode x trial position* interaction with mean amplitude values pooled over both probe types indicated significant differences for the comparison of trial positions B and C at electrode position Cz (higher mean amplitudes at trial position C; see Appendix P).

T-tests for mean amplitudes of target versus non-target conditions separately at each trial position revealed higher values for target trials at trial position A for electrode Pz and at trial positions A and C for electrode Cz (and just below threshold at trial position B for Cz; p = .05). Descriptive statistics of mean amplitude values between 300 and 700 ms post-stimulus for all conditions are shown in Appendix Q.

Table 10: T-tests for mean amplitudes (300-700 ms post-stimulus) comparing target versus non-target conditions separately at each trial position for electrode positions Pz (left) and Cz (right). Significant results are indicated with asterisks (* p<.05, ** p<.01).

Pz			**Cz**		
targets vs. non-targets	**t-value**	**p-value**	**targets vs. non-targets**	**t-value**	**p-value**
trial position A	2.6	=.017 *	**trial position A**	5.5	<.001 **
trial position B	1.9	=.07	**trial position B**	2.1	=.05
trial position C	1.8	=.09	**trial position C**	3.8	=.001 **

3.3.3.3 Event-related potentials – Differences between probe types and trial positions

Some apparent differences between target and non-target ERPs are described qualitatively in the following paragraph, based on the grand average ERP waveforms for targets and for non-target probes and on the visual inspection of the difference waves between probe type conditions (separately for each trial position).

Between 200 and 400 ms post-stimulus, differences between target and non-target trials were prominent over bilateral parietal brain regions and also at fronto-central electrode sites (N303). Target trials showed relatively higher negative voltage values than non-target trials over bilateral parietal electrode sites and most pronounced on the left side. The N303 component over fronto-central electrodes was mainly produced by a negative deflection of the non-target condition whereas the target condition showed voltage values near zero.

Both, the early and the late components of the P3b component (P367, P520, respectively) showed higher amplitude values for the target condition compared with the non-target condition at centro-parietal electrodes and this difference was more pronounced over the left hemisphere. The concurrent negative deflection at frontal electrode sites (N510) showed

higher negative amplitude values for the target condition. Furthermore, target trials showed higher negative amplitude values than non-target trials between 400 and 700 ms at frontal electrode sites, more pronounced over the right compared with the left hemisphere.

ERPs for target and non-target conditions and for the difference wave of target minus non-target trials are depicted in Appendix R.

Difference waves for target trials minus non-target trials were also computed separately for each trial position. When comparing these three difference waves, it is obvious that the difference wave obtained from stimuli presented at trial position A showed the highest amplitude values. This was the case for most of the previously described differences, whereas the difference wave from trial position C showed less pronounced amplitudes, indicating smaller differences between target and non-target trials at trial position C. Difference waves separately for all three trial positions are shown in Appendix S.

The present paragraph contains a qualitative description of differences between ERPs derived at different trial positions (A, B, and C). This description is based on a visual inspection of separate ERPs for all six conditions (targets and non-targets at each trial position).

At electrode positions PO8 and PO7, the P111 component showed smallest amplitude values at trial position A, for target and for non-target trials. The most prominent difference between trial positions was identified for the N170 component. For target trials as well as for non-target trials, the N170 amplitude at electrode sites PO7 and PO8 was smallest at trial position A (mainly at PO8) and largest at trial position C (mainly at PO7). A detailed examination of these position effects would be far beyond the scope of the present work. Therefore, separate ERPs for all probe conditions are illustrated for further visual orientation in Appendix T.

3.3.4 Source analysis – Integration of fMRI and EEG data

3.3.4.1 Location of the calculated regional sources

For the SA, activation peaks derived from fMRI (contrasts: *T vs. fix*; *N vs. fix*) were transferred to RSs as described in the SA Methods section (beginning on page 54). The resulting RSs were located bilaterally in inferior frontal gyri (IFG), in left middle frontal gyrus (MFG), superior frontal gyrus (SFG, including medial frontal parts), anterior cingulate cortex (ACC), left precuneus, right parahippocampal gyrus, left fusiform gyrus, left inferior occipital gyrus (IOG), right middle occipital gyrus (MOG), left insula and right lentiform nucleus (putamen). Corresponding coordinates are listed in Table 9 on page 65 and source locations are shown in Figure 16 on page 71.

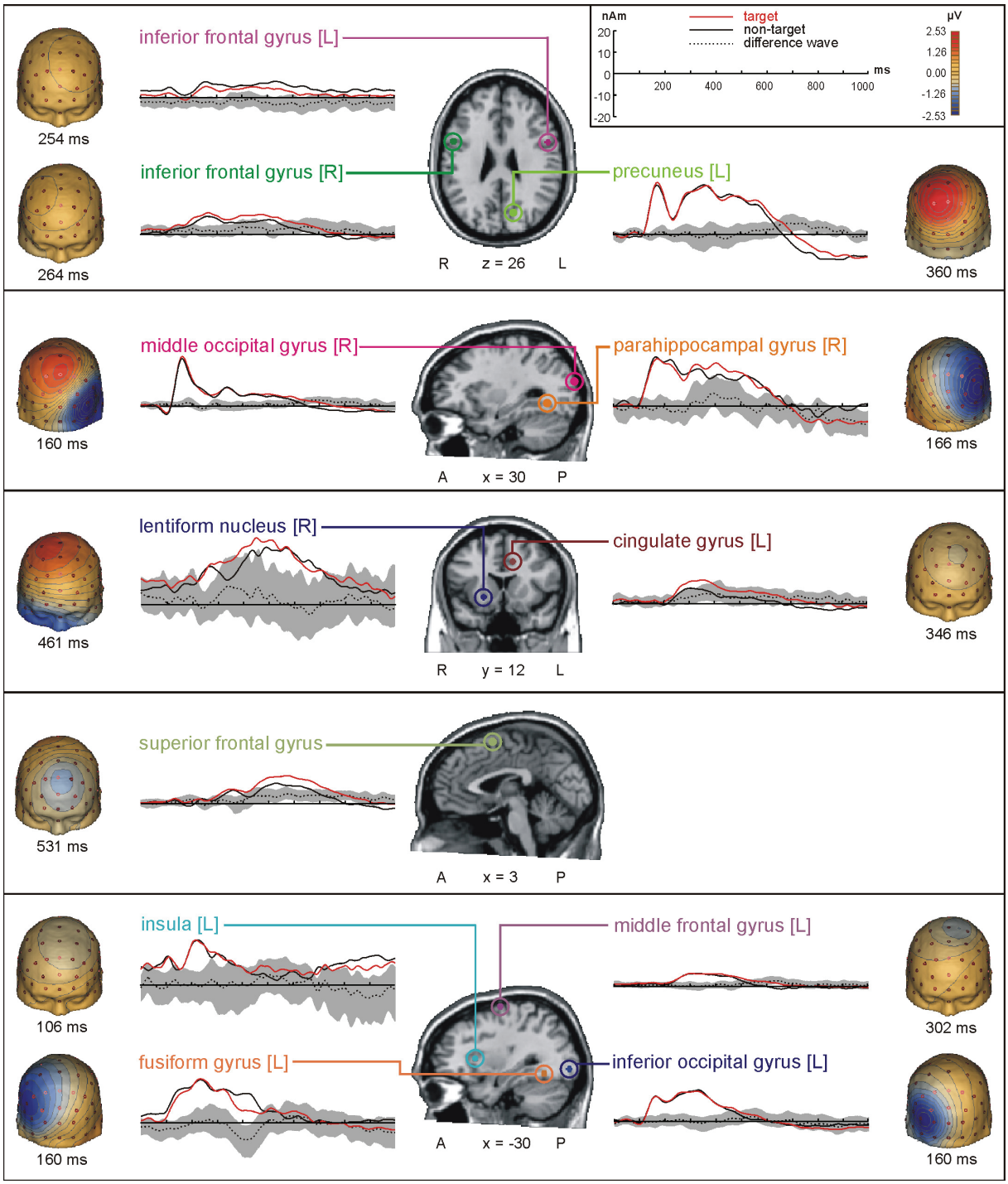

Figure 16: Middle: Positions of all regional sources projected onto the Talairach-transformed MNI brain. For each regional source, the corresponding source waveform time course of the first dipole component is shown for the probe presentation epoch (0-999 ms). Source waveforms of the target condition are colored in red and source waveforms of the non-target condition in black. The dotted line shows the difference source wave (targets minus non-targets) and the area shaded in gray represents the 95%-confidence interval computed with the bootstrap BCa method. On both sides, topographical scalp voltage maps are shown separately for the source activity of each regional source at a time point when the corresponding regional source shows peaking source activities. Abbreviations: A = anterior; P = posterior; R = right hemisphere; L = left hemisphere.

3.3.4.2 Chronological sequence of regional source activities

In the following, the chronological sequence of grand average source activities is described. These grand average source activities are derived from the source model applied to the grand average ERP where all conditions are combined, regardless of probe type and trial position. These source waveforms reflect the activity of the first dipole component, which was oriented at the maximum amplitude of source activity over the whole examined time interval. Therefore, source waveforms are described with regard to their peak amplitudes and to the shape of the waveform and not with regard to their polarity. Source waveforms are shown in Figure 16 on page 71 separately for the target condition and for the non-target condition.

The RSs in right MOG and left IOG showed transient responses peaking at 160 ms post-stimulus and contributing to the P111 and also to the N170 component of the scalp ERP. A second deflection of the MOG RS was rather transient with a peak at 336 ms whereas the second deflection of the IOG RS showed a broader and more pronounced response peaking at 325 ms. Both second components showed a contribution to the positive deflection over parietal electrode positions at the scalp (P3b). The RS in left precuneus initially showed a comparable pattern with a narrow source activity peaking at 170 ms and contributing to the concurrent positive deflection at parietal midline electrodes and second a broad a sustained component peaking at 360 ms and contributing to the first peak of the P3b component. RSs in right parahippocampal and left fusiform gyri showed an earlier onset of source activity than all other posterior RSs, and both showed a small contribution to the P111 scalp response. The source activity of the parahippocampal RS showed a positive deflection with two peaks at 166 and 217 ms contributing to the N170 scalp potential. The source activity then changed into a more transient deflection comparable to the precuneus response but with a maximum at 326 ms and a contribution to the P3b scalp potential. Source activity of the RS in fusiform gyrus showed a first peak at 160 ms and a second larger peak at 233 ms, both contributing to the N170 deflection at the scalp. Source activity in SFG showed a small peak at 133 ms, which contributed to the concurrent negative deflection at fronto-central scalp electrodes. Further SFG source activity peaked at 234 ms and another deflection peaking at 360 ms contributed to the negative deflection at fronto-central electrodes (N303). A broad and sustained response of the source activity derived from the SFG RS peaked at 531 ms and contributed to the negative deflection at frontal midline electrodes (N510).

Source activity of the lentiform nucleus RS showed a small sustained response peaking at 274 ms, followed by a broad and sustained activity between 350 and 800 ms contributing to the

positive deflection at central scalp electrodes (second P3b peak). The source activity of the RS located in left IFG showed a broad sustained deflection with a peak at 254 ms, which had a small contribution to a negative deflection at lateral frontal scalp electrodes over the left hemisphere. The corresponding IFG RS in the right hemisphere showed a comparable pattern of source activity with an amplitude maximum at 264 ms and with almost no contribution to the scalp signal.

The RS in left insula showed a transient source activity deflection peaking at 106 ms and contributing to the concurrent negative deflection at fronto-central scalp electrodes. This deflection was followed by a second source waveform response peaking at 217 ms with almost no contribution to the scalp signal. The source waveform of the RS in left MFG showed a sustained activation between 200 and 600 ms reaching its maximum at 302 ms and contributing to the negative scalp potential over frontal brain regions (N303). Source activity in ACC gyrus showed also a sustained response with an amplitude maximum at 346 ms and contributed to the negative deflection at fronto-central scalp electrodes (N303).

3.3.4.3 Differences between source activities for targets and non-targets

The BCa bootstrap approach applied to the pooled difference source wave (source waveform of the target condition minus source waveform of the non-target condition, each pooled over all trial positions) revealed differences for several RSs between source activities of the target condition and of the non-target condition (see Figure 16 and Table 11). The following description of differences is restricted to significant time epochs which persisted over more than 30 ms.

The RS in right MOG showed source activity differences between 582 and 756 ms post-stimulus and the RS in left precuneus between 650 and 773 ms and between 797 and 846 ms, both with higher source activities in the target condition because the activity of the target condition decreased more slowly than the activity of the non-target condition. For the left fusiform gyrus RS, source activity showed higher amplitude values for non-target trials and an earlier decrease of activation in the target condition, leading to probe type differences between 382 and 436 ms. Source activity of the SFG RS was more pronounced for the target condition, leading to differences in a time window ranging from 451 to 875 ms. Left IFG RS showed higher source activities for the non-target condition between 37 and 68 ms, between 287 and 326 ms and also between 904 and 980 ms. For the RS in right IFG, the activity of the target condition showed higher amplitude values and decreased more slowly than the activity of the non-target condition. These source activity patterns produced probe type differences

between 617 and 710 ms. Probe type differences in source activity for the left MFG RS were significant between 539 and 676 ms because the activation of the target condition persisted for a longer time than the activation of the non-target condition. For the ACC RS, significant source activity differences between 313 and 441 ms were generated by a higher peak amplitude of the source waveform derived from the target condition.

Table 11: Left column: Time epochs (in ms, for probe presentation: 0-999 ms) where the bootstrap 95%-confidence interval for the pooled difference source wave (source waveform of the target condition minus source waveform of the non-target condition, each pooled over all trial positions) did not include zero. Significant epochs for the difference source waves separately at each trial position are listed in the three columns on the right side. Time epochs lasting less than 30 ms are put in parentheses. Epochs in boldface indicate time epochs where source activities were higher for the non-target condition compared with the target condition. In all other cases, target source activities were higher than non-target source activities.

Regional sources	**Grand average difference wave**	**Trial positions A**	**B**	**C**
right middle occipital gyrus	582-756 (804-820)	(537-563) 568-770 787-834	(697-719)	**(240-256)**
left inferior occipital gyrus				**(0-18)**
left precuneus	(68-94) 650-773 797-846 (895-908)	**(25-41)**		39-70 150-197 (824-852)
right parahippocampal gyrus				**926-999**
left fusiform gyrus	**382-436**			**(412-440)**
superior frontal gyrus	(185-207) 451-875	(559-586) 632-717 777-826	0-39 406-607 664-701	
left inferior frontal gyrus	**(0-15)** **37-68** **(109-127)** **(232-244)** **287-326** **(617-644)** **904-980**		**27-123** **260-332** **(508-537)**	
right inferior frontal gyrus	(197-208) (386-400) 617-710 (795-822)	684-721	(641-660)	(190-205) 445-482 590-650 (791-816)
left middle frontal gyrus	539-676	637-852	606-684	
cingulate gyrus	(255-273) 313-441 (585-601) (658-671) (701-730) (841-855)		(256-276) (295-313)	

3.3.4.4 Differences between source activities at different trial positions

Bootstrap 95%-confidence intervals were also computed separately for the difference waves at trial positions A, B and C (see Appendix U, Appendix V, Appendix W, respectively). The corresponding time windows showing significant differences between targets and non-targets at each trial position are listed in the three rightmost columns of Table 11 on page 74. In the current paragraph, differences between source activities of target and non-target trials based on the pooled difference wave (as described previously, see page 73, and see also the leftmost column showing significant time windows of Table 11 on page 74), are compared qualitatively to differences found when examining the confidence intervals separately at each trial position.

For the right MOG RS, the difference between targets and non-targets seen in the pooled difference wave (582-756 ms) seemed to be dominated by a difference at trial position A, but there was also a temporary difference between 697 and 719 ms at trial position B (< 30 ms duration). The difference for pooled data in left precuneus from 650 to 773 might be explained by differences at trial position A whereas the difference between 797 and 846 ms seemed to be dominated by trial position C, because trial position C showed differences between 824 and 852 ms (<30 ms duration). Higher activities in the pooled data for the non-target condition in left fusiform gyrus (382-436 ms) might be explained by differences at trial position C (< 30 ms duration).

For pooled data, SFG showed persisting higher activities in the target condition (451-875 ms) and this difference between probe types was also present at trial positions A and B.

Differences for pooled data in left IFG with a higher source activity for non-target compared to target trials (37-68 ms, 287-326 ms, 904-980 ms) were presumably dominated by the differences at trial position B (27-123 ms, 260-332 ms). The higher source activity for target trials in right IFG found in pooled data (617-710 ms) was reflected in differences at all trial positions. The difference in pooled data for left MFG might be explained by higher source activity for the target condition at trial positions A and B.

3.4 Discussion

In the beginning of the discussion section, results obtained with different methods (behavioral data, fMRI data, EEG data, SA data) are discussed separately. In the Preliminary Conclusions section, findings from all methods are integrated and discussed with regard to each other.

3.4.1 Behavioral data

Behavioral data revealed a comparable pattern for RTs and error rates: Performance decreased with increasing trial position for non-target trials whereas for target trials performance was lowest at trial position B.

For non-target trials, there were significant differences between all trial positions for RTs and error rates of the EEG session, whereas for the fMRI session error rates were solely higher at trial position C compared with positions A and B. This outcome indicates increasing task demands with increasing retention duration for non-target probes. For target trials, RTs at position B were higher than RTs at position C for both measurement sessions and also compared with position A in the EEG session.

There are several potential influencing factors, which might account together for this RT data pattern of the target condition (position B > A and C). On the one hand, it is important to note that, with the present design, the probability of target presentation increased with increasing trial position (from 25 to 33.3 and to 50 percent), whereas the probability of non-target presentation decreased with increasing trial position (accordingly: 75, 66.3, 50 percent). Therefore, at trial position C target and non-target probes were equally probable whereas at position B non-targets were more probable than target trials. It is a frequent finding that RTs to events with a higher probability are shorter than RTs to events with lower probabilities (Braver, Barch, Gray, Molfese, & Snyder, 2001; Gordon, 1967). Based on the assumption of a linear influence of stimulus frequency on RTs, this influence alone would have caused highest RTs to targets at position A and lowest RTs at position C. On the other hand, increasing the cognitive load, the task difficulty or both with increasing retention duration would have led to higher RTs with increasing trial position as seen for non-target trials especially in the EEG session, because RTs are thought to provide a measure of cognitive load (see Braver et al., 1997). Another influence might have been induced by the distracting previous probe stimulus in the same trial (at trial position A) on the processing of probes at trial position B. At position A, a non-target probe was presented, producing a distracting stimulation and leading

to the requirement to maintain the target stimulus further on in spite of this distraction. To respond properly to the target stimulus at trial position B, a response alternation was necessary with respect to the previous non-target probe at trial position A. Indeed, the same situation requiring response alternation with respect to the previous stimulus was also present at trial position C. However, the distracting effect of non-target probes might have been highest for the target stimulus which followed the first distractor (target at trial position B) and diminish after the second distractor (target at trial position C), when it had already been possible to maintain the target representation in WM in spite of the first distracting stimulus (non-target at position A). Thus, the distraction might have contributed to the finding of higher RTs at trial position B compared with positions A and C. Alternatively, if stimulus frequency would not show a linear influence on RTs (varying with the proportion of both stimulus categories), but rather a distinction between present or absent differences in stimulus frequency, RTs of the EEG session could be explained by this effect together with the effect of increasing demand with rising trial position (an interpretation of RTs measured during the fMRI session is given in the following).

To sum up, processing demands for non-target trials seemed to increase with increasing trial position, whereas target processing might have been influenced by effects of stimulus frequency, cognitive load or task difficulty and distraction.

In some studies, higher RTs for the fMRI session are clearly visible in the RT illustrations, but most of them do not discuss these findings (e.g., Natale, Marzi, Girelli, Pavone, & Pollmann, 2006; Swainson et al., 2003). In the present study, the longer fixation period in the fMRI session together with tiresome surrounding conditions (monotonous noise, horizontal position) might have led to a tiredness causing higher RTs in the fMRI session. Indeed, in the present study, differences between RTs for both measurement sessions were especially pronounced for all non-target conditions (53-95 ms difference between RTs obtained in the EEG and in the fMRI sessions). After the fMRI session, some participants stated they had the impression that they had to press the right response button (assigned to the non-target condition) tighter than the left response button. This might be caused by mechanical wear of the left mouse button because it had been used more frequently in former fMRI experiments. Therefore, RTs of the fMRI session should be interpreted with caution. Indeed, it is interesting to note that RTs of the fMRI session would parallel the observed RT pattern of the EEG session if about 50 ms would be subtracted from the RTs of all non-target conditions of the fMRI session.

Other studies also reported – as observed in the present EEG session at trial positions A and B – higher RTs when responding to target trials compared to non-target trials (Guo et al., 2008; Leung, Gore, & Goldman-Rakic, 2005).

Altogether, the direct comparisons of target and non-target trials at different trial positions yielded decreased performance for target trials at trial positions A and B and no differences between both probe types at trial position C (for error rates of both measurement sessions and for RTs of the EEG session).

If behavioral or electrophysiological correlates had shown opposite tendencies for targets in comparison to non-targets in the present study, an interpretation in terms of a linear effect of stimulus frequency would be appropriate. Nevertheless, even if there are no clearly opposing effects for target and non-target trials, an influence of stimulus probability cannot be ruled out. An influence of stimulus frequency might account for the finding that differences between target and non-target trials are reduced at trial position C where the occurrence of both probe types was equally probable.

Subjective evaluation of task difficulty confirmed comparable subjective task difficulty in both measurement sessions and also a comparable strategy use. These results validated the present selection of complex shapes and their randomized assignment to the measurement sessions. This is an important finding because different shapes were used in both sessions and they were not counterbalanced across measurement sessions.

3.4.2 FMRI data

3.4.2.1 Brain regions involved in target processing compared to non-target processing

FMRI data revealed consistent activation patterns for the comparison of target and non-target trials at position A and B (see page 63). All regions, which were active at trial position A (medial frontal gyrus, right IFG, sub-lobar (claustrum / insula), bilateral lingual gyri, midbrain) also showed activation at trial position B. Additional brain regions were exclusively activated at trial position B (right MFG, right IFG, lentiform nucleus, precentral gyrus, sub-gyral clusters in temporal, parietal and occipital lobe). In contrast, even with a more liberal threshold, no cluster comprising more than six contiguous voxels was found for the target versus non-target comparison at trial position C. At trial position C, target and non-target trials had the same frequency of occurrence. When considering this fact, one might

come to the conclusion that differences between probe types at trial positions A and B might result primarily from the circumstance that non-target stimuli were presented more frequently. However, more widespread activation patterns were found at trial position B where the ratio between target and non-target trials (33.3 percent to 66.6 percent) was more similar than the ratio at trial position B (targets: 25 percent; non-targets: 75 percent).

Nevertheless, the outcome that no supra-threshold clusters were found at trial position C is in line with the results of Leung and colleagues (2005), who did not find any activated clusters when contrasting targets and non-targets. Indeed, they used delay durations of 18 seconds, whereas other studies examining probe-related differences in WM mainly used shorter delay periods (Druzgal & D'Esposito, 2001: 8 s; Jiang et al., 2000: 4-20 s). This finding might indicate that processing mechanisms for target and non-target probes might differ either more consistently or to a greater extent when retrieval occurs early in the trial, whereas processing differences seem to diminish or become more inconsistent, when the decision about the WM status occurs late in the trial. To test this assumption, further studies are required where comparisons between target and non-target probe presentation after different delay durations are examined using a constant ratio of stimulus frequency between probe types.

Some regions which showed activation for the *T vs. N* contrasts (at positions A and/or B), were also reported to show activation in comparable contrasts of other WM studies. For example, activations in the right IFG are in line with the finding of inferior frontal activations by Jiang and colleagues (2000). Left precentral gyrus was activated in the present probe type contrast at position B and Druzgal and D'Esposito (2001) also reported activation in left precentral gyrus for target compared with non-target trials.

3.4.2.2 Probe processing independent of trial position and probe type

Target retrieval, contrasted with the fixation period and combined over all trial positions (conjunction null, *T vs. fix*, see page 65), was assumed to reveal brain areas generally associated with target recognition. Peak activations were obtained in left IFG, left SFG, bilateral MFG and precentral gyri, left insula, left lingual gyrus and cerebellum. In order to detect brain areas which reflect the processing of correct rejections, non-target trials were contrasted with the fixation period (and combined over all trial positions, conjunction null, *N vs. fix*, see page 65). Peak activations were located in right superior and medial frontal gyri, anterior and posterior cingulate gyri, right fusiform gyrus, bilateral MOG, right lentiform nucleus and in the midbrain. The coordinates of these peak activations obtained with both conjunctions were used to compute the positions of 12 RSs. These contrasts were chosen for

the computation of the RS positions because brain areas involved in target recognition, as well as in the correct rejection of non-targets, were needed. Both were required to build a general SA model, which could be reasonably applied to both probe conditions.

The positions of the obtained activated clusters are well in line with the locations of activations reported in other WM studies when contrasting the retrieval epoch (regardless of probe type) against a low-level baseline (Bledowski et al., 2006; Cabeza et al., 2002; Ranganath et al., 2003). This outcome assures that reasonable activation foci were used for the computation of RS locations in the present study.

3.4.2.3 Comparing peak activations from the target versus non-target contrasts with the regional source positions

In the following, peak activations from the *T vs. N* contrasts at trial positions A and B (see page 63) are compared with the location of the RSs, which had been obtained with the contrasts *T vs. fix* and *N vs. fix* (see page 65). It is important to note that these qualitative comparisons rely on comparisons of the Talairach coordinates of the *T vs. N* activations with the original target and non-target peak activations (versus fixation) and also with the resulting averaged RS locations. This approach is applied because some RS coordinates (e.g., the right lentiform nucleus RS) were obtained by an averaging procedure and therefore integrated several peak activations (correspondingly: lentiform nucleus, insula, sub-lobar; see Table 9, page 65). For example, when comparing these insula peak coordinates (32, 23, 1) with the IFG activations from the *T vs. N* contrast (position A: 34, 25, -3; position B: 32, 27, -3; see Table 8, page 63), it is apparent that they have similar locations (distance between the insula peak and the „*T vs. N* peaks": at position A = 0.49 cm; at position B = 0.57 cm). The distance between the „*T vs. N* peaks" and the averaged lentiform nucleus RS location was 1.91 cm (position A) and 1.94 cm (position B). With regard to the limited spatial resolution of the SA approach, it can be assumed that source activities from the lentiform nucleus RS additionally cover activation originating in these inferior frontal regions. Therefore, it is interesting to explore, for which RSs corresponding activation clusters are present in the *T vs. N* contrast.

For three RS locations, no corresponding comparable activation clusters in the *T vs. N* contrasts at trial positions A or B were found: For the RS in left precuneus, the RS in left fusiform gyrus and for the right parahippocampal gyrus RS.

Nearby Talairach coordinates of three other RSs, activation clusters for the *T vs. N* contrast were found solely at trial position B: Right IFG RS corresponded to a cluster with a right IFG

peak activation (*T vs. N*), left IFG RS corresponded to a cluster with a left precentral peak and left MFG RS corresponded to another cluster showing a left precentral peak activation.

For the remaining RSs (right lentiform nucleus, ACC, SFG, left IOG, right MOG and left insula), corresponding activations in the *T vs. N* contrast were found at both trial positions (A and B). The lentiform nucleus RS and their corresponding activations from the *T vs. N* contrasts were already described as an example at the beginning of this paragraph.

The medial frontal clusters (from the *T vs. N* contrast at positions A and B) were surrounded by two RS clusters: The ACC RS was located more anterior and inferior and the SFG RS was located more superior than the medial frontal activations. However, there was a shorter distance between the SFG RS and the medial frontal clusters, compared with the distance between the medial frontal clusters and the ACC RS. The peak coordinates of the medial frontal clusters were located in the RCZp (according to Picard & Strick, 1996), whereas the SFG RS (averaged coordinates) was located in pre-SMA, although two of the three peak activations, which were used to compute the SFG RS, were also located in the RCZp. The ACC RS was located at the inferior border of the RCZp. Interpretations of the RCZp activations are given in the General Discussion section (beginning on page 98), because this region was also activated in the morphing task.

Left IOG RS (and especially its target peak in lingual gyrus) corresponded to clusters with peak activations in lingual gyrus in the *T vs. N* contrast at both trial positions. The RS in right MOG corresponded roughly to the right-hemispheric lingual gyrus clusters (*T vs. N*, at positions A and B).

The location of the RS in left insular cortex was corresponding to the location of sub-lobar clusters from the *T vs. N* contrasts (position A: claustrum at a range of 3mm; position B: insula at a range of 3mm).

Altogether, there were 12 RS locations of which only three did not show a corresponding activation in the contrast of target trials versus non-target trials. This finding might indicate that the majority of brain regions involved in probe processing per se also shows a differential contribution related to the processing of different probe types, with a specific engagement in the processing of target probes.

3.4.3 EEG data

The succession of ERP deflections is well in line with the findings of another study examining WM retrieval (Bledowski et al., 2006), with the difference that the N303 in the

present study is described as P308 by Bledowski and colleagues. This discrepancy in polarity can be attributed to the use of an additional frontal reference electrode „FCz“ in their study whereas average-reference was used in the current study.

3.4.3.1 P3b mean amplitudes

The P3b component showed two distinct peaks at 367 ms (Pz) and 520 ms (CPz) post-stimulus. The temporal occurrence, especially of the first P3b peak, corroborates well with P3b peak latencies reported by Bledowski and colleagues (2006; P366, P585).

In the present study, P3b mean amplitudes showed higher values for target trials compared with non-target trials at electrode position Cz at trial positions A and C (with a trend at position B) and at electrode position Pz at trial position A.

This finding can be linked to effects found in LTM tasks, because is in line with the parietal old/new effect, showing higher P3b amplitudes in response to target stimuli compared with non-target stimuli (Friedman & Johnson, 2000; Gomarus et al., 2006; Rugg & Curran, 2007). In agreement with findings from long-term recognition experiments (Friedman & Johnson, 2000; Rugg & Curran, 2007), a visual inspection indicated that this effect was more pronounced over the left hemisphere (see Appendix R), The fact that the parietal old/new effect at electrode position Pz was solely significant at trial position A, may indicate an influence of stimulus probability on P3b mean amplitudes Pz, because differences in stimulus frequency between target and non-target trials were highest at trial position A (targets: 25 percent, non-targets: 75 percent). Generally, for P3b amplitude and stimulus probability, an inverse relation is observed, with higher amplitude values for infrequent trials (Banquet, Renault, & Lesèvre, 1981; Donchin & Coles, 1988; Sutton et al., 1965). This effect might have induced higher mean amplitudes in the infrequent target condition and lower amplitudes in the frequent non-target condition.

When using completely new stimuli in a WM task, Guo and colleagues (2008) found more pronounced differences in P3b activation between target and non-target stimuli, compared to the differences between targets and non-targets when familiar stimuli were used. In the present study, a limited number of shapes was used and therefore, at the beginning of the experiment all stimuli were new and became more and more familiar throughout the course of the experiment. Thus, the differences between target and non-target probes might have been more pronounced if only new shapes had been used. In the present study, a limited set of shapes was used intentionally to accentuate WM processing mechanisms. By the use of constantly recurring stimuli as targets and non-targets, participants could not rely on

familiarity judgments (familiar / unfamiliar) in their decision whether the presented stimulus was the current target or a non-target stimulus.

The Electrode x Trial Position interaction yielded higher P3b mean amplitudes at trial position C compared with position B at electrode Cz, independent of probe type. Since P3b amplitudes are reported to decrease with increasing WM load (Gevins et al., 1996; Kotchoubey et al., 1996; Looren de Jong et al., 1988; McEvoy et al., 1998; Mecklinger et al., 1992; Wijers et al., 1989), this might be an indicator for higher cognitive demands at trial position B, as also expressed in higher RTs at trial position B. This outcome might be caused – as already discussed for RTs – by a distracting effect of the first non-target probe stimulus.

Indeed, RTs were solely higher at trial position B for target trials whereas P3b mean amplitudes showed higher values for both probe types at trial position B. For several reasons, an unambiguous explanation of P3b mean amplitude effects is not possible with the present design: The influences of cognitive load, probe type and stimulus probability might interact with each other and additionally, the present design evoked two P3b peaks (labeled P367 and P520 according to their occurrence in the grand average), which might have been differentially influenced by the afore-mentioned influencing factors.

3.4.3.2 ERP differences between target and non-target trials

The qualitative description of further differences between ERPs of target and of non-target trials (see page 69) revealed a negative deflection over fronto-central brain regions around 300 ms for non-target trials (N303) whereas target trials showed values near zero. This effect may be linked to the early frontal old/new effect (FN400 according to Curran, 2000; Paller, Voss, & Boehm, 2007), which is usually found around 400 ms post-stimulus in LTM tasks. This effect is characterized as a negative deflection between 300 and 500 ms with higher amplitude values for new than old items (Curran, 2000; Friedman & Johnson, 2000; Mecklinger, 2000; Rugg & Curran, 2007).

Indeed, the present negative deflection (N303) and also the probe type-related effect visible in the difference wave (targets minus non-targets, see Appendix S) occurred earlier than the typically reported FN400 effect.

Generally, the difference wave for target versus non-target trials showed most pronounced deflections at trial position A and least pronounced differences between both probe types at trial position C, indicating that differences between processing mechanisms for both probe types seemed to decrease with increasing trial position or when stimulus frequency for both probe types became more similar.

This finding will be discussed together with similar findings from other measurement techniques in the preliminary conclusions section (see page 91).

3.4.4 Source analysis

3.4.4.1 Sequence of regional source activities

Source analysis revealed early activities in right MOG, left IOG, left fusiform and right parahippocampal gyrus. All four RSs showed a contribution to the positive deflection at the scalp peaking at 111 ms in the grand average (generally referred to as P1 component) and to the negative deflection at the scalp peaking at 170 ms in the grand average (generally referred to as N1 component). The former two RSs showed a more pronounced contribution to the P1 deflection and the latter two RSs especially to the N1 scalp potential. Both IFG sources showed less pronounced sustained activities with almost no contribution to the signal at the scalp. Left precuneus contributed mainly to the scalp P3b component, right MOG also showed a small contribution to the P3b deflection and lentiform nucleus also contributed with a sustained activation to the more central P3b component. ACC, SFG and left MFG RSs contributed to the concurrent negative deflection at the scalp (N303) and the SFG RS also showed a contribution to the later negative deflection at frontal electrodes (N510).

Since source potentials do not depend on the reference electrode (Michel et al., 2004; Scherg & Von Cramon, 1986), the present data can be compared directly with the SA data by Bledowski and colleagues for the retrieval epoch of a WM task (2006). They reported early transient activities located in bilateral inferior temporal cortices which contributed to the N1 component. In the present study, right MOG, left IOG, right parahippocampal and left fusiform gyri contributed to the N1 component (N170 in the grand average), in line with studies reporting N1 generators in ventral occipito-temporal regions as well as in dorsal extrastriate cortex (Clark, Fan, & Hillyard, 1995; Di Russo, Martinez, Sereno, Pitzalis, & Hillyard, 2002; Martinez et al., 2006). The N1 component is thought to reflect discrimination processes between different stimuli (Hopf, Vogel, Woodman, Heinze, & Luck, 2002; Ritter, Simson, Vaughan, & Macht, 1982; Ritter, Simson, & Vaughan, 1988; Vogel & Luck, 2000) and is suggested to be composed of different sub-components depending on the position of the stimulus in the visual field (Clark et al., 1995).

In the study of Bledowski and colleagues (2006), their inferior temporal RS showed source activities in both dipoles, the first dipole showed a transient deflection contributing to the N1

scalp component, whereas their second dipole showed a more sustained activity pattern contributing to the P3b scalp deflection. The left IOG RS of the present study showed a combined pattern with an initially transient activation contributing to the scalp N1 response and a subsequent sustained activation with a small contribution to the P3b scalp component. In the present study, the left IOG RS was located more medial, posterior and a bit more superior than the inferior temporal RS reported by Bledowski and colleagues. Here, it is important to note that SA does not provide a spatial resolution in the order of millimeters and therefore a comparison of RSs across studies with slightly differing RS coordinates is possible.

The present source activity in precuneus showed a similar pattern as the source activity of the posterior parietal RS in the study by Bledowski and colleagues, with an initial transient peak followed by a broad and sustained response contributing to the P3b component. The sustained activity patterns of the present right parahippocampal and left fusiform source activities were comparable with the sustained responses of the second inferior temporal dipoles found in the Bledowski study, even if their RSs were located more lateral and posterior than the RSs of the present study.

In the present study, RSs in SFG, left MFG and bilateral IFG showed less pronounced responses, in agreement with the response patterns of medial frontal, left motor cortex and left precentral RSs of Bledowski and colleagues. The right lentiform nucleus RS showed a broad sustained activity contributing to the P3b deflection and was located more medial and notably more inferior than the right VLPFC RS of Bledowski and colleagues, which also showed a P3b contribution.

The present findings support the assumption that the P3b potential does not reflect a unitary component but integrates activities from posterior (precuneus RS) as well as frontal (lentiform nucleus RS) brain regions (see Bledowski et al., 2006).

Reinvang and colleagues (1998) analyzed data of a perceptual memory task using a SA approach with four sources (analysis time window: 200-600ms post-stimulus) and found early peaking occipital source activities (at 340 ms). This is in line with the present finding of activation peaks at 336 and 325 ms after probe-onset in occipital source waveforms (right MOG and left IOG RSs).

3.4.4.2 Differences in source activity between probe types

Differences between source activities for target and non-target trials (see Table 11 on page 74) were found mainly in late time windows (>500 ms post-stimulus) and can be subdivided

into three patterns: Firstly, some RSs (right MOG, left precuneus, right IFG, left middle fontal gyrus) showed an earlier and faster decrease of activity in the non-target condition compared with the target condition. This pattern was visible around response execution and the respective RSs showed no contributions to the scalp ERP response during these time epochs. This finding might be explained by the fact that RTs for non-target trials were shorter than for target trials (at trial positions A and B), potentially causing an earlier decrease of activation after response execution for the non-target condition.

Secondly, two other RSs (left IFG, left fusiform gyrus) showed higher non-target activities compared with target activities. Left IFG RS showed a generally less pronounced response pattern and higher amplitude values for the non-target condition over the whole analysis interval. Significant time epochs from the bootstrap procedure were distributed over the whole trial, indicating that the difference between probe types was rather unspecific and presumably simply caused by a baseline-shift of the consistently higher non-target activity. Left fusiform gyrus RS, whose position had been obtained with the *N vs. fix* contrast, showed higher source activity amplitudes in the non-target condition around 400 ms. Earlier activation in fusiform gyrus, with contributions to the P1 and N1 scalp responses, yielded no differences between probe types. In the fMRI contrast of *T vs. N* trials, there was no corresponding activation in left fusiform gyrus. These observations support the suggestion that left fusiform gyrus might be particularly engaged in non-target probe processing. This interpretation is described in more detail in the preliminary conclusions section (beginning on page 93).

Thirdly, ACC and SFG RSs showed higher source waveform amplitudes in the target condition, compared with the non-target condition. The ACC RS exhibited a significant bootstrap epoch between 313 and 441 ms post-stimulus. A visible increase in source activity amplitude for the target condition compared with the non-target condition started at about 250 ms post-stimulus (see Figure 16). During this time, the ACC RS contributed to the negative deflection at the scalp (N303) and showed a rather positive voltage distribution at fronto-central scalp electrodes for the target condition (or values near zero) and a negative fronto-central voltage scalp distribution for the non-target condition (see Appendix X). Thus, the qualitatively described differences in N303 amplitude in the ERP data might be mainly determined by the ACC RS causing relatively higher positive amplitudes in the target condition and higher negative amplitude values for the non-target condition. Furthermore, it is noticeable that the position of the ACC RS (Talairach coordinates x, y, z: -10, 15, 32) was obtained with the *N vs. fix* contrast (conjunction over all trial positions), whereas the bootstrap procedure showed higher source activity amplitudes for the target condition in this region. To

further examine this prima facie discrepancy, the *T vs. fix* contrast was computed with a lowered threshold (uncorrected, p<.001). This threshold adjustment resulted in an activated medial frontal cluster with a sub-peak (-10, 13, 34) located nearby the ACC RS, demonstrating that this region also participated in target probe processing. This activation probably had failed to reach significance with the FDR-corrected threshold for target trials, because the conjunction statistic was computed over all three single contrasts (targets at trial position A vs. fixation; targets at position B vs. fixation; targets at position C vs. fixation), thus requiring that the resulting clusters showed significant activation in each of all three single contrasts. Indeed, when the contrast „targets at trial position B versus fixation" was computed separately (FDR-corrected, p <.05), no sub-peak was located nearby the ACC RS coordinate and this outcome probably caused the absence of supra-threshold activation in this region in the conjunction contrast with FDR correction.

Another RS showing higher target source activity amplitudes was located in the SFG and showed the longest significant bootstrap epoch of all RSs (451-875 ms). During this time window, the SFG RS contributed to the negative scalp deflection over fronto-central electrode positions, which showed higher amplitudes in the target compared with the non-target condition (N510, see Appendix T). This indicates a particular engagement of superior frontal brain regions in the processing of target probes compared with non-target probe processing. The Talairach coordinates of the SFG RS had been obtained from one great cluster from the *T vs. fix* contrast and from two smaller clusters from the *N vs. fix* contrast (see Table 9 on page 65). Furthermore, for the *T vs. N* contrasts, medial frontal activations were present at trial positions A and B. These activations were located a bit more inferior compared with the location of the SFG RS. However, the peak of the target condition (*T vs. fix*; -4, 8, 49), which was used for the calculation of the SFG RS coordinate, was comparable with the sub-peaks of the *T vs. N* contrasts at trial positions A and B (both -4, 10, 46). This finding is consistent with the fact that significant differences with the bootstrap approach were obtained at trial positions A and B and these results emphasize a specific contribution of this region to target processing mechanisms, especially at early positions in the trial or especially when the infrequent condition acted as target. Interpretations of ACC- and SFG activation patterns are given in the preliminary conclusions section (beginning on page 93).

Reinvang and colleagues (1998) successfully applied their SA model with four sources to the presentation of test stimuli which occurred either one or ten seconds after the first stimulus. This finding indicates that the same SA model can be applied successfully to different task

conditions, e.g., to WM-related task conditions and to task conditions without WM demands. In the SA of the present task, the explained variances computed separately for both probe type conditions (see SA Methods section, beginning on page 54), supported the assumption that the current model was adequate for the target condition as well as for the non-target condition.

3.4.5 Critical reflections

The present fMRI results demonstrate one important difficulty in the interpretation of fMRI data: The obtained activation clusters depend on the selected contrast and on the choice of the threshold applied to the data. Some regions, which were found active only for the *N vs. fix* contrast and not for the *T vs. fix* contrast (ACC and MOG) showed activation in the *T vs. N* contrast. This apparently counterintuitive outcome reflects the fact that different statistics were applied in both cases. Contrasting two conditions separately against the same baseline (e.g., *T vs. fix*; *N vs. fix*) does not permit the conclusion that anatomical regions, which only show activation in one of the two contrasts (e.g., *N vs. fix*), show higher activity in the corresponding (non-target) condition compared with the other (target) condition. In the contrast of *T vs. fix*, the effect size could have been smaller or the variability could have been larger, leading to absent supra-threshold voxels in the brain areas under consideration. The right way to examine differences between two conditions in fMRI is to perform a direct contrast between these two conditions, therefore only activation patterns from the *T vs. N* contrast can be interpreted as showing more consistent activation in the target condition compared with the non-target condition.

Linking study results which were obtained with different methodological approaches can shed light on cognitive processing mechanisms and lead to a more complete description of the examined cognitive processes than one technique alone.

As described above, ACC activation (present in the contrast of *N vs. fix*, and in the *T vs. N* contrast) seemed to indicate an ambiguous result. Bootstrap differences revealed higher ACC source activities for targets compared with non-targets early in the trial, indicating transient differences in probe type processing. When interpreting and linking the present data from different methods, it has to be considered that fMRI activation clusters are dependent on previously determined parameters like the computed contrast (e.g., “which cognitive processes occur in both contrasted conditions and are therefore cancelled out in the comparison?”) and the selected threshold. Results from SA depend on the applied model

(head model, number of sources, their location and orientation, see Luck, 2005a) and are sensitive to more transient processes, which may not be detected with fMRI.

In the present study, source sensitivity images showed that the RSs of the present study contributed to specific brain regions. Nevertheless, the amount of interdependence between different sources cannot be examined in detail with source sensitivity images. A technically more demanding but also more precise approach to measure the interaction between different sources would be the computation of the so-called "crosstalk" (see Bledowski et al., 2006), requiring the implementation of a model simulation.

The number and location of RSs has a great influence on an obtained SA solution (Luck, 2005b). With the selected approach, the user-dependence of the SA approach is minimized concerning the selection of the source locations (because RS positions were derived from fMRI clusters, Bledowski et al., 2007). Nevertheless, the researcher still has to determine which of the resulting RSs are finally included in the model. In the present thesis, sources in midbrain and cerebellum were excluded, whereas the RS located in right lentiform nucleus was included in the model. This decision was based on a personal communication with the BESA® support (K. Hoechstetter, April 02, 2008). Indeed, source activity in lentiform nucleus showed remarkably high amplitude values and a large variability was visible in the broad 95%-confidence interval computed with the bootstrap procedure. Therefore, the source waveforms of this RS should be interpreted cautiously.

The SA approach applied in the present study included an interpolation to a standard 81 electrode montage and a co-registration between the electrode montage and the Talairach-transformed MNI template. These steps provided the basis to a reasonable comparison between EEG and fMRI data, however, at the expense of inter-individual differences in the data. The digitized electrode positions obtained for each participant could not be included with this approach. Nevertheless, the activated clusters derived from fMRI also originated from group statistics. It should just be considered that the reported data are based on group statistics and the applied methodological procedures minimize individual variability.

Furthermore, there are generally known potential mismatches between activity found with fMRI and sources found with SA (see Im, 2007). Firstly, these possible mismatches comprise sources, which are only visible in fMRI ("fMRI extra sources"), e.g., deeply located sources or closed field sources, which do not produce measurable deflections at the scalp surface; and secondly, they comprise sources which are only visible in EEG ("fMRI invisible sources"), e.g., sources which are activated only transiently. Thirdly, they comprise mismatches, which

are caused by fundamental differences between both techniques ("fMRI discrepancy sources").

Constraints from fMRI were used for the SA procedure in the present study. Therefore, "fMRI extra sources" might have been included in the model. Nevertheless, "fMRI invisible sources" and "fMRI discrepancy sources" are not considered with the present approach. One approach to incorporate these sources would be to include additional sources in the SA model and examine if the SA fitting algorithm would result in plausible source locations and source waveforms which indicate that these regions might show a reasonable contribution to retrieval processing.

Although the precise relation between neuronal generators of hemodynamic and electrophysiological effects still remains unexplained, a correspondence between BOLD responses and synaptic responses of cell populations is likely (see Arthurs & Boniface, 2002).

In neuroscientific research with human participants, the outcome of a study is critically dependent on the selected study design, because it is necessary to collect a sufficient amount of data within a very limited time. Hence, to implement a study design with target and non-target probe trials and three parametrically increasing retention durations (3, 7, 11 s), it was necessary to present multiple stimuli during one trial at different trial positions. The implementation of this design resulted in differing stimulus frequencies for target and non-target probes at different positions in the trial. Indeed, it is unclear if the subjects even noticed the frequency variation at different trial positions. Nevertheless, this circumstance had to be considered when interpreting the current data and might have had a considerable influence on some of the results (e.g., on P3 mean amplitudes). Unfortunately, it is impossible to disentangle effects of delay duration (trial position) and stimulus frequency with the present design.

3.4.6 Preliminary conclusions – Integration of behavioral, EEG, and fMRI data

3.4.6.1 Link to long-term memory research

Results from different methodological approaches revealed differences as well as similarities when different probe types were processed. To date, there are only few WM studies comparing different probe types. Indeed, one field of research where retrieval processing and the comparison between different probe types (old/new items) has been a matter of particular interest is LTM research. Retrieval from LTM involves the activation of the recollected

information in WM because WM offers the possibility to link LTM information to current cognitive processing mechanisms and to manipulate the activated representations according to the current task demands. Therefore, a (nevertheless limited) comparison of findings from LTM studies with findings from WM studies investigating retrieval mechanisms is supposable and this link between WM and LTM data is visible in old/new effects (e.g., in P3b mean amplitudes) in the present ERP data. Other recently published WM studies (Danker et al., 2008; Guo et al., 2008) also support the presence of old/new effects in WM tasks.

During the significant bootstrap time window, the ACC RS contributed to the N303 ERP deflection (together with the SFG and the left MFG RSs). In the EEG discussion, it was suggested that the N303 reflects processing mechanisms known from LTM tasks (potentially related to the FN400 component). The FN400 component has been linked to familiarity processing (Curran, 2000). LTM effects may have been provoked in the present design because a limited number of shapes were repeated throughout the experiment and thus, became more and more familiar during the course of the experiment. As most shapes were encoded verbally and the participants indicated for each verbally encoded shape the assigned name at the end of the experiment (in the questionnaires on the applied encoding strategies), it is possible that LTM representations for at least some of the shapes had been formed during the course of the experiment. Indeed, the processing of the current target stimulus might have involved a higher degree of familiarity than a non-target stimulus, because of its recent presentation during encoding. However, it has to be noted that the N303 component of the present study occurred earlier than common frontal FN400 effects in LTM tasks. Nevertheless, the significant bootstrap epoch with probe type differences overlapped with the time window of the typical FN400 old/new effect.

3.4.6.2 Differences in cognitive processing between probe types at different trial positions

The finding that there were no differences between target and non-target trials at trial position C for RTs of the EEG session is consistent with the outcome that there were no suprathreshold activation clusters when contrasting target and non-target trials at trial position C and also with the results that P3b mean amplitudes did not show probe type differences at trial position C and that the ERP difference wave was least pronounced at trial position C.

These findings indicate that there seemed to be a difference in probe stimulus processing depending on the type of the probe stimulus only when the probe stimulus was presented early or in the middle of the trial, whereas at the end of the trial (position C), probe stimulus

processing yielded minor differences or even no differences at all between targets and non-targets. In the design of the present study, stimulus frequency was different for target and non-target trials at trial positions A and B, but not at position C. This might be the most obvious explanation for the present findings. However, the (linear) influence of stimulus frequency alone would have caused most pronounced differences between both probe type conditions at trial position A as observed in the EEG difference waves. Indeed, the behavioral data and the fMRI contrast between targets and non-targets yield most pronounced probe type differences at trial position B. When it is assumed that increased RTs serve as a measure of increased load (see Braver et al., 1997), this pattern might be explained by the additional assumption that target processing might have been especially demanding at trial position B (due to the influence of the first distracting probe stimulus at trial position A, as previously mentioned in the discussion sections of RT data and P3b mean amplitudes). Furthermore, P3b mean amplitudes at electrode position Pz showed higher values at trial position C compared to trial position B, which might also indicate higher cognitive load at trial position B.

Accordingly, processing demands for non-target probes might have increased gradually with increasing trial position because of decreasing non-target probability. Indeed, at position A, processing demands for target probes might have been higher (compared with non-target probes) due to a lower stimulus frequency. At trial position B, processing demands for targets might have been even higher; firstly due to the lower stimulus frequency and secondly, due to the need to regain the held-in-mind target representation after the first probe stimulus (presented at trial position A) and to compare this recovered representation with the presented stimulus (potential higher cognitive load). Processing demands at trial position C might have been comparable for target and non-target probes because of equal stimulus probabilities and perhaps additionally, because the second recovery and processing of the target representation (after the second probe stimulus at trial position B) might have been less demanding compared to trial position B.

The proper explanation for the reported findings cannot be elucidated with the present design. Therefore, further studies comparing target and non-target probes are required which separately explore influences of delay duration and stimulus frequency on probe type processing.

3.4.6.3 Brain regions contributing differentially to target and non-target processing

It is noticeable that 6 of the current 12 RSs were located in anatomical regions reported to show higher activities to target trials compared with non-target trials (Druzgal & D'Esposito, 2001; Jiang et al., 2000). The present RSs located within these anatomical regions (left MFG, right MOG, bilateral IFG, left fusiform gyrus and left insula) showed differing patterns with regard to the bootstrap analysis of probe type differences. Left MFG, right MOG and right IFG RSs showed a faster decrease of source activity in the non-target condition. Left insular RS did not show differences in source activity between probe types. However, left IFG and left fusiform gyrus showed higher source activities for the non-target condition. This finding seems to be contradictory to their reported involvement in target retrieval but differences between both conditions might have been too transient to be detectable with fMRI. As previously discussed, the left IFG RS showed no specific pattern of bootstrap differences between probe types and no contribution to the scalp signal. Therefore, it is assumed that the corresponding bootstrap differences might not express meaningful differences between probe types.

Indeed, it was already suggested that left fusiform gyrus might show a specific engagement in non-target processing (see SA discussion, beginning on page 85). This suggestion was derived from the finding that higher source activity amplitudes for non-target trials were found in the fusiform RS around 400 ms. During the significant bootstrap time window (382-436 ms), source activities of the non-target condition showed a clear peak whereas the target condition showed decreasing activity (see Figure 16 on page 71).

The ventral temporal cortex/(left) fusiform gyrus has been reported to show specific sub-regions related to category-related processing of visual stimuli (Ishai, Ungerleider, Martin, & Haxby, 2000), e.g., with a sub-region involved in the processing of face stimuli (Kanwisher, McDermott, & Chun, 1997) or another sub-region involved in the processing of letters or word forms (Cohen & Dehaene, 2004). Furthermore, the left ventral temporal cortex has been linked to image generation (D'Esposito et al., 1997) and to visual imagery of visual objects in the same category-specific cortical regions where stimulus processing is carried out (Ishai et al., 2000; O'Craven & Kanwisher, 2000). After investigating brain activation with fMRI during a visual mental imagery task and a visual perception task, Ganis and colleagues (2004) concluded that fusiform gyrus might be engaged in storage and re-activation of visual objects.

These proposals about the function of left fusiform gyrus may shed light on the finding of higher source waveform activities in response to non-target stimuli in the present study.

Visual processing of the non-target probe stimulus might involve a mental representation of the target stimulus in order to compare this representation with the presented probe stimulus. This comparison might be necessary in order to enable the decision process if the presented stimulus is the target stimulus or not. Indeed, visual processing of the target stimulus should not require mental imagery because the held-in-mind target stimulus is identical with the presented stimulus and therefore no additional imagery demand should be needed for the decision process. The temporal occurrence of source waveform differences (considerably before response execution) would be in line with this explanation.

The RS in ACC yielded higher source activities for the target condition compared with the non-target condition before response execution (313-441 ms post-stimulus), showing a temporal overlap with the bootstrap differences in left fusiform gyrus. However, the source waveform of the ACC RS showed an earlier peak compared to the source waveform of the fusiform RS and differences in source activities between probe types also started earlier in ACC compared with left fusiform gyrus.

According to Bush and colleagues (2000), the ACC can be subdivided into a dorsal cognitive division and a rostral-ventral affective division. Whereas activation in the first-mentioned division is linked to cognitive processing in rather demanding tasks, activation patterns involving the last-mentioned division have been shown to occur during tasks with emotional content. The ACC RS of the present study was located in the dorsal cognitive division of the ACC (according to Bush et al., 2000, see Figure 2a), in line with the requirement of complex cognitive processing rather than affective processing in the present task. According to the classification by Picard and Strick (1996), the ACC RS was located just below the inferior border of the RCZp.

Generally, activity in the cingulate gyrus, especially in the ACC, has been shown to vary with cognitive load (Braver et al., 1997; Callicott et al., 1999) and task difficulty (Barch et al., 1997; Hautzel, Mottaghy, Schmidt, Müller, & Krause, 2003). Anterior cingulate cortex function is linked to several higher-cognitive processing operations, inter alia conflict monitoring (Botvinick et al., 2004; van Veen, Cohen, Botvinick, Stenger, & Carter, 2001), response selection (Awh & Gehring, 1999; Devinsky, Morrell, & Vogt, 1995) or attentional control (Botvinick, Braver, Barch, Carter, & Cohen, 2001; Crottaz-Herbette & Menon, 2006).

The present finding of higher source activities in ACC for target trials compared with non-target trials is contradictory to results of three fMRI studies examining probe type differences in WM tasks (Druzgal & D'Esposito, 2001; Leung, Gore, & Goldman-Rakic, 2005; Zhang,

Leung, & Johnson, 2003). In the first study (Druzgal & D'Esposito, 2001), higher PSC values in ACC were observed for non-target stimuli compared with target stimuli and in the region-of-interest analysis of the second study (Leung, Gore, & Goldman-Rakic, 2005), no PSC differences between probe types were found in ACC. In the third study (Zhang et al., 2003), ACC showed activation in the contrast of non-target versus target trials. Higher ACC activation for non-target trials was interpreted to reflect a higher degree of performance monitoring (Druzgal & D'Esposito, 2001), caused by a response bias towards a target response or by increasing response competition for non-target responses. In line with this interpretation, two of these three studies reported higher RTs for non-target trials (Druzgal & D'Esposito, 2001; Zhang et al., 2003). In the present study, higher source activities for the target condition before response execution might reflect performance monitoring or conflict monitoring mechanisms, which were not present in the afore-mentioned studies. In all three studies, target and non-target trials had an equal probability of occurrence. In contrast, the presently applied design with unequal stimulus frequencies for target and non-target trials might have caused response conflict. Braver and colleagues (2001) demonstrated in an fMRI study that ACC was involved when responses to low-frequency stimuli were executed, no matter whether the applied task was an oddball task, a go/no-go task or a two-alternative forced-choice task. They concluded that motor planning and selection of the appropriate response might have been more demanding when responding to low-frequent trials. Thus, in the present study, the increase in ACC source activity in the target condition might be explained by the detection of response conflict at trial positions A and B where the target stimulus was infrequent compared with the non-target stimulus. The RT pattern of the EEG session showing higher RTs for target compared with non-target trials at trial positions A and B corroborates this interpretation. Furthermore, error rates were higher for targets compared with non-targets at trial positions A and B, this might also indicate a higher degree of conflict on infrequent target trials.

When examining bootstrap epochs for the ACC RS at the individual trial positions (see Table 11 on page 74), there were no significant epochs during the time window of significant differences in the grand average that could confirm the assumption that the effect was mainly caused by trial positions A and B. Indeed, previous to the significant epoch in the grand average, temporary (< 30 ms) significant bootstrap differences were observed at trial position B. This indicated that differences between probe types were present at trial position B, even when there was no temporal overlap with the differences observed in the grand average data. Likewise, instead of conflict detection or conflict monitoring processes, response selection

mechanisms might have been more demanding for target trials at trial positions A and B when the infrequent response had to be selected.

The SFG RS also showed higher source activities for targets compared with non-targets in a broad time window between 451 and 875 ms. This effect occurred immediately after the probe type differences in the ACC. Although the SFG RS and the ACC RS were located relatively close to each other (distance: 2.74 cm), the source waveforms of both RSs showed clearly distinguishable activities, confirming that both RSs covered differential activity. The source waveform of the ACC RS showed a narrower peak and the SFG RS showed a broad sustained deflection when activity in the ACC RS was already decreasing.

According to the classification by Picard and Strick (1996), the SFG RS was located in pre-SMA (anterior to the vertical plane through the anterior commissure). Activations in pre-SMA have been associated with response planning and preparation processes (Picard & Strick, 1996). Furthermore, in contrast to the SMA proper, pre-SMA has bilateral connections to the PFC and is regarded as a region involved in cognitive rather than motor processing (Picard & Strick, 2001). Activations in pre-SMA are a frequent finding in WM tasks (e.g., Linden et al., 2003; Petit et al., 1998; Pollmann & von Cramon, 2000), and activation patterns including the pre-SMA have been shown to vary with cognitive load (Bledowski et al., 2006; Zarahn, Rakitin, Abela, Flynn, & Stern, 2005). Furthermore, apart from the ACC, which showed higher responses to low-frequency stimuli in the study by Braver and colleagues (2001), a second region located in pre-SMA (Talairach coordinates: 2, 3, 48) showed the same activity pattern in their study. The SFG source of the present study was located slightly more anterior and superior (3, 5, 54), compared to the pre-SMA activation reported by Braver and colleagues. Nevertheless, the distance between these two regions (0.64 cm) was well below the spatial resolution of the SA approach. Thus, the explanation given for probe type differences in ACC – higher response conflict on target trials at trial positions A and B due to lower stimulus frequency – could also be a possible explanation for probe type differences in SFG. Indeed, consistent with the previously mentioned consideration, bootstrap analyses separately for all trial positions indicated that the SFG RS showed significant source activity differences between probe types at trial positions A and B (see Table 11, page 74).

When comparing source activities of the ACC and the SFG RSs, it is obvious that source activities of the SFG RS showed a later and more sustained deflection. With regard to these source activities, it might be concluded that the cognitive process discriminating between probe types (possibly conflict management for target trials at trial positions A and B) might

be accomplished by two separate mechanisms. The first might be carried out in ACC and the second might be performed by superior frontal brain structures. In line with the proposals of ACC and pre-SMA function, activity of the ACC RS might reflect either conflict monitoring per se, response selection or attentional control mechanisms whereas activity of the superior-frontal RS might reflect response planning or response execution mechanisms. This explanation is in line with the temporal occurrence of source waveform activities as well as source waveform differences of both sources. The ACC might provide rather executive processing mechanisms assigned to the detection and handling of response conflict whereas SFG might provide more response-related processing mechanisms in order to put forward response preparative and executive operations.

The specific processing stage (conflict detection, conflict monitoring or response selection), where differences in probe type processing were generated, cannot be definitely determined with the present design. Nevertheless, the reason for probe type differences might be the same for the RSs in ACC and SFG: a higher demand with regard to conflict management processes caused by the processing of infrequent target stimuli.

Altogether, the data obtained with different methods (behavioral, fMRI, EEG and SA data) point to the presence of processing differences between target and non-target probes. The results further indicate that differences between probe type processing were reduced at trial position C, probably induced by the influence of stimulus probability or delay duration on probe processing. Furthermore, task processing might have been most demanding for probes at trial position B. The results were discussed with regard to the frequency of occurrence of target and non-target probes at different trial positions and with regard to the possibility that distraction might have been evoked by non-target probe stimuli presented in the same trial, leading to a higher degree of cognitive load at trial position B.

Results from SA further support the idea that ACC and SFG were specifically involved in the processing of target probes, possibly engaged in conflict managing operations because target stimuli had a lower stimulus frequency (at trial positions A and B). Furthermore, the left fusiform gyrus showed a specific contribution to the processing of non-target probes, potentially associated with the mental imagination of the target stimulus in order to facilitate a comparison between this held-in-mind target stimulus and the presented non-target shape.

4 General Discussion

At the beginning of the general discussion, both experiments are compared with each other to point out in which aspects the studies resembled each other and which aspects were different for both studies, particularly with regard to the applied task designs. Then, both studies are compared and linked with regard to the results and a final conclusion is drawn. Finally, future prospects are provided on further possibilities to examine WM processing in more detail.

4.1 Differences and similarities of both experiments

In both studies, different designs were used to suit different requirements. In Experiment 1, the use of dynamic shapes during the retention period placed emphasis on the maintenance period and permitted an examination of this sustained process under conditions of distraction. A baseline using a simple circle was applied, resulting in low WM demands in order to obtain activation in brain regions involved in WM maintenance. Area MT+ was investigated in more detail due to its particular engagement in this task variant including dynamic stimulation. In Experiment 2, the task including static stimuli provided the opportunity to compare the momentary point in time of WM retrieval to the moment when a probe stimulus was accurately recognized as non-target stimulus. There was no necessity to apply a low-level WM baseline because target and non-target conditions could be compared directly. Furthermore, for an fMRI-constrained SA of EEG data, not only brain regions concerned with WM processing had to be determined but also brain regions concerned with stimulus processing per se and with response execution.

In both experiments, comparable complex shapes were utilized and memory load was varied using different maintenance durations before the target shape reappeared.

In summary, although different stages of WM processing were examined in both tasks, the application of similar stimulus material and the use of delay durations with varying length facilitated a comparison between both tasks.

In both task designs, it was impossible to separate memory-related and attention-related processing mechanisms during data analysis. During the delay epoch, attention should have been directed to the current memory content to maintain the target representation „on-line“, whereas during memory retrieval, attention should also have been guided to the held-in-mind representation in order to perform a comparison with the presented stimulus. Indeed, there are WM studies and explanatory models (Cowan, 1999; Herrmann, Munk, & Engel, 2004), which

emphasize a close link between attention and WM or even propose that WM might be considered a kind of attention (Fuster, 2006). Generally, when interpreting data from WM tasks, one has to keep in mind that some processes, which are aggregated under the concept of WM, can also be interpreted as a by-product of normal information processing (see Buckner & Koutstaal, 1998). This suggestion corroborates the assumption that some (e.g., inferior frontal) brain regions, which usually show activation in WM tasks, are also associated with executive processing mechanisms in other cognitive tasks and that these regions are described to be part of an interactive network which subserves cognitive control functions (see Cole & Schneider, 2007).

4.2 Integration of results

The participants' subjective evaluations of task difficulty in both experiments indicated that the tasks were of medium difficulty (minimum difficulty: 1; maximum: 10; mean difficulty: 5.1 in Experiment 1; 4.3 for the EEG session of Experiment 2; 4.2 for the fMRI session). In both studies, verbalization was the encoding strategy mostly used, although all shape stimuli had been selected to be hard to verbalize. This outcome corresponds well to the finding that object WM tasks involve a verbal component, even when the stimuli were chosen to be „nonverbalizable" (Postle, D'Esposito, & Corkin, 2005). Furthermore, this finding emphasizes the importance of post-test evaluations in WM research in order to be able to reconstruct what the participants did during task solution and which strategies were used to memorize the stimulus material.

When comparing fMRI activations obtained with both tasks, it is obvious that several brain regions were involved in task processing in both experiments. This corroborates the finding that a distributed network of brain regions is frequently reported to show activation in WM studies (see Wager & Smith, 2003). This network comprises various brain regions, which are activated in different types of WM tasks, during different task phases (encoding, maintenance, retrieval), and also when cognitive load in WM tasks is manipulated.

When comparing the activation patterns of both tasks qualitatively, it is obvious that the results of Experiment 1 were dominated by a large parieto-occipital activation pattern, whereas the results of Experiment 2 showed more focused activation clusters without a clear dominance of activation in posterior brain areas. It is important to note that the threshold applied for the fMRI data of Experiment 1 (FDR-corrected, $p<.001$) was more conservative

than the threshold applied in Experiment 2 (FDR-corrected, p<.05). A quite conservative threshold had to be applied to the data of Experiment 1 because with a more liberal threshold (FDR-corrected, p<.05, as used in Experiment 2) the obtained clusters were too large (cluster size: up to 21213 voxels, instead of 5585 voxels at maximum with the current threshold of p<.001) to permit a reasonable interpretation of the results. Indeed, when looking at data from Experiment 1, one has to consider that activation patterns in other brain regions which also might contribute to WM maintenance might have been hidden due to the selection of a rather conservative threshold. Thus, a more conservative threshold was selected to achieve a discrimination of separate clusters and to accentuate a reasonable activation pattern, potentially at the expense of smaller or less consistently activated clusters which nevertheless might have contributed to task resolution.

In the following, brain regions activated during the maintenance epoch of Experiment 1 (complex versus simple, conjunction over all delay durations) are compared with brain regions activated during the retrieval epoch of Experiment 2. This is done in order to examine which brain areas showed activation during WM maintenance as well as retrieval.

For Experiment 2, different suprathreshold clusters are available, firstly obtained with the contrasts against the fixation baseline (*T vs. fix*; *N vs. fix*, and the corresponding averaged coordinates of the RSs), and secondly obtained with the *T vs. N* contrasts at trial positions A and B.

Both tasks were accomplished by different samples of study participants and the reported suprathreshold clusters are group activations, which integrate activations from several participants with differing brain anatomy. Therefore, activated clusters of both studies are compared qualitatively with each other when they were located near to each other according to the Talairach coordinates, even when the anatomical labels assigned to their peak coordinates were different.

The following peak activations retrieved from Experiment 1 corresponded at least roughly to activations found in Experiment 2: Bilateral clusters in MFG (Talairach coordinates: left hemisphere: -28,-1, 55; right: 30, 1, 57), bilateral clusters in IFG (left: -32, 21, -3; right: 32, 25, -5), another right-hemispheric IFG cluster (50, 11, 22) and a medial frontal cluster located in the RCZp (-4, 14, 47). Notably, these shared activations were all located in frontal cortex.

Bilateral MFG (BA 6, dorsal premotor cortex) showed activation in Experiment 1 and in Experiment 2 (RS in left MFG / right MFG in the contrast of targets versus non-targets at trial

position B). In WM studies, activations in premotor cortex are frequently reported, for the maintenance epoch as well as for the retrieval epoch (e.g., Manoach, Greve, Lindgren, & Dale, 2003; Rypma & D'Esposito, 1999). Indeed, the dorsal premotor cortex is also reported to show activation across a wide range of other cognitive tasks and is thought to be part of an interactive „cognitive control network" of brain regions which together subserve executive functions (Cole & Schneider, 2007).

Activation in right IFG in Experiment 1 was located near by the right IFG RS used in Experiment 2.

Furthermore, another set of bilateral IFG activations from Experiment 1 roughly corresponded to activations in Experiment 2, namely to the RS in left insula and to the right-hemispheric insular sub-peak used for the computation of the lentiform nucleus RS. The IFG clusters from Experiment 1 corresponded also to activations found in the target versus non-target contrasts of Experiment 2 at trial positions A (cluster in left claustrum and right IFG) and at trial position B (cluster in left insula and right IFG). It is important to note that the IFG activations obtained in Experiment 1 extended into the anterior insulae. Activations in IFG (Owen et al., 2005; Postle & Hamidi, 2007; Wager & Smith, 2003), as well as in insular cortex (Cairo et al., 2004; Manoach et al., 2003) are a frequent finding in WM tasks.

Activation in IFG was discussed to be linked to the assignment of responses to stimuli and to the accomplishment of a plan to recall or remember (see Owen et al., 2005). Inferior frontal activation extending to anterior insula has also been linked to the processing of task difficulty (Duncan & Owen, 2000). Furthermore, in an fMRI study, Courtney and colleagues (1997) observed sustained activity during WM maintenance in clusters spanning both anatomical regions (IFG, insula). In the study by Bledowski and colleagues (2006), the location of the bilateral VLPFC RSs were obtained by averaging three coordinates for each hemisphere, two of them were located in insular cortex and one in IFG.

Therefore, it remains to be clarified whether IFG and insular brain regions may act in concert or whether they make different contributions to WM processing and their conjoint activation may be attributed solely to inter-subject variance and the imprecise location of activated clusters due to the normalization procedure and the application of a group statistic over several participants.

Activation in the posterior portion of the rostral cingulate zone (RCZp, according to Picard & Strick, 1996) was found for the maintenance period of the morphing task, as well as for the

retrieval epoch (contrasts vs. fixation, as well as *T vs. N* contrasts) of the DMTS task using static stimuli. Picard and Strick reported activation in the more caudal part of the RCZp in tasks involving arm movements (arm region), whereas the rostral part was activated in tasks requiring oculomotor and speech processing (face region). According to their classification (Picard & Strick, 1996; Figure 5D, page 346), the activation foci of Experiment 2 (task with static stimuli) of the *T vs. N* contrast were located in the arm region of the RCZp. Two sub-peaks, which were used to compute the SFG RS (2, -1, 50 and -4, 8, 49) were also located in the RCZp arm region. In contrast, the activation foci of Experiment 1 (task with morphing stimuli) lay within the face region of the RCZp (-4, 14, 47 and 6, 16, 45) and the ACC RS from Experiment 2 was located at the inferior border of the RCZp face region (-10, 15, 32). A study by Barch and colleagues (2001) could not confirm the RCZp somatotopy for Stroop-like tasks requiring either vocal/eye or manual responses, whereas the meta-analysis by Laird and colleagues (2005) confirmed differing activations in RCZp hand and verbal regions in Stroop tasks with differing response modalities. During the retrieval epoch of the present static task, a manual response was required, in agreement with activations in the RCZp arm region. In the maintenance epoch of the morphing task, no response was executed, but a verbal subvocal rehearsal mechanism could have been used to rehearse the (verbally encoded) representation of the current target shape, and this might have led to activations in the RCZp face region. Alternatively, small eye movements might have been performed to track the morphing shape and they might have caused activation in the RCZp face region.

Activation in the ACC RS which contributed to the N303 scalp potential and showed higher amplitudes for target trials compared with non-target trials (bootstrap statistic) before response execution cannot be reliably linked with one specific portion of the RCZp (hand or verbal) because of the reduced spatial resolution of the SA approach. Nevertheless, Braver and colleagues (2001) suggested that the AC region corresponding to the RCZp might act as a "generic conflict detector", indicated by higher ACC activity in response to infrequent stimuli compared with frequent stimuli. This is in line with the higher ACC source activity for target trials and with the present RCZp activation in the contrasts of targets versus non-targets at trial positions A and B, where non-target trials were more frequent than target trials. In almost the same manner, this region might have been engaged during the morphing task, because of the necessity to detect and process distracting shapes under conditions of enhanced cognitive load (complex shapes).

The brain regions discussed above showed fMRI activations in both experiments, during maintenance as well as retrieval processing. This finding is in line with findings from other studies examining different phases of WM tasks (e.g. Cairo et al., 2004; Manoach et al., 2003) and with the proposal that brain regions may interact in a complex way to subserve task solution (see Carpenter, Just, & Reichle, 2000; Fuster, 2001). Additionally, the present design of Experiment 1 might have led to retrieval-like processing mechanisms already during the maintenance period because participants continuously compared the current morphing stimulus with the held-in-mind target representation.

4.3 Final conclusions

Experiment 1 aimed at a characterization of a network of brain areas involved in maintenance processing under conditions of higher cognitive load (stimulus complexity), but identical visual stimulation. During the delay, continuously morphing stimuli were presented. A widespread activation pattern could be identified, in line with WM networks reported in other studies. This network was consistently involved in maintenance processing, even when different retention durations were applied. It is remarkable that such a widespread network of brain areas was obtained even if the only difference between both contrasted conditions was the complexity of the held-in-mind target stimulus. Furthermore, PSC in motion-sensitive area MT+ yielded a modulation with stimulus complexity as well as with delay duration, pointing towards a higher engagement of area MT+ when complex stimuli were maintained in WM.

In Experiment 2, different methodological approaches were used to characterize processing differences between probe types (targets, non-targets) during the retrieval epoch of a DMTS task with static stimuli presented at different positions in the trial. Neuronal correlates of WM retrieval could be successfully identified and the resulting activation foci were used for an fMRI-constrained SA.

Processing differences between probe types were identified in the left fusiform gyrus, the ACC and the SFG. When examining probe stimuli at different positions in the trial, reduced differences between target and non-target processing were observed at trial position C, pointing towards influences of stimulus frequency and/or of delay duration. Furthermore, findings with different methodological approaches indicated a cognitive load effect with higher load at trial position B.

Altogether, two different approaches were used to gain insight into neuronal correlates of maintenance and retrieval processing in WM tasks. Both tasks shared activations in frontal brain areas, indicating that these frontal regions were involved in the processing of different stages of WM tasks (maintenance, retrieval). Nevertheless, it might be possible that these brain regions accomplished the same cognitive operation (e.g., the management of conflicting information) during both tasks.

4.4 Suggestions for further research

An overwhelming quantity of WM studies has been conducted so far. Nevertheless, important questions remain unanswered until now, e.g., the question: "which brain areas are involved and how do they interact to complete WM processing mechanisms?"

With regard to this question, one has to consider that all obtained results are dependent on several factors: the applied design and selected type of WM task (DMTS, n-back…), the task period which is focused on (maintenance, retrieval), the stimulus material (verbal, spatial, object), the measurement method and so on. Therefore, it is possible that a definite answer to the question posed previously does not exist. Further studies might help to figure out which are the processing mechanisms underlying cognitive operations across several tasks. Moreover, further studies are required to integrate current research findings from different neuroscientific research fields (like, e.g., linking studies investigating mnemonic, executive or attentional processing mechanisms).

Future research might point to the necessity to consider the brain as an interactive network, where several cognitive processes might be bound to a fixed location within the brain but other processes emerge from the dynamic interaction between several brain regions (e.g., see Postle, 2006).

An analysis of the maintenance epochs of Experiment 2 (fMRI and/or EEG data) could be used to examine the suggestion that cognitive load might be higher at trial position B because of the previously interfering first probe stimulus. During the second maintenance epoch (trial position B), participants had to regain the representation of the target shape after the presentation of the distracting probe stimulus. It might have been easier at trial position C to handle the distraction and to retain the representation of the target because this mechanism had already been performed at trial position B. Nevertheless, it is critical to examine two different task phases of the same WM task because these task phases can never be presented

in a randomized order. For example, the encoding epoch is always followed by the delay epoch and the delay epoch always precedes retrieval. Therefore, long-lasting modulations during one trial, e.g., an increase or decrease in tonic arousal, are likely to affect more than one task phase. This circumstance leads to multicollinearity and the violation of the assumption of independent task events (see Cairo et al., 2004). To reduce multicollinearity, the duration of the task phases might be jittered (Cairo et al., 2004), or the length of the delay epoch might be increased (Jha & McCarthy, 2000; Leung, Gore, & Goldman-Rakic, 2002; Rypma & D'Esposito, 1999). There are also other methodological options to handle this problem, e.g., to use subject-specific empirically derived shapes of the hemodynamic response function to allow for a better differentiation between activity of different task phases (Postle, Zarahn, & D'Esposito, 2000; Rypma & D'Esposito, 1999); or to apply finite impulse response (FIR) models in order to estimate the hemodynamic response function without prior assumptions about its shape (Manoach et al., 2003). Another frequently used strategy is the variation of WM load (e.g., Jha & McCarthy, 2000; Rypma & D'Esposito, 1999), but this approach does not exclusively reveal activation in brain regions associated with WM processing but also in brain regions associated with executive or strategic processing.

A comparison of electrophysiological or SA data with PSC data from fMRI could either reveal comparable activity patterns in task-relevant brain regions or differences between both methodologies. Indeed, with the present design of Experiment 2, only a comparison between targets and non-targets separately at each trial position would be reasonable because PSC data at trial positions B and C might have been influenced by the previously presented stimuli due to the lag of the hemodynamic response function. Furthermore, there is evidence for a closer link between the BOLD signal and fast oscillations, compared with the relationship between the BOLD signal and evoked potentials (Foucher, Otzenberger, & Gounot, 2003). Therefore, fMRI data could be compared with oscillatory responses, e.g., induced gamma activity during the retrieval epoch, because gamma activity has been linked to object representation (Tallon-Baudry & Bertrand, 1999) and to the matching of stimulus-related information with the current memory content as well as subsequent processing mechanisms (Herrmann et al., 2004). The comparability of findings and models derived from this methodological approach with results reported in the present study is severely limited because induced oscillatory responses are cancelled out in averaged ERPs (as used in the present Experiment 2), due to their latency variations (Tallon-Baudry & Bertrand, 1999).

In Experiment 2, several ERP deflections showed interesting patterns which differentiated between probe types (N303, N510 in the grand average) or between trial positions (P1, N1). A detailed analysis of these components was beyond the scope of the present study, but it could probably result in new insights into the influence of probe type or trial position on these ERP components.

Furthermore, interesting approaches to confirm the validity of the SA result would be either to accomplish another SA without fMRI constraints in order to compare the resulting model with the present fMRI-constrained SA model or to use additional probe sources added to the currently used model to check for fMRI invisible sources, which might also contribute to retrieval processing. Until now, no definite solution is offered to the question of the validity of the resulting SA model. Further research is required to solve this problem and accordingly, improve the explanatory power of SA results.

References

Allman, J. M., & Kaas, J. H. (1971). A representation of the visual field in the caudal third of the middle temporal gyrus of the owl monkey (aotus trivirgatus). *Brain Research, 31*(1), 85-105.

Arthurs, O. J., & Boniface, S. (2002). How well do we understand the neural origins of the fMRI BOLD signal? *Trends in Neurosciences, 25*(1), 27-31.

Atkinson, R. C., & Shiffrin, R. M. (1968). Human memory: A proposed system and its control processes. In K. W. Spence, & J. T. Spence (Eds.), *The Psychology of Learning and Motivation: Advances in Research and Theory* (pp. 89-195). New York: Academic Press.

Atkinson, R. C., & Shiffrin, R. M. (1971). The control of short-term memory. *Scientific American, 224*, 82-90.

Awh, E., & Gehring, W. J. (1999). The anterior cingulate cortex lends a hand in response selection. *Nature Neuroscience, 2*(10), 853-854.

Baddeley, A. D. (2000). The episodic buffer: A new component of working memory? *Trends in Cognitive Sciences, 4*(11), 417-423.

Baddeley, A. D. (2003). Working memory: Looking back and looking forward. *Nature Reviews. Neuroscience, 4*(10), 829-839.

Baddeley, A. D., & Hitch, G. J. (1974). Working memory. In G. A. Bower (Ed.), *The Psychology of Learning and Motivation* (pp. 47-90). New York: Academic Press.

Baddeley, A. D., & Logie, R. H. (1999). Working memory: The multiple-component model. In A. Miyake, & P. Shah (Eds.), *Models of working memory: Mechanisms of active maintenance and executive control* (pp. 28-61). Cambridge: Cambridge University Press.

Banquet, J. P., Renault, B., & Lesèvre, N. (1981). Effect of task and stimulus probability on evoked potentials. *Biological Psychology, 13*, 203-214.

Barch, D. M., Braver, T. S., Akbudak, E., Conturo, T., Ollinger, J., & Snyder, A. (2001). Anterior cingulate cortex and response conflict: Effects of response modality and processing domain. *Cerebral Cortex, 11*(9), 837-848.

Barch, D. M., Braver, T. S., Nystrom, L. E., Forman, S. D., Noll, D. C., & Cohen, J. D. (1997). Dissociating working memory from task difficulty in human prefrontal cortex. *Neuropsychologia, 35*(10), 1373-1380.

Bashore, T. R. (1990). Stimulus-response compatibility viewed from a cognitive psychophysiological perspective. In R. W. Proctor, & T. G. Reeve (Eds.), *Stimulus-response compatibility: An integrated perspective* (pp. 183-223). Amsterdam: Elsevier.

Benjamini, Y., & Hochberg, Y. (1995). Controlling the false discovery rate: A practical and powerful approach to multiple testing. *Journal of the Royal Statistical Society,* (Series B. 57), 289-300.

Bledowski, C., Kadosh, K. C., Wibral, M., Rahm, B., Bittner, R. A., Hoechstetter, K., et al. (2006). Mental chronometry of working memory retrieval: A combined functional magnetic resonance imaging and event-related potentials approach. *Journal of Neuroscience, 26*(3), 821-829.

Bledowski, C., Linden, D. E., & Wibral, M. (2007). Combining electrophysiology and functional imaging - different methods for different questions. *Trends in Cognitive Sciences, 11*(12), 500-502.

Bledowski, C., Prvulovic, D., Hoechstetter, K., Scherg, M., Wibral, M., Goebel, R., et al. (2004). Localizing P300 generators in visual target and distractor processing: A combined event-related potential and functional magnetic resonance imaging study. *Journal of Neuroscience, 24*(42), 9353-9360.

Botvinick, M. M., Braver, T. S., Barch, D. M., Carter, C. S., & Cohen, J. D. (2001). Conflict monitoring and cognitive control. *Psychological Review, 108*(3), 624-652.

Botvinick, M. M., Cohen, J. D., & Carter, C. S. (2004). Conflict monitoring and anterior cingulate cortex: An update. *Trends in Cognitive Sciences, 8*(12), 539-546.

Braver, T. S., Barch, D. M., Gray, J. R., Molfese, D. L., & Snyder, A. (2001). Anterior cingulate cortex and response conflict: Effects of frequency, inhibition and errors. *Cerebral Cortex, 11*(9), 825-836.

Braver, T. S., Cohen, J. D., Nystrom, L. E., Jonides, J., Smith, E. E., & Noll, D. C. (1997). A parametric study of prefrontal cortex involvement in human working memory. *NeuroImage, 5*(1), 49-62.

Buckner, R. L., & Koutstaal, W. (1998). Functional neuroimaging studies of encoding, priming, and explicit memory retrieval. *Proceedings of the National Academy of Sciences of the United States of America, 95*(3), 891-898.

Bunge, S. A., Ochsner, K. N., Desmond, J. E., Glover, G. H., & Gabrieli, J. D. (2001). Prefrontal regions involved in keeping information in and out of mind. *Brain, 124*(Pt 10), 2074-2086.

Bush, G., Luu, P., & Posner, M. I. (2000). Cognitive and emotional influences in anterior cingulate cortex. *Trends in Cognitive Sciences, 4*(6), 215-222.

Cabeza, R., Dolcos, F., Graham, R., & Nyberg, L. (2002). Similarities and differences in the neural correlates of episodic memory retrieval and working memory. *NeuroImage, 16*(2), 317-330.

Cabeza, R., & Nyberg, L. (2000a). Imaging cognition II: An empirical review of 275 PET and fMRI studies. *Journal of Cognitive Neuroscience, 12*(1), 1-47.

Cabeza, R., & Nyberg, L. (2000b). Neural bases of learning and memory: Functional neuroimaging evidence. *Current Opinion in Neurology, 13*(4), 415-421.

Cairo, T. A., Liddle, P. F., Woodward, T. S., & Ngan, E. T. C. (2004). The influence of working memory load on phase specific patterns of cortical activity. *Cognitive Brain Research, 21*(3), 377-387.

Callicott, J. H., V, M., Bertolino, A., Finn, K., Coppola, R., Frank, J. A., et al. (1999). Physiological characteristics of capacity constraints in working memory as revealed by functional MRI. *Cerebral Cortex, 9*(1), 20-26.

Carpenter, P. A., Just, M. A., & Reichle, E. D. (2000). Working memory and executive function: Evidence from neuroimaging. *Current Opinion in Neurobiology, 10*(2), 195-199.

Chafee, M. V., & Goldman-Rakic, P. S. (1998). Matching patterns of activity in primate prefrontal area 8a and parietal area 7ip neurons during a spatial working memory task. *Journal of Neurophysiology, 79*(6), 2919-2940.

Chawla, D., Rees, G., & Friston, K. J. (1999). The physiological basis of attentional modulation in extrastriate visual areas. *Nature Neuroscience, 2*(7), 671-676.

Clark, V. P., Fan, S., & Hillyard, S. A. (1995). Identification of early visual evoked potential generators by retinotopic and topographic analyses. *Human Brain Mapping, 2*, 170-187.

Cohen, L., & Dehaene, S. (2004). Specialization within the ventral stream: The case for the visual word form area. *NeuroImage, 22*(1), 466-476.

Cole, M. W., & Schneider, W. (2007). The cognitive control network: Integrated cortical regions with dissociable functions. *NeuroImage, 37*(1), 343-360.

Constantinidis, C., & Steinmetz, M. A. (1996). Neuronal activity in posterior parietal area 7a during the delay periods of a spatial memory task. *Journal of Neurophysiology, 76*(2), 1352-1355.

Courtney, S. M., Ungerleider, L. G., Keil, K., & Haxby, J. V. (1997). Transient and sustained activity in a distributed neural system for human working memory. *Nature, 386*(6625), 608-611.

Cowan, N. (1988). Evolving conceptions of memory storage, selective attention, and their mutual constraints within the human information-processing system. *Psychological Bulletin, 104*(2), 163-191.

Cowan, N. (1995). *Attention and memory: An integrated framework*. New York: Oxford University Press.

Cowan, N. (1999). An embedded-processes model of working memory. In A. Miyake, & P. Shah (Eds.), *Models of working memory: Mechanisms of active maintenance and executive control* (pp. 62-101). Cambridge: Cambridge University Press.

Crottaz-Herbette, S., & Menon, V. (2006). Where and when the anterior cingulate cortex modulates attentional response: Combined fMRI and ERP evidence. *Journal of Cognitive Neuroscience, 18*(5), 766-780.

Culham, J. C., Cavanagh, P., & Kanwisher, N. G. (2001). Attention response functions: Characterizing brain areas using fMRI activation during parametric variations of attentional load. *Neuron, 32*(4), 737-745.

Curran, T. (2000). Brain potentials of recollection and familiarity. *Memory & Cognition, 28*(6), 923-938.

Dale, A. M., & Halgren, E. (2001). Spatiotemporal mapping of brain activity by integration of multiple imaging modalities. *Current Opinion in Neurobiology, 11*(2), 202-208.

Danker, J. F., Hwang, G. M., Gauthier, L., Geller, A., Kahana, M. J., & Sekuler, R. (2008). Characterizing the ERP old-new effect in a short-term memory task. *Psychophysiology, 45(5),* 784-793.

De Fockert, J. W., Rees, G., Frith, C. D., & Lavie, N. (2001). The role of working memory in visual selective attention. *Science, 291*(5509), 1803-1806.

Della-Maggiore, V., Chau, W., Peres-Neto, P. R., & McIntosh, A. R. (2002). An empirical comparison of SPM preprocessing parameters to the analysis of fMRI data. *NeuroImage, 17*(1), 19-28.

D'Esposito, M., Aguirre, G. K., Zarahn, E., Ballard, D., Shin, R. K., & Lease, J. (1998). Functional MRI studies of spatial and nonspatial working memory. *Cognitive Brain Research, 7*(1), 1-13.

D'Esposito, M., Detre, J. A., Aguirre, G. K., Stallcup, M., Alsop, D. C., Tippet, L. J., et al. (1997). A functional MRI study of mental image generation. *Neuropsychologia, 35*(5), 725-730.

D'Esposito, M., Postle, B. R., Jonides, J., & Smith, E. E. (1999). The neural substrate and temporal dynamics of interference effects in working memory as revealed by event-related functional MRI. *Proceedings of the National Academy of Sciences of the United States of America, 96*(13), 7514-7519.

D'Esposito, M., Postle, B. R., & Rypma, B. (2000). Prefrontal cortical contributions to working memory: Evidence from event-related fMRI studies. *Experimental Brain Research, 133*(1), 3-11.

Devinsky, O., Morrell, M. J., & Vogt, B. A. (1995). Contributions of anterior cingulate cortex to behaviour. *Brain, 118* (Pt 1), 279-306.

De Zubicaray, G. I., McMahon, K., Wilson, S. J., & Muthiah, S. (2001). Brain activity during the encoding, retention, and retrieval of stimulus representations. *Learning and Memory, 8*(5), 243-251.

Dien, J., Spencer, K. M., & Donchin, E. (2004). Parsing the late positive complex: Mental chronometry and the ERP components that inhabit the neighborhood of the P300. *Psychophysiology, 41*(5), 665-678.

Di Russo, F., Martinez, A., Sereno, M. I., Pitzalis, S., & Hillyard, S. A. (2002). Cortical sources of the early components of the visual evoked potential. *Human Brain Mapping, 15*(2), 95-111.

Donchin, E. (1981). Surprise!...surprise? *Psychophysiology, 18*(5), 493-513.

Donchin, E., & Coles, M. G. H. (1988). Is the P300 component a manifestation of context updating? *Behavioral and Brain Sciences, 11*, 357-374.

Druzgal, T. J., & D'Esposito, M. (2001). A neural network reflecting decisions about human faces. *Neuron, 32*(5), 947-955.

Duncan, J., & Owen, A. M. (2000). Common regions of the human frontal lobe recruited by diverse cognitive demands. *Trends in Neurosciences, 23*(10), 475-483.

Efron, B., & Tibshirani, R. J. (1993). *An introduction to the bootstrap*. New York: Chapman & Hall.

Falkenstein, M., Hohnsbein, J., & Hoormann, J. (1994). Effects of choice complexity on different subcomponents of the late positive complex of the event-related potential. *Electroencephalography and Clinical Neurophysiology, 92*(2), 148-160.

Falkenstein, M., Koshlykova, N. A., Kiroj, V. N., Hoormann, J., & Hohnsbein, J. (1995). Late ERP components in visual and auditory Go/Nogo tasks. *Electroencephalography and Clinical Neurophysiology, 96*(1), 36-43.

Fan, J., Hof, P. R., Guise, K. G., Fossella, J. A., & Posner, M. I. (2008). The functional integration of the anterior cingulate cortex during conflict processing. *Cerebral Cortex, 18*(4), 796-805.

Foucher, J. R., Otzenberger, H. e., & Gounot, D. (2003). The BOLD response and the gamma oscillations respond differently than evoked potentials: An interleaved EEG-fMRI study. *BMC Neuroscience, 4*, 22.

Friedman, D., & Johnson, R.,Jr. (2000). Event-related potential (ERP) studies of memory encoding and retrieval: A selective review. *Microscopy Research and Technique, 51*(1), 6-28.

Friston, K. J., Frith, C. D., Turner, R., & Frackowiak, R. S. (1995). Characterizing evoked hemodynamics with fMRI. *NeuroImage, 2*(2), 157-165.

Friston, K. J., Holmes, A. P., Price, C. J., Büchel, C., & Worsley, K. J. (1999). Multisubject fMRI studies and conjunction analyses. *NeuroImage, 10*(4), 385-396.

Friston, K. J., Holmes, A. P., & Worsley, K. J. (1999). How many subjects constitute a study? *NeuroImage, 10*(1), 1-5.

Funahashi, S., Bruce, C. J., & Goldman-Rakic, P. S. (1989). Mnemonic coding of visual space in the monkey's dorsolateral prefrontal cortex. *Journal of Neurophysiology, 61*(2), 331-349.

Fuster, J. M. (2001). The prefrontal cortex - an update: Time is of the essence. *Neuron, 30*(2), 319-333.

Fuster, J. M. (2006). The cognit: A network model of cortical representation. *International Journal of Psychophysiology, 60*(2), 125-132.

Fuster, J. M., & Alexander, G. E. (1971). Neuron activity related to short-term memory. *Science, 173*(997), 652-654.

Ganis, G., Thompson, W. L., & Kosslyn, S. M. (2004). Brain areas underlying visual mental imagery and visual perception: An fMRI study. *Cognitive Brain Research, 20*(2), 226-241.

Genovese, C. R., Lazar, N. A., & Nichols, T. (2002). Thresholding of statistical maps in functional neuroimaging using the false discovery rate. *NeuroImage, 15*(4), 870-878.

Gevins, A., Smith, M. E., Le, J., Leong, H., Bennett, J., Martin, N., et al. (1996). High resolution evoked potential imaging of the cortical dynamics of human working memory. *Electroencephalography and Clinical Neurophysiology, 98*(4), 327-348.

Goldman-Rakic, P. S. (1992). Working memory and the mind. *Scientific American, 267*(3), 110-117.

Goldman-Rakic, P. S. (1995). Architecture of the prefrontal cortex and the central executive. *Annals of the New York Academy of Sciences, 769*, 71-83.

Goldman-Rakic, P. S. (1996). The prefrontal landscape: Implications of functional architecture for understanding human mentation and the central executive. *Philosophical Transactions of the Royal Society of London. Series B, Biological Sciences, 351*(1346), 1445-1453.

Goldstein, A., Spencer, K. M., & Donchin, E. (2002). The influence of stimulus deviance and novelty on the P300 and novelty P3. *Psychophysiology, 39*(6), 781-790.

Gomarus, H. K., Althaus, M., Wijers, A. A., & Minderaa, R. B. (2006). The effects of memory load and stimulus relevance on the EEG during a visual selective memory search task: An ERP and ERD/ERS study. *Clinical Neurophysiology, 117*(4), 871-884.

Gordon, I. E. (1967). Stimulus probability and simple reaction time. *Nature, 215*(5103), 895-896.

Gould, R. L., Brown, R. G., Owen, A. M., Ffytche, D. H., & Howard, R. J. (2003). fMRI BOLD response to increasing task difficulty during successful paired associates learning. *NeuroImage, 20*(2), 1006-1019.

Guo, C., Lawson, A. L., Zhang, Q., & Jiang, Y. (2008). Brain potentials distinguish new and studied objects during working memory. *Human Brain Mapping, 29*(4), 441-452.

Hartley, A. A., & Speer, N. K. (2000). Locating and fractionating working memory using functional neuroimaging: Storage, maintenance, and executive functions. *Microscopy Research and Technique, 51*(1), 45-53.

Hautzel, H., Mottaghy, F. M., Schmidt, D., Müller, H. W., & Krause, B. J. (2003). Neurocognition and PET. Strategies for data analysis in activation studies on working memory. *Nuklearmedizin, 42*(5), 197-209.

Hazy, T. E., Frank, M. J., & O'Reilly, R. C. (2006). Banishing the homunculus: Making working memory work. *Neuroscience, 139*(1), 105-118.

Hazy, T. E., Frank, M. J., & O'Reilly, R. C. (2007). Towards an executive without a homunculus: Computational models of the prefrontal cortex/basal ganglia system. *Philosophical Transactions of the Royal Society of London. Series B, Biological Sciences, 362*(1485), 1601-1613.

Heeger, D. J., & Ress, D. (2002). What does fMRI tell us about neuronal activity? *Nature Reviews. Neuroscience, 3*(2), 142-151.

Helmholtz, H. (1853). Ueber einige Gesetze der Vertheilung elektrischer Ströme in körperlichen Leitern mit Anwendung auf die thierisch-elektrischen Versuche. *Annalen der Physik und Chemie* pp. 211-233.

Herrmann, C. S., Munk, M. H., & Engel, A. K. (2004). Cognitive functions of gamma-band activity: Memory match and utilization. *Trends in Cognitive Sciences, 8*(8), 347-355.

Hohnsbein, J., Falkenstein, M., Hoormann, J., & Blanke, L. (1991). Effects of crossmodal divided attention on late ERP components. I. simple and choice reaction tasks. *Electroencephalography and Clinical Neurophysiology, 78*(6), 438-446.

Holmes, A. P., & Friston, K. J. (1998). Generalisability, random effects and population inference. *NeuroImage, 7*, S754.

Hopf, J. M., Vogel, E., Woodman, G., Heinze, H. J., & Luck, S. J. (2002). Localizing visual discrimination processes in time and space. *Journal of Neurophysiology, 88*(4), 2088-2095.

Hopfinger, J. B., Khoe, W., & Song, A. (2005). Combining electrophysiology with structural and functional neuroimaging: ERP's, PET, MRI, fMRI. In T. C. Handy (Ed.), *Event-Related Potentials. A Methods Handbook* (pp. 345-379). Cambridge, MA: MIT Press.

Horwitz, B., Friston, K. J., & Taylor, J. G. (2000). Neural modeling and functional brain imaging: An overview. *Neural Networks, 13*(8-9), 829-846.

Huettel, S. A., Song, A. W., & McCarthy, G. (2004). *Functional Magnetic Resonance Imaging*. Sunderland, Mass.: Sinauer.

Ille, N., Berg, P., & Scherg, M. (2002). Artifact correction of the ongoing EEG using spatial filters based on artifact and brain signal topographies. *Journal of Clinical Neurophysiology, 19*(2), 113-124.

Im, C. (2007). Dealing with mismatched fMRI activations in fMRI constrained EEG cortical source imaging: A simulation study assuming various mismatch types. *Medical & Biological Engineering & Computing, 45*(1), 79-90.

Ishai, A., Ungerleider, L. G., Martin, A., & Haxby, J. V. (2000). The representation of objects in the human occipital and temporal cortex. *Journal of Cognitive Neuroscience, 12 Supplement 2*, 35-51.

Jaeggi, S. M., Seewer, R., Nirkko, A. C., Eckstein, D., Schroth, G., Groner, R., et al. (2003). Does excessive memory load attenuate activation in the prefrontal cortex? Load-dependent processing in single and dual tasks: Functional magnetic resonance imaging study. *NeuroImage, 19*(2), 210-225.

James, W. (1890). *The Principles of Psychology*. New York: Holt.

Jha, A. P., & McCarthy, G. (2000). The influence of memory load upon delay-interval activity in a working-memory task: An event-related functional MRI study. *Journal of Cognitive Neuroscience, 12 Supplement 2*, 90-105.

Jiang, Y., Haxby, J. V., Martin, A., Ungerleider, L. G., & Parasuraman, R. (2000). Complementary neural mechanisms for tracking items in human working memory. *Science, 287*(5453), 643-646.

Johnson, R.,Jr. (1986). A triarchic model of P300 amplitude. *Psychophysiology, 23*(4), 367-384.

Johnstone, T., Ores Walsh, K. S., Greischar, L. L., Alexander, A. L., Fox, A. S., Davidson, R. J., et al. (2006). Motion correction and the use of motion covariates in multiple-subject fMRI analysis. *Human Brain Mapping, 27*(10), 779-788.

Jonides, J., Lewis, R. L., Nee, D. E., Lustig, C. A., Berman, M. G., & Moore, K. S. (2008). The mind and brain of short-term memory. *Annual Review of Psychology, 59*, 193-224.

Jovicich, J., Peters, R. J., Koch, C., Braun, J., Chang, L., & Ernst, T. (2001). Brain areas specific for attentional load in a motion-tracking task. *Journal of Cognitive Neuroscience, 13*(8), 1048-1058.

Kanwisher, N., McDermott, J., & Chun, M. M. (1997). The fusiform face area: A module in human extrastriate cortex specialized for face perception. *Journal of Neuroscience, 17*(11), 4302-4311.

Kieras, D. E., Meyer, D. E., Mueller, S., & Seymour, T. (1999). Insights into working memory from the perspective of the EPIC architecture for modeling skilled perceptual-motor and cognitive human performance. In A. Miyake, & P. Shah (Eds.), *Models of working memory: Mechanisms of active maintenance and executive control.* (pp. 183-223). New York: Cambridge University Press.

Kok, A. (2001). On the utility of P3 amplitude as a measure of processing capacity. *Psychophysiology,* (38), 557-577.

Kotchoubey, B. I., Jordan, J. S., Grozinger, B., Westphal, K. P., & Kornhuber, H. H. (1996). Event-related brain potentials in a varied-set memory search task: A reconsideration. *Psychophysiology, 33*(5), 530-540.

Kwong, K. K., Belliveau, J. W., Chesler, D. A., Goldberg, I. E., Weisskoff, R. M., Poncelet, B. P., et al. (1992). Dynamic magnetic resonance imaging of human brain activity during primary sensory stimulation. *Proceedings of the National Academy of Sciences of the United States of America, 89*(12), 5675-5679.

LaBar, K. S., Gitelman, D. R., Parrish, T. B., & Mesulam, M. (1999). Neuroanatomic overlap of working memory and spatial attention networks: A functional MRI comparison within subjects. *NeuroImage, 10*(6), 695-704.

Laird, A. R., McMillan, K. M., Lancaster, J. L., Kochunov, P., Turkeltaub, P. E., Pardo, J. V., et al. (2005). A comparison of label-based review and ALE meta-analysis in the stroop task. *Human Brain Mapping, 25*(1), 6-21.

Lavie, N. (1995). Perceptual load as a necessary condition for selective attention. *Journal of Experimental Psychology: Human Perception & Performance, 21*(3), 451-468.

Lavie, N., Hirst, A., de Fockert, J. W., & Viding, E. (2004). Load theory of selective attention and cognitive control. *Journal of Experimental Psychology: General, 133*(3), 339-354.

Leung, H. C., Gore, J. C., & Goldman-Rakic, P. S. (2002). Sustained mnemonic response in the human middle frontal gyrus during on-line storage of spatial memoranda. *Journal of Cognitive Neuroscience, 14*(4), 659-671.

Leung, H. C., Gore, J. C., & Goldman-Rakic, P. S. (2005). Differential anterior prefrontal activation during the recognition stage of a spatial working memory task. *Cerebral Cortex, 15*(11), 1742-1749.

Leung, H. C., Seelig, D., & Gore, J. C. (2004). The effect of memory load on cortical activity in the spatial working memory circuit. *Cognitive, Affective and Behavioral Neuroscience, 4*(4), 553-563.

Linden, D. E. J., Bittner, R. A., Muckli, L., Waltz, J. A., Kriegeskorte, N., Goebel, R., et al. (2003). Cortical capacity constraints for visual working memory: Dissociation of fMRI load effects in a fronto-parietal network. *NeuroImage, 20*(3), 1518-1530.

Looren de Jong, H., Kok, A., & van Rooy, J. C. (1988). Early and late selection in young and old adults: An event-related potential study. *Psychophysiology, 25*(6), 657-671.

Lovett, M. C., Reder, L. M., & Lebiere, C. (1999). Modeling working memory in a unified architecture: An ACT-R perspective. In A. Miyake, & P. Shah (Eds.), *Models of working memory: Mechanisms of active maintenance and executive control.* (pp. 135-182). New York: Cambridge University Press.

Luck, S. J. (2005a). *An Introduction to the Event-Related Potential Technique*. Cambridge, Mass.: MIT Press.

Luck, S. J. (2005b). ERP localization. In S. J. Luck (Ed.), *An Introduction to the Event-Related Potential Technique* (pp. 267-301). Cambridge, Mass.: MIT Press.

Manoach, D. S., Greve, D. N., Lindgren, K. A., & Dale, A. M. (2003). Identifying regional activity associated with temporally separated components of working memory using event-related functional MRI. *NeuroImage, 20*(3), 1670-1684.

Martinez, A., Teder-Salejarvi, W., Vazquez, M., Molholm, S., Foxe, J. J., Javitt, D. C., et al. (2006). Objects are highlighted by spatial attention. *Journal of Cognitive Neuroscience, 18*(2), 298-310.

Mayer, J. S., Bittner, R. A., Nikolic, D., Bledowski, C., Goebel, R., & Linden, D. E. (2007). Common neural substrates for visual working memory and attention. *NeuroImage, 36*(2), 441-453.

McEvoy, L. K., Smith, M. E., & Gevins, A. (1998). Dynamic cortical networks of verbal and spatial working memory: Effects of memory load and task practice. *Cerebral Cortex, 8*(7), 563-574.

Mecklinger, A. (2000). Interfacing mind and brain: A neurocognitive model of recognition memory. *Psychophysiology, 37*(5), 565-582.

Mecklinger, A., Kramer, A. F., & Strayer, D. L. (1992). Event related potentials and EEG components in a semantic memory search task. *Psychophysiology, 29*(1), 104-119.

Mecklinger, A., & Meinshausen, R. M. (1998). Recognition memory for object form and object location: An event-related potential study. *Memory & Cognition, 26*(5), 1068-1088.

Menon, V., Ford, J. M., Lim, K. O., Glover, G. H., & Pfefferbaum, A. (1997). Combined event-related fMRI and EEG evidence for temporal-parietal cortex activation during target detection. *Neuroreport, 8*(14), 3029-3037.

Michel, C. M., Murray, M. M., Lantz, G., Gonzalez, S., Spinelli, L., & Grave de Peralta, R. (2004). EEG source imaging. *Clinical Neurophysiology, 115*(10), 2195-2222.

Miller, E. K., & Cohen, J. D. (2001). An integrative theory of prefrontal cortex function. *Annual Review of Neuroscience, 24*, 167-202.

Miller, E. K., Erickson, C. A., & Desimone, R. (1996). Neural mechanisms of visual working memory in prefrontal cortex of the macaque. *Journal of Neuroscience, 16*(16), 5154-5167.

Miller, E. K., Li, L., & Desimone, R. (1993). Activity of neurons in anterior inferior temporal cortex during a short-term memory task. *Journal of Neuroscience, 13*(4), 1460-1478.

Miller, G. A. (1956). The magical number seven plus or minus two: Some limits on our capacity for processing information. *Psychological Review, 63*(2), 81-97.

Miller, G. A., Galanter, E., & Pribram, K. H. (1960). *Plans and the Structure of Behavior*. New York: Holt, Rinehart & Winston.

Miyake, A., & Shah, P. (1999). Toward unified theories of working memory: Emerging general consensus, unresolved theoretical issues, and future research directions. In A. Miyake, & P. Shah (Eds.), *Models of working memory: Mechanisms of active maintenance and executive control* (pp. 442-482). Cambridge: Cambridge University Press.

Miyashita, Y., & Chang, H. S. (1988). Neuronal correlate of pictorial short-term memory in the primate temporal cortex. *Nature, 331*(6151), 68-70.

Naghavi, H. R., & Nyberg, L. (2005). Common fronto-parietal activity in attention, memory, and consciousness: Shared demands on integration? *Consciousness and Cognition, 14*(2), 390-425.

Narayanan, N. S., Prabhakaran, V., Bunge, S. A., Christoff, K., Fine, E. M., & Gabrieli, J. D. E. (2005). The role of the prefrontal cortex in the maintenance of verbal working memory: An event-related FMRI analysis. *Neuropsychology, 19*(2), 223-232.

Natale, E., Marzi, C. A., Girelli, M., Pavone, E. F., & Pollmann, S. (2006). ERP and fMRI correlates of endogenous and exogenous focusing of visual-spatial attention. *European Journal of Neuroscience, 23*(9), 2511-2521.

Nichols, T., Brett, M., Andersson, J., Wager, T., & Poline, J. B. (2005). Valid conjunction inference with the minimum statistic. *NeuroImage, 25*(3), 653-660.

O'Craven, K. M., & Kanwisher, N. (2000). Mental imagery of faces and places activates corresponding stimulus-specific brain regions. *Journal of Cognitive Neuroscience, 12*(6), 1013-1023.

O'Craven, K. M., Rosen, B. R., Kwong, K. K., Treisman, A., & Savoy, R. L. (1997). Voluntary attention modulates fMRI activity in human MT-MST. *Neuron, 18*(4), 591-598.

Ogawa, S., Tank, D. W., Menon, R., Ellermann, J. M., Kim, S. G., Merkle, H., et al. (1992). Intrinsic signal changes accompanying sensory stimulation: Functional brain mapping with magnetic

resonance imaging. *Proceedings of the National Academy of Sciences of the United States of America, 89*(13), 5951-5955.

Oldfield, R. C. (1971). The assessment and analysis of handedness: The Edinburgh inventory. *Neuropsychologia, 9*(1), 97-113.

Olivers, C. N. L., Meijer, F., & Theeuwes, J. (2006). Feature-based memory-driven attentional capture: Visual working memory content affects visual attention. *Journal of Experimental Psychology: Human Perception & Performance, 32*(5), 1243-1265.

O'Reilly, R. C. (1998). Six principles for biologically-based computational models of cortical cognition. *Trends in Cognitive Sciences, 2*(11), 455-462.

O'Reilly, R. C., & Frank, M. J. (2006). Making working memory work: A computational model of learning in the prefrontal cortex and basal ganglia. *Neural Computation, 18*(2), 283-328.

Owen, A. M., Herrod, N. J., Menon, D. K., Clark, J. C., Downey, S. P., Carpenter, T. A., et al. (1999). Redefining the functional organization of working memory processes within human lateral prefrontal cortex. *European Journal of Neuroscience, 11*(2), 567-574.

Owen, A. M., McMillan, K. M., Laird, A. R., & Bullmore, E. (2005). N-back working memory paradigm: A meta-analysis of normative functional neuroimaging studies. *Human Brain Mapping, 25*(1), 46-59.

Paller, K. A., Voss, J. L., & Boehm, S. G. (2007). Validating neural correlates of familiarity. *Trends in Cognitive Sciences, 11*(6), 243-250.

Paulesu, E., Frith, C. D., & Frackowiak, R. S. (1993). The neural correlates of the verbal component of working memory. *Nature, 362*(6418), 342-345.

Paus, T., Koski, L., Caramanos, Z., & Westbury, C. (1998). Regional differences in the effects of task difficulty and motor output on blood flow response in the human anterior cingulate cortex: A review of 107 PET activation studies. *Neuroreport, 9*(9), R37-47.

Petit, L., Courtney, S. M., Ungerleider, L. G., & Haxby, J. V. (1998). Sustained activity in the medial wall during working memory delays. *Journal of Neuroscience, 18*(22), 9429-9437.

Petrides, M., Alivisatos, B., Evans, A. C., & Meyer, E. (1993). Dissociation of human mid-dorsolateral from posterior dorsolateral frontal cortex in memory processing. *Proceedings of the National Academy of Sciences of the United States of America, 90*(3), 873-877.

Picard, N., & Strick, P. L. (1996). Motor areas of the medial wall: A review of their location and functional activation. *Cerebral Cortex, 6*(3), 342-353.

Picard, N., & Strick, P. L. (2001). Imaging the premotor areas. *Current Opinion in Neurobiology, 11*(6), 663-672.

Polich, J. (2004). Neuropsychology of P3a and P3b: A theoretical overview. In N. C. Moore, & K. Arikan (Eds.), *Brainwaves and Mind: Recent Developments* (pp. 15-29). Wheaton, IL: Kjellberg Inc.

Polich, J. (2007). Updating P300: An integrative theory of P3a and P3b. *Clinical Neurophysiology, 118*(10), 2128-2148.

Pollmann, S., & von Cramon, D. Y. (2000). Object working memory and visuospatial processing: Functional neuroanatomy analyzed by event-related fMRI. *Experimental Brain Research, 133*(1), 12-22.

Postle, B. R. (2006). Working memory as an emergent property of the mind and brain. *Neuroscience, 139*(1), 23-38.

Postle, B. R., D'Esposito, M., & Corkin, S. (2005). Effects of verbal and nonverbal interference on spatial and object visual working memory. *Memory & Cognition, 33*(2), 203-212.

Postle, B. R., Druzgal, T. J., & D'Esposito, M. (2003). Seeking the neural substrates of visual working memory storage. *Cortex, 39*(4-5), 927-946.

Postle, B. R., & Hamidi, M. (2007). Nonvisual codes and nonvisual brain areas support visual working memory. *Cerebral Cortex, 17*(9), 2151-2162.

Postle, B. R., Zarahn, E., & D'Esposito, M. (2000). Using event-related fMRI to assess delay-period activity during performance of spatial and nonspatial working memory tasks. *Brain Research. Brain Research Protocols, 5*(1), 57-66.

Pritchard, W. S. (1981). Psychophysiology of P300. *Psychological Bulletin, 89*(3), 506-540.

Ranganath, C., Johnson, M. K., & D'Esposito, M. (2003). Prefrontal activity associated with working memory and episodic long-term memory. *Neuropsychologia, 41*(3), 378-389.

Reinvang, I., Magnussen, S., Greenlee, M. W., & Larsson, P. G. (1998). Electrophysiological localization of brain regions involved in perceptual memory. *Experimental Brain Research, 123*(4), 481-484.

Repovs, G., & Baddeley, A. D. (2006). The multi-component model of working memory: Explorations in experimental cognitive psychology. *Neuroscience, 139*(1), 5-21.

Rickham, P. P. (1964). Human Experimentation. Code of Ethics of the World Medical Association. Declaration of Helsinki. *British Medical Journal, 2*(5402), 177.

Ridderinkhof, K. R., Ullsperger, M., Crone, E. A., & Nieuwenhuis, S. (2004). The role of the medial frontal cortex in cognitive control. *Science, 306*(5695), 443-447.

Ritter, W., Simson, R., & Vaughan, H. G.,Jr. (1988). Effects of the amount of stimulus information processed on negative event-related potentials. *Electroencephalography and Clinical Neurophysiology, 69*(3), 244-258.

Ritter, W., Simson, R., Vaughan, H. G.,Jr, & Macht, M. (1982). Manipulation of event-related potential manifestations of information processing stages. *Science, 218*(4575), 909-911.

Rösler, F. (1988). The P300 event-related potentials: A one-humped dromedary's saddle on a two-humped camel. *Behavioral and Brain Sciences,* (11), 392-393.

Rowe, J. B., Toni, I., Josephs, O., Frackowiak, R. S., & Passingham, R. E. (2000). The prefrontal cortex: Response selection or maintenance within working memory? *Science, 288*(5471), 1656-1660.

Rugg, M. D. (1995). ERP studies of memory. In M. D. Rugg, & M. G. H. Coles (Eds.), *Electrophysiology of Mind: Event-Related Brain Potentials and Cognition.* (pp. 132-170). Oxford: Oxford University Press.

Rugg, M. D., & Coles, M. G. H. (Eds.). (1997). *Electrophysiology of Mind: Event-Related Brain Potentials and Cognition*. Oxford: Oxford University Press.

Rugg, M. D., & Curran, T. (2007). Event-related potentials and recognition memory. *Trends in Cognitive Sciences, 11*(6), 251-257.

Rypma, B., & D'Esposito, M. (1999). The roles of prefrontal brain regions in components of working memory: Effects of memory load and individual differences. *Proceedings of the National Academy of Sciences of the United States of America, 96*(11), 6558-6563.

Rypma, B., Prabhakaran, V., Desmond, J. E., Glover, G. H., & Gabrieli, J. D. (1999). Load-dependent roles of frontal brain regions in the maintenance of working memory. *NeuroImage, 9*(2), 216-226.

Scherg, M., & Berg, P. (1996). New concepts of brain source imaging and localization. *Electroencephalography and Clinical Neurophysiology. Supplement, 46*, 127-137.

Scherg, M., & Von Cramon, D. (1986). Evoked dipole source potentials of the human auditory cortex. *Electroencephalography and Clinical Neurophysiology, 65*(5), 344-360.

Schmiedt, C., Meistrowitz, A., Schwendemann, G., Herrmann, M., & Basar-Eroglu, C. (2005). Theta and alpha oscillations reflect differences in memory strategy and visual discrimination performance in patients with Parkinson's disease. *Neuroscience Letters, 388*(3), 138-143.

Slotnick, S. D. (2005). Source localization of ERP generators. In T. C. Handy (Ed.), *Event-Related Potentials. A Methods Handbook* (pp. 149-166). Cambridge, MA: MIT Press.

Smith, E. E., & Jonides, J. (1997). Working memory: A view from neuroimaging. *Cognitive Psychology, 33*(1), 5-42.

Squires, N., Squires, K., & Hillyard, S. A. (1975). Two varieties of long-latency positive waves evoked by unpredictable auditory stimuli in man. *Electroencephalography and Clinical Neurophysiology,* (38), 387-401.

Stern, C. E., Sherman, S. J., Kirchhoff, B. A., & Hasselmo, M. E. (2001). Medial temporal and prefrontal contributions to working memory tasks with novel and familiar stimuli. *Hippocampus, 11*(4), 337-346.

Sternberg, S. (1966). High-speed scanning in human memory. *Science, 153*(736), 652-654.

Sutton, S., Braren, M., Zubin, J., & John, E. R. (1965). Evoked-potential correlates of stimulus uncertainty. *Science, 150*(700), 1187-1188.

Swainson, R., Cunnington, R., Jackson, G. M., Rorden, C., Peters, A. M., Morris, P. G., et al. (2003). Cognitive control mechanisms revealed by ERP and fMRI: Evidence from repeated task-switching. *Journal of Cognitive Neuroscience, 15*(6), 785-799.

Talairach, J., & Tournoux, P. (1988). *Co-Planar Stereotaxic Atlas of the Human Brain*. Stuttgart, Germany: Georg Thieme Verlag.

Tallon-Baudry, C., & Bertrand, O. (1999). Oscillatory gamma activity in humans and its role in object representation. *Trends in Cognitive Sciences, 3*(4), 151-162.

Taylor, K., Mandon, S., Freiwald, W. A., & Kreiter, A. K. (2005). Coherent oscillatory activity in monkey area V4 predicts successful allocation of attention. *Cerebral Cortex, 15*(9), 1424-1437.

Treue, S., & Maunsell, J. H. (1996). Attentional modulation of visual motion processing in cortical areas MT and MST. *Nature, 382*(6591), 539-541.

Van Essen, D. C., Maunsell, J. H., & Bixby, J. L. (1981). The middle temporal visual area in the macaque: Myeloarchitecture, connections, functional properties and topographic organization. *Journal of Comparative Neurology, 199*(3), 293-326.

Van Veen, V., Cohen, J. D., Botvinick, M. M., Stenger, V. A., & Carter, C. S. (2001). Anterior cingulate cortex, conflict monitoring, and levels of processing. *NeuroImage, 14*(6), 1302-1308.

Verleger, R. (1997). On the utility of P3 latency as an index of mental chronometry. *Psychophysiology, 34*(2), 131-156.

Verleger, R. (2008). P3b: Towards some decision about memory. *Clinical Neurophysiology, 119*(4), 968-970.

Vogel, E. K., & Luck, S. J. (2000). The visual N1 component as an index of a discrimination process. *Psychophysiology, 37*(2), 190-203.

Von Zerssen, D. (1994). Persönlichkeitszüge als Vulnerabilitätsindikatoren - Probleme bei ihrer Erfassung. *Fortschritte der Neurologie-Psychiatrie, 62*, 1-13.

Wager, T. D., & Smith, E. E. (2003). Neuroimaging studies of working memory: A meta-analysis. *Cognitive, Affective and Behavioral Neuroscience, 3*(4), 255-274.

Wijers, A. A., Mulder, G., Okita, T., & Mulder, L. J. (1989). Event-related potentials during memory search and selective attention to letter size and conjunctions of letter size and color. *Psychophysiology, 26*(5), 529-547.

Wittfoth, M., Buck, D., Fahle, M., & Herrmann, M. (2006). Comparison of two simon tasks: Neuronal correlates of conflict resolution based on coherent motion perception. *NeuroImage, 32*(2), 921-929.

Wolf, R. C., Vasic, N., & Walter, H. (2006). Differential activation of ventrolateral prefrontal cortex during working memory retrieval. *Neuropsychologia, 44*(12), 2558-2563.

Yoon, J. H., Curtis, C. E., & D'Esposito, M. (2006). Differential effects of distraction during working memory on delay-period activity in the prefrontal cortex and the visual association cortex. *NeuroImage, 29*(4), 1117-1126.

Zarahn, E., Rakitin, B., Abela, D., Flynn, J., & Stern, Y. (2005). Positive evidence against human hippocampal involvement in working memory maintenance of familiar stimuli. *Cerebral Cortex, 15*(3), 303-316.

Zeki, S., Watson, J. D., Lueck, C. J., Friston, K. J., Kennard, C., & Frackowiak, R. S. (1991). A direct demonstration of functional specialization in human visual cortex. *Journal of Neuroscience, 11*(3), 641-649.

Zhang, J. X., Leung, H. C., & Johnson, M. K. (2003). Frontal activations associated with accessing and evaluating information in working memory: An fMRI study. *NeuroImage, 20*(3), 1531-1539.

List of Tables

List of Figures

List of Text boxes

Acknowledgements

I would like to thank everyone who contributed to this doctoral thesis in some way.

Especially, I want to express my gratitude to my supervisor, Prof. Dr. Dr. Manfred Herrmann, for providing the opportunity to accomplish my thesis in his department and for his invaluable support and guidance. Furthermore, I would like to thank my second adviser, Prof. Dr. Andreas K. Kreiter, for his kind support and inspiring cooperation.

This thesis would not have been possible without my mentor Thorsten Fehr, who kindly taught me to do research and gave me professional advice whenever required.

Katja Schmuck actively accompanied the entire process of this project, she provided invaluable assistance professionally as well as personally. Sina Alexa Trautmann has provided support in numerous ways: she shared this experience and motivated me whenever I needed it. I am grateful that I could enjoy the impressive teamwork with her.

Furthermore, I would like to express my gratitude to my other colleagues:

Sascha Clamer (technical support), Barbara Muntz (moral support), Stephan Miedl, Sascha Frühholz and Daniel Wiswede for useful discussions and collegial support. Ekkehard Küstermann, Peter Erhard and Melanie Löbe for support with regard to the fMRI measurements and Wolf Zinke for an informative cooperation with inspiring discussions. Furthermore, I would like to thank Caroline Haak for her kindly assistance in EEG data recording.

Sincere thanks go to Karsten Hoechstetter for support with regard to the BESA® software and to Christoph Bledowski for providing the Talairach-transformed MNI template. The volunteers are thanked for their participation in the experiments. Moreover, I would like to express my gratitude to Annette Göddemeyer and Christina Regenbogen who proofread this work.

Many thanks to my friends Maren Maetze, Frauke Husmann, Patricia Pennacchio and Gudrun Wessling who enlightened the whole process with mental support and distraction.

I am grateful to my family, particularly to my parents Angelika and Klaus Buck, my sister Dorothee and my grandparents Hannelore and Heinrich Briel. You all gave me strength and motivation. Thank you for your understanding and patience when I was busy.

Special thanks go to Orlando, for your tireless support and just for being you, the best husband ever. Julina Sophie, I would like to thank you for such a wonderful pregnancy, you let me know when I had to slow down and you gave me enough time to complete this work. Your presence lighted up the writing time and now you light up our whole life. Thank you!

Appendix

Appendix A: Consent Form - General

Universität Bremen

Abteilung für Neuropsychologie & Verhaltensneurobiologie

Einwilligungserklärung

für die Teilnahme am Projekt von Dipl.-Psych. Daniela Galashan

Proband/in: _____ Geburtsdatum: _____

Mir ist bekannt, dass die Teilnahme an der wissenschaftlichen Studie freiwillig ist und ich sie jederzeit ohne Angabe von Gründen und ohne persönlichen Nachteil widerrufen kann. Meine Daten werden dann vollständig gelöscht.

Über Art und Durchführung der geplanten ❒ neuropsychologischen Untersuchung / ❒ EEG- / ❒ MRT-Untersuchung im Rahmen dieser wissenschaftlichen Studie hat mich Frau/Herr _____ in einem Aufklärungsgespräch ausführlich informiert. Auch habe ich das entsprechende Informationsblatt gelesen (im Fall einer EEG- und/oder MRT-Untersuchung). Ich konnte alle mir wichtig erscheinenden Fragen, z.B. über spezielle Risiken und mögliche Komplikationen und über Neben- und Folgemaßnahmen stellen, die zur Vorbereitung oder während der Untersuchung erforderlich sind. Die mir erteilten Informationen habe ich inhaltlich verstanden.

Ich weiß, dass bei der Untersuchung persönliche Daten elektronisch erfasst und anonym in einer für die Öffentlichkeit nicht zugänglichen Datenbank gespeichert werden. Informationen zu Ihrer Person werden im Rahmen datenschutzrechtlicher Bedingungen verwaltet. Sie werden mittels elektronischer Datenverarbeitung weiterverarbeitet, nur für dieses Forschungsvorhaben verwendet und eventuell im Rahmen wissenschaftlicher Veröffentlichungen eingesetzt. Sobald es der Forschungszweck zulässt, werden die personenbezogenen Daten gelöscht bzw. vernichtet. Dieses wird spätestens im Dezember 2009 sein.

Die Verantwortlichkeit für die Daten obliegt der „Abteilung für Neuropsychologie & Verhaltensneurobiologie“ der Universität Bremen.

Sollte ich zur Speicherung meiner Daten Fragen haben oder Auskünfte benötigen, kann ich mich an die folgenden Personen wenden:

- Dipl.-Psych. Daniela Galashan (Tel.: 0421-218-2863)
- Prof. Dr. Dr. M. Herrmann (Sekretariat Frau Muntz: 0421-218-8225)

Ich bin mit der anonymisierten Speicherung, Verarbeitung und Veröffentlichung dieser Daten einverstanden. Auch diese Einwilligung kann ich jederzeit ohne Angabe von Gründen widerrufen.

Ich gebe hiermit meine Einwilligung, dass bei mir im Rahmen eines Forschungsvorhabens Verhaltensdaten erhoben und/oder eine EEG- und/oder eine MRT-Untersuchung (wie oben angekreuzt) des Gehirns durchgeführt wird/werden.

Das Probandeninformationsblatt (im Falle einer EEG- und/oder MRT-Untersuchung) sowie ein Exemplar dieser Einwilligungserklärung habe ich erhalten.

1. Messung		
Ort, Datum	Unterschrift: Patient/Proband	Unterschrift: Untersucher
2. Messung		
Ort, Datum	Unterschrift: Patient/Proband	Unterschrift: Untersucher

Appendix B (1): Information on fMRI measurement – Part I (general)

Informationsblatt für Probanden

Sehr geehrte Probandin, sehr geehrter Proband,

vielen Dank für Ihr Interesse an einer Studie, bei der die Aktivität im Gehirn während des Lösens von Aufgaben untersucht werden soll.
Wir möchten Sie zunächst über den Ablauf informieren, um Ihnen einen Überblick über die geplanten Messungen zu ermöglichen und Ihnen das Ziel der Untersuchung zu erklären. Die Untersuchungen werden mit einem Magnetresonanztomographen (kurz MRT) durchgeführt, der uns Messungen der Durchblutung im Gehirn schmerzfrei und ohne zusätzliche Gabe von Medikamenten ermöglicht. Einige Personen werden die Untersuchung schon einmal erlebt haben, wenn hochauflösende Bilder vom Kopf im Rahmen der medizinischen Diagnostik durchgeführt wurden.

Ziel der Untersuchung

Die Studie soll die Aktivität im Gehirn während der Durchführung einer visuell präsentierten Aufgabe bestimmen.

Was ist eine Magnetresonanztomographie?

Im Rahmen der Studie ist eine funktionelle Magnetresonanztomographie des Gehirns vorgesehen. Mit Hilfe dieser Methode ist es möglich, die Durchblutung in Ihrem Gehirn zu messen und daraus Rückschlüsse auf die bei der Aufgabe beteiligten Bereiche zu ziehen.
Hierbei treffen Radiowellen, die in dem Magnetfeld erzeugt worden sind, auf den Körper, der Signale zurückschickt. Diese Echosignale werden von speziellen Antennen aufgefangen und in einem Computer ausgewertet.
Ein Kontrastmittel ist **nicht** erforderlich. Es werden **keine** Röntgenstrahlen eingesetzt.

Wie läuft die Untersuchung ab?

Vor der Untersuchung werden Sie vom Untersuchungsleiter ausführlich über die für den Tag geplanten Messungen und Ziele informiert. Sie haben das Recht, ohne Angabe von Gründen die Teilnahme an der Messung abzulehnen. Auch im Verlauf der Untersuchung werden Sie vom Untersucher jederzeit gehört. Für die Untersuchung müssen Sie sich auf eine Liege legen. Im Messbereich wird eine Kopfspule angebracht. Mit der Liege werden Sie dann langsam in die Röhre des Kernspintomographen geschoben. Dort befinden Sie sich während der gesamten Untersuchung, die normalerweise 60 Minuten dauert, in einem starken Magnetfeld, das für die Untersuchung benötigt wird. Während der eigentlichen Messung sind sehr laute Klopfgeräusche zu hören, die völlig normal sind und von elektromagnetischen Schaltungen herrühren. Das Magnetfeld selbst können Sie weder spüren noch hören. Es ist für die Qualität der Messungen von großer Bedeutung, dass Sie während der Untersuchung möglichst ruhig liegen bleiben. Um dies zu erleichtern, werden Ihr Kopf und Arme mit Polstern und anderen Hilfsmitteln schmerzfrei gelagert. Die Aufgaben, die Sie während der Untersuchung zu bearbeiten haben, werden Ihnen über einen an der Kopfspule angebrachten Spiegel dargeboten.

Appendix B (2): Information on fMRI measurement – Part II (risks)

Mögliche Risiken der Methode?

Der Kernspintomograph hält alle für die Sicherheit des Betriebes und insbesondere die Sicherheit der Probanden erforderlichen Grenzwerte ein. Er wurde vom TÜV einer Sicherheitsprüfung unterzogen und wird darüber hinaus in den vorgeschriebenen Intervallen überprüft. Dennoch müssen folgende Punkte beachtet werden.

1. Auf ferromagnetische Gegenstände (z.B. Gegenstände, die Eisen oder Nickel enthalten) im Bereich des Magneten (z.B. Messer, Schraubenzieher, Kugelschreiber, Münzen, Haarspangen, ..) wird eine starke Anziehungskraft ausgeübt. Dadurch werden die Gegenstände mit großer Geschwindigkeit in den Magneten gezogen und können Personen erheblich verletzen.
2. Metallkörper und andere Fremdkörper wie Geschossteile können ebenfalls ferromagnetisch sein, durch magnetische Kräfte ihre Position im Körper verändern und dadurch innere Verletzungen hervorrufen.
3. Kleine Metallsplitter im Auge können durch magnetische Kräfte bewegt oder gedreht werden und das Auge verletzen.
4. Personen mit Chochlea-Implantaten, Defibrillatoren oder Pumpensystemen sollten nicht einem starken Magnetfeld ausgesetzt werden, da es auch in diesen Fällen zu Risiken durch magnetische Kräfte kommen kann.
5. Herzschrittmacher können im Magnetfeld ihre Funktionsfähigkeit verlieren. Deshalb dürfen Personen mit Herzschrittmachern nicht an Untersuchungen teilnehmen.
6. Bei der Messung mit dem Kernspintomographen kommt es zur Abstrahlung von hochfrequenter elektromagnetischer Strahlung, wie sie z.B. bei Radiosendern und Funktelefonen auftritt. Dies kann zu einer geringfügigen Erwärmung des untersuchten Gewebes führen.
7. Das Schalten der Magnetfeldgradienten führt in Teilen des Gradientensystems zu mechanischen Verformungen, die Geräusche mit Lautstärken über 100 dB erzeugen können. Deshalb müssen Sie bei allen Messungen entweder schallabsorbierende Kopfhörer oder Lärmschutzstopfen tragen, die von uns zur Verfügung gestellt werden. Bei Einhaltung dieser Vorsichtsmaßnahmen kann eine Schädigung des Hörsystems ausgeschlossen werden.
8. Manche Menschen erleben enge Räume als bedrohlich. Sie berichten über Unwohlsein z.B. in Fahrstühlen oder in großen Menschenansammlungen. Obwohl diese Angsterkrankung meist über die Anamnese ausgeschlossen werden kann, ist ein erstmaliges Auftreten während der Messung im Kernspintomographen möglich. Der Untersucher ist bei der Messung anwesend; bei dem Auftreten von Symptomen kann der Proband über Sprechkontakt bzw. über eine Notklingel jederzeit auf sich aufmerksam machen, so dass bei Symptomen eine rasche Intervention gewährleistet ist.

Appendix C: Questionnaire with exclusion criteria for fMRI measurements

Fragebogen für Teilnehmer/innen an Kernspinresonanzuntersuchungen

Name:.....
Vorname:.....Geschlecht:.....
Geburtsdatum:.....
Straße/Hausnummer:.....
Wohnort:.....
Telefon:.....
Beruf:.....

Beantworten Sie bitte folgende Fragen zu möglichen Gegenanzeigen für Ihre Teilnahme an den Untersuchungen (Zutreffendes unterstreichen):

Sind Sie Träger eines Herzschrittmachers oder anderer elektrischer Geräte?	□ ja	□ weiß nicht	□ nein
Besitzen Sie metallische Implantate (z.B. Zahnschrauben oder metallische, mechanische Verhütungsmittel)?	□ ja	□ weiß nicht	□ nein
Befinden sich in Ihrem Körper andere metallische Fremdkörper?	□ ja	□ weiß nicht	□ nein
Wurde bei Ihnen eine Gefäßoperation durchgeführt?	□ ja	□ weiß nicht	□ nein
Haben Sie eine Allergie gegen Medikamente?	□ ja	□ weiß nicht	□ nein
Haben Sie Piercings oder Tätowierungen?	□ ja	□ weiß nicht	□ nein
Haben Sie jemals eine allergische Reaktion auf die Gabe eines Kontrastmittels gehabt?	□ ja	□ weiß nicht	□ nein
Leiden Sie unter Platzangst?	□ ja	□ weiß nicht	□ nein
Sind bei Ihnen oder in Ihrer Familie Anfallsleiden (Epilepsie, Fallsucht) aufgetreten?	□ ja	□ weiß nicht	□ nein
Besteht die Möglichkeit, dass Sie schwanger sind?	□ ja	□ weiß nicht	□ nein

Beantworten Sie bitte folgende für unsere Untersuchungen wichtigen Fragen:

Sind Sie linkshändig?	□ ja	□ weiß nicht	□ nein
Sind Sie Brillenträger/in?	□ ja	□ weiß nicht	□ nein
Tragen Sie Kontaktlinsen?	□ ja	□ weiß nicht	□ nein
Haben Sie Hörprobleme?	□ ja	□ weiß nicht	□ nein
Sind Sie mehrsprachig aufgewachsen?	□ ja	□ weiß nicht	□ nein

Ich habe alle Fragen auf dieser Seite wahrheitsgemäß und nach bestem Wissen beantwortet.

_____ _____
Ort, Datum Unterschrift der Probandin/des Probanden

Appendix D: Consent Form for fMRI measurements

Einwilligungserklärung

Über die geplante kernspintomographische Untersuchung im Rahmen einer wissenschaftlichen Studie hat mich Frau / Herr ..... in einem Aufklärungsgespräch ausführlich informiert. Auch habe ich das entsprechende Informationsblatt gelesen und den Fragebogen zu möglichen Ausschlusskriterien ausgefüllt.
Ich konnte alle mir wichtig erscheinenden Fragen, z.B. über die in meinem Fall speziellen Risiken und möglichen Komplikationen und über die Neben- und Folgemaßnahmen stellen, die zur Vorbereitung oder während der Untersuchung erforderlich sind.

Die mir erteilten Informationen habe ich inhaltlich verstanden. Mir ist bekannt, dass ich meine Einwilligung jederzeit ohne Angaben von Gründen widerrufen kann.
Ich weiß, dass die bei Untersuchungen mit mir gewonnenen Daten auf der Basis elektronischer Datenverarbeitung weiterverarbeitet und eventuell für wissenschaftliche Veröffentlichungen verwendet werden sollen.
Ich bin mit der anonymisierten Verarbeitung und Veröffentlichung dieser Daten einverstanden. Auch diese Einwilligung kann ich jederzeit ohne Angabe von Gründen widerrufen.

Ich gebe hiermit meine Einwilligung, dass bei mir im Rahmen eines Forschungsvorhabens eine Kernspintomographie des Gehirns durchgeführt wird.

Ich erkläre mich damit einverstanden, dass meine persönlichen Daten in einer für die Öffentlichkeit nicht zugänglichen Datenbank erfasst werden. Die Speicherung meiner Daten dient ausschließlich der Möglichkeit einer erneuten Kontaktaufnahme des Instituts zum Zwecke der Vereinbarung weiterer Untersuchungen.
Informationen zu Ihrer Person werden im Rahmen datenschutzrechtlicher Bedingungen verwaltet.

Ort, Datum	Unterschrift Proband/in	Unterschrift Untersucher/in

PROBANDENCODE:_____

Appendix E: Example page of the Encoding Questionnaire used in Experiment 1. All shapes are shown in Figure 2 (see page 21).

Wie haben Sie sich die links abgebildete Figur gemerkt? (Es können immer mehrere Möglichkeiten angekreuzt werden)	**Wie oft haben Sie sich die Figur so gemerkt?**				
☐ als ..... bezeichnet	☐ immer	☐ häufig	☐ manchmal	☐ selten	☐nie
☐ Anzahl der Ecken gemerkt	☐ immer	☐ häufig	☐ manchmal	☐ selten	☐nie
☐ Richtung der Ecken gemerkt (wenn es bestimmte Ecken waren, in der Figur umkreisen)	☐ immer	☐ häufig	☐ manchmal	☐ selten	☐nie
☐ ein bestimmtes Merkmal der Figur gemerkt, nämlich.....(in der Figur umkreisen)	☐ immer	☐ häufig	☐ manchmal	☐ selten	☐nie

Wie haben Sie sich die links abgebildete Figur gemerkt?	**Wie oft haben Sie sich die Figur so gemerkt?**				
☐ als ..... bezeichnet	☐ immer	☐ häufig	☐ manchmal	☐ selten	☐nie
☐ Anzahl der Ecken gemerkt	☐ immer	☐ häufig	☐ manchmal	☐ selten	☐nie
☐ Richtung der Ecken gemerkt (wenn es bestimmte Ecken waren, in der Figur umkreisen)	☐ immer	☐ häufig	☐ manchmal	☐ selten	☐nie
☐ ein bestimmtes Merkmal der Figur gemerkt, nämlich.....(in der Figur umkreisen)	☐ immer	☐ häufig	☐ manchmal	☐ selten	☐nie

Wie haben Sie sich die links abgebildete Figur gemerkt?	**Wie oft haben Sie sich die Figur so gemerkt?**				
☐ als ..... bezeichnet	☐ immer	☐ häufig	☐ manchmal	☐ selten	☐nie
☐ Anzahl der Ecken gemerkt	☐ immer	☐ häufig	☐ manchmal	☐ selten	☐nie
☐ Richtung der Ecken gemerkt (wenn es bestimmte Ecken waren, in der Figur umkreisen)	☐ immer	☐ häufig	☐ manchmal	☐ selten	☐nie
☐ ein bestimmtes Merkmal der Figur gemerkt, nämlich.....(in der Figur umkreisen)	☐ immer	☐ häufig	☐ manchmal	☐ selten	☐nie

Appendix F: Post-test evaluation questions used after all experiments.

Uns interessieren nun abschließend folgende Fragen:

- Wie schätzen Sie momentan ihre Müdigkeit ein (auf einer Skala von 1[wenig] bis 10 [viel])? .....
- Und ihr psychisches **Wohlbefinden** (auf einer Skala von 1[wenig] bis 10 [viel])? .....
- Wie würden Sie persönlich die Aufgabenschwierigkeit auf einer Skala von 1-10 (1=sehr leicht, 10=sehr schwer) beurteilen? .....
- Wie viele unterschiedliche Zeitepochen sind Ihnen aufgefallen? .....
- Hatten Sie Schwierigkeiten (z.B. mangelnde Konzentration, Instruktionsschwierigkeiten, etc.) während der Messung? Wenn ja, welche?
  .....
  .....
- Sind Ihnen Gesetzmäßigkeiten, beispielsweise in der Abfolge der Figuren, etc. aufgefallen? Wenn ja, welche?
  .....
  .....
- Haben Sie sonstige Anmerkungen zum Experiment?
  .....
  .....
  .....

Appendix G: Glass brains showing activation patterns obtained with a conjunction analysis for the maintenance of complex trials vs. maintenance of simple circle trials, over all delay durations (FDR-corrected, p<.001).

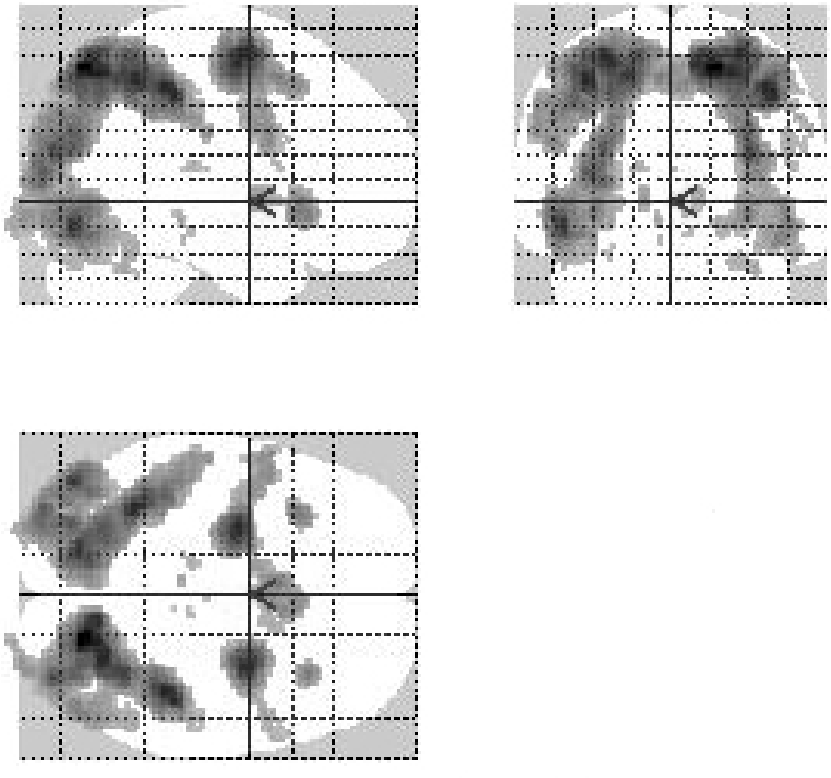

Appendix H: Information on EEG measurement

Informationsblatt für Probanden

Sehr geehrte Probandin, sehr geehrter Proband,

vielen Dank für Ihr Interesse an einer Studie, bei der die Aktivität im Gehirn während des Lösens von Aufgaben untersucht werden soll.

Wir möchten Sie zunächst über den Ablauf informieren, um Ihnen einen Überblick über die geplanten Messungen zu ermöglichen und Ihnen das Ziel der Untersuchung zu erklären. Die Untersuchungen werden mit Hilfe der Elektroenzephalographie (kurz EEG) durchgeführt, die Messungen der Nervenzell-Aktivität im Gehirn ohne Eingriff, schmerzfrei und ohne zusätzliche Gabe von Medikamenten ermöglicht.

Ziel der Untersuchung

Die Studie soll die Aktivität im Gehirn während der Durchführung einer visuell präsentierten Aufgabe bestimmen.

Was ist ein Elektroenzephalogramm (EEG)?

Aufgrund der Aktivität der Nervenzellen lässt sich an der Kopfoberfläche fortlaufend eine elektrische Spannung messen – das Elektroenzephalogramm (EEG). Für die EEG-Messung müssen an verschiedenen Stellen des Kopfes Elektroden platziert werden, die eine Verbindung zwischen Kopfoberfläche und Messgerät herstellen.

Die Elektroden bestehen aus Silber/Silberchlorid, Zinn oder Gold. Zur Verbesserung der Leitfähigkeit wird eine Paste verwendet, die im Wesentlichen aus Wasser, Kochsalz und Verdickungsmittel besteht. Um zwischen Haut und Elektrode einen hinreichend guten Kontakt herzustellen, werden die Elektroden an einer speziellen Haube, ähnlich einer Badekappe, fixiert.

Wie läuft die Untersuchung ab?

Vor der Untersuchung werden Sie vom Untersuchungsleiter ausführlich über die für den Tag geplanten Messungen und Ziele informiert. Sie haben das Recht, jederzeit ohne Angabe von Gründen und ohne persönlichen Nachteil, die Teilnahme an der Messung abzulehnen oder während der Messung abzubrechen.

Während der Messung sitzen Sie auf einem Stuhl. Um Störungen der Messung zu vermeiden, findet die Untersuchung in einem eigenen, abgeschirmten und störungsarmen Raum statt. Während der Messung sind Sie zusammen mit einem Mitarbeiter der Abteilung in einem Raum und können sich jederzeit an ihn wenden.

Mögliche Risiken der Methode?

Die EEG-Messung ist vollständig gefahrlos. Für das EEG werden nur solche Geräte verwendet, die den einschlägigen Sicherheitsbestimmungen genügen. Sie werden in gleicher Form auch für die klinische Routine eingesetzt.

Appendix I: Encoding questionnaire showing all stimuli used in the EEG session of Experiment 2.

Fragebogen zur Merkstrategie der einzelnen Zielreize [EEG]
VPN-code: Datum:

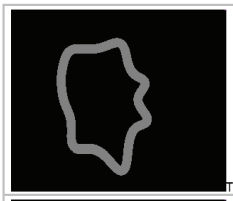 T102	☐ Figur wurde hauptsächlich durch Anzahl & Richtung der Ecken oder ein charakteristisches Merkmal gemerkt (bitte markieren).	☐ Figur wurde hauptsächlich als ..... bezeichnet.	☐ Figur wurde hauptsächlich anders gemerkt, und zwar	☐ erinnere diese Figur, bzw. meine angewandte Merkstrategie nicht
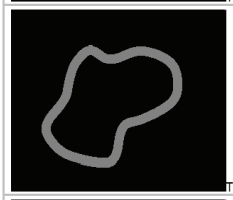 T103	☐ Figur wurde hauptsächlich durch Anzahl & Richtung der Ecken oder ein charakteristisches Merkmal gemerkt (bitte markieren).	☐ Figur wurde hauptsächlich als ..... bezeichnet.	☐ Figur wurde hauptsächlich anders gemerkt, und zwar	☐ erinnere diese Figur, bzw. meine angewandte Merkstrategie nicht
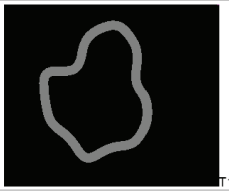 T105	☐ Figur wurde hauptsächlich durch Anzahl & Richtung der Ecken oder ein charakteristisches Merkmal gemerkt (bitte markieren).	☐ Figur wurde hauptsächlich als ..... bezeichnet.	☐ Figur wurde hauptsächlich anders gemerkt, und zwar	☐ erinnere diese Figur, bzw. meine angewandte Merkstrategie nicht
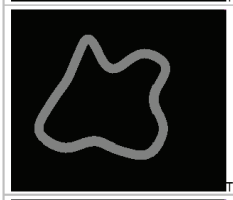 T108	☐ Figur wurde hauptsächlich durch Anzahl & Richtung der Ecken oder ein charakteristisches Merkmal gemerkt (bitte markieren).	☐ Figur wurde hauptsächlich als ..... bezeichnet.	☐ Figur wurde hauptsächlich anders gemerkt, und zwar	☐ erinnere diese Figur, bzw. meine angewandte Merkstrategie nicht
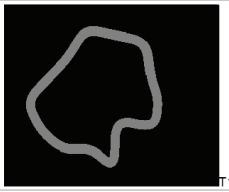 T110	☐ Figur wurde hauptsächlich durch Anzahl & Richtung der Ecken oder ein charakteristisches Merkmal gemerkt (bitte markieren).	☐ Figur wurde hauptsächlich als ..... bezeichnet.	☐ Figur wurde hauptsächlich anders gemerkt, und zwar	☐ erinnere diese Figur, bzw. meine angewandte Merkstrategie nicht
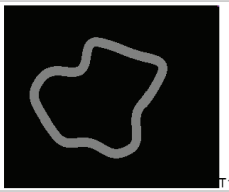 T112	☐ Figur wurde hauptsächlich durch Anzahl & Richtung der Ecken oder ein charakteristisches Merkmal gemerkt (bitte markieren).	☐ Figur wurde hauptsächlich als ..... bezeichnet.	☐ Figur wurde hauptsächlich anders gemerkt, und zwar	☐ erinnere diese Figur, bzw. meine angewandte Merkstrategie nicht
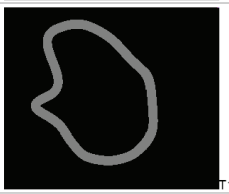 T128	☐ Figur wurde hauptsächlich durch Anzahl & Richtung der Ecken oder ein charakteristisches Merkmal gemerkt (bitte markieren).	☐ Figur wurde hauptsächlich als ..... bezeichnet.	☐ Figur wurde hauptsächlich anders gemerkt, und zwar	☐ erinnere diese Figur, bzw. meine angewandte Merkstrategie nicht
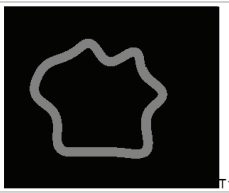 T129	☐ Figur wurde hauptsächlich durch Anzahl & Richtung der Ecken oder ein charakteristisches Merkmal gemerkt (bitte markieren).	☐ Figur wurde hauptsächlich als ..... bezeichnet.	☐ Figur wurde hauptsächlich anders gemerkt, und zwar	☐ erinnere diese Figur, bzw. meine angewandte Merkstrategie nicht

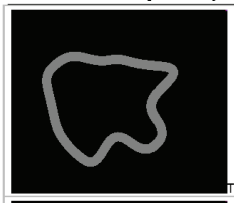 T130	☐ Figur wurde hauptsächlich durch Anzahl & Richtung der Ecken oder ein charakteristisches Merkmal gemerkt (bitte markieren).	☐ Figur wurde hauptsächlich als ..... bezeichnet.	☐ Figur wurde hauptsächlich anders gemerkt, und zwar	☐ erinnere diese Figur, bzw. meine angewandte Merkstrategie nicht
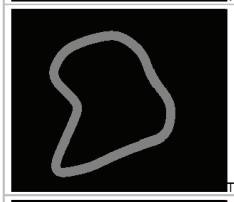 T133	☐ Figur wurde hauptsächlich durch Anzahl & Richtung der Ecken oder ein charakteristisches Merkmal gemerkt (bitte markieren).	☐ Figur wurde hauptsächlich als ..... bezeichnet.	☐ Figur wurde hauptsächlich anders gemerkt, und zwar	☐ erinnere diese Figur, bzw. meine angewandte Merkstrategie nicht
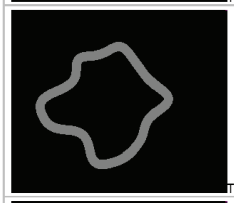 T138	☐ Figur wurde hauptsächlich durch Anzahl & Richtung der Ecken oder ein charakteristisches Merkmal gemerkt (bitte markieren).	☐ Figur wurde hauptsächlich als ..... bezeichnet.	☐ Figur wurde hauptsächlich anders gemerkt, und zwar	☐ erinnere diese Figur, bzw. meine angewandte Merkstrategie nicht
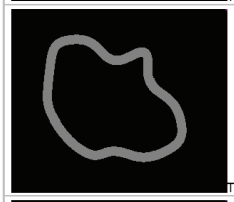 T139	☐ Figur wurde hauptsächlich durch Anzahl & Richtung der Ecken oder ein charakteristisches Merkmal gemerkt (bitte markieren).	☐ Figur wurde hauptsächlich als ..... bezeichnet.	☐ Figur wurde hauptsächlich anders gemerkt, und zwar	☐ erinnere diese Figur, bzw. meine angewandte Merkstrategie nicht
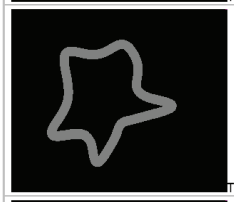 T14	☐ Figur wurde hauptsächlich durch Anzahl & Richtung der Ecken oder ein charakteristisches Merkmal gemerkt (bitte markieren).	☐ Figur wurde hauptsächlich als ..... bezeichnet.	☐ Figur wurde hauptsächlich anders gemerkt, und zwar	☐ erinnere diese Figur, bzw. meine angewandte Merkstrategie nicht
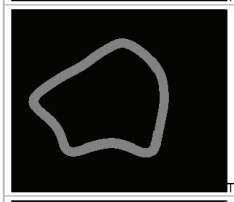 T141	☐ Figur wurde hauptsächlich durch Anzahl & Richtung der Ecken oder ein charakteristisches Merkmal gemerkt (bitte markieren).	☐ Figur wurde hauptsächlich als ..... bezeichnet.	☐ Figur wurde hauptsächlich anders gemerkt, und zwar	☐ erinnere diese Figur, bzw. meine angewandte Merkstrategie nicht
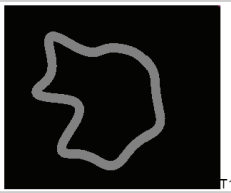 T143	☐ Figur wurde hauptsächlich durch Anzahl & Richtung der Ecken oder ein charakteristisches Merkmal gemerkt (bitte markieren).	☐ Figur wurde hauptsächlich als ..... bezeichnet.	☐ Figur wurde hauptsächlich anders gemerkt, und zwar	☐ erinnere diese Figur, bzw. meine angewandte Merkstrategie nicht
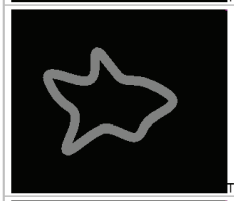 T146	☐ Figur wurde hauptsächlich durch Anzahl & Richtung der Ecken oder ein charakteristisches Merkmal gemerkt (bitte markieren).	☐ Figur wurde hauptsächlich als ..... bezeichnet.	☐ Figur wurde hauptsächlich anders gemerkt, und zwar	☐ erinnere diese Figur, bzw. meine angewandte Merkstrategie nicht
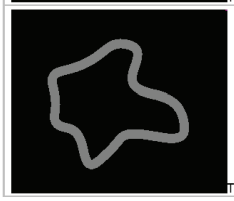 T166	☐ Figur wurde hauptsächlich durch Anzahl & Richtung der Ecken oder ein charakteristisches Merkmal gemerkt (bitte markieren).	☐ Figur wurde hauptsächlich als ..... bezeichnet.	☐ Figur wurde hauptsächlich anders gemerkt, und zwar	☐ erinnere diese Figur, bzw. meine angewandte Merkstrategie nicht

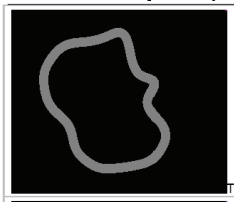 T176	☐ Figur wurde hauptsächlich durch Anzahl & Richtung der Ecken oder ein charakteristisches Merkmal gemerkt (bitte markieren).	☐ Figur wurde hauptsächlich als ..... bezeichnet.	☐ Figur wurde hauptsächlich anders gemerkt, und zwar	☐ erinnere diese Figur, bzw. meine angewandte Merkstrategie nicht
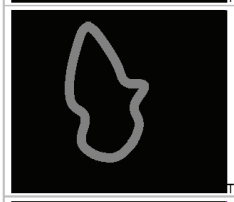 T177	☐ Figur wurde hauptsächlich durch Anzahl & Richtung der Ecken oder ein charakteristisches Merkmal gemerkt (bitte markieren).	☐ Figur wurde hauptsächlich als ..... bezeichnet.	☐ Figur wurde hauptsächlich anders gemerkt, und zwar	☐ erinnere diese Figur, bzw. meine angewandte Merkstrategie nicht
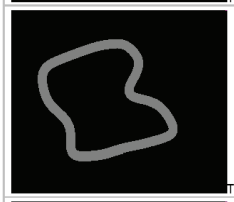 T18	☐ Figur wurde hauptsächlich durch Anzahl & Richtung der Ecken oder ein charakteristisches Merkmal gemerkt (bitte markieren).	☐ Figur wurde hauptsächlich als ..... bezeichnet.	☐ Figur wurde hauptsächlich anders gemerkt, und zwar	☐ erinnere diese Figur, bzw. meine angewandte Merkstrategie nicht
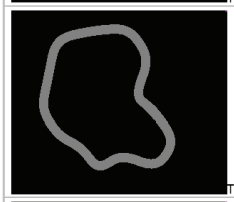 T181	☐ Figur wurde hauptsächlich durch Anzahl & Richtung der Ecken oder ein charakteristisches Merkmal gemerkt (bitte markieren).	☐ Figur wurde hauptsächlich als ..... bezeichnet.	☐ Figur wurde hauptsächlich anders gemerkt, und zwar	☐ erinnere diese Figur, bzw. meine angewandte Merkstrategie nicht
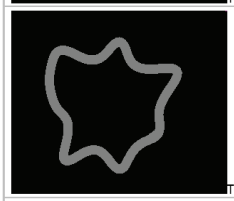 T182	☐ Figur wurde hauptsächlich durch Anzahl & Richtung der Ecken oder ein charakteristisches Merkmal gemerkt (bitte markieren).	☐ Figur wurde hauptsächlich als ..... bezeichnet.	☐ Figur wurde hauptsächlich anders gemerkt, und zwar	☐ erinnere diese Figur, bzw. meine angewandte Merkstrategie nicht
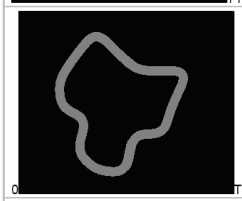 T190	☐ Figur wurde hauptsächlich durch Anzahl & Richtung der Ecken oder ein charakteristisches Merkmal gemerkt (bitte markieren).	☐ Figur wurde hauptsächlich als ..... bezeichnet.	☐ Figur wurde hauptsächlich anders gemerkt, und zwar	☐ erinnere diese Figur, bzw. meine angewandte Merkstrategie nicht
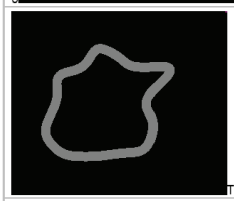 T192	☐ Figur wurde hauptsächlich durch Anzahl & Richtung der Ecken oder ein charakteristisches Merkmal gemerkt (bitte markieren).	☐ Figur wurde hauptsächlich als ..... bezeichnet.	☐ Figur wurde hauptsächlich anders gemerkt, und zwar	☐ erinnere diese Figur, bzw. meine angewandte Merkstrategie nicht
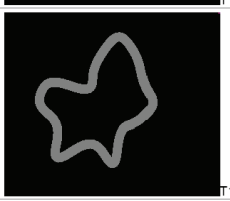 T194	☐ Figur wurde hauptsächlich durch Anzahl & Richtung der Ecken oder ein charakteristisches Merkmal gemerkt (bitte markieren).	☐ Figur wurde hauptsächlich als ..... bezeichnet.	☐ Figur wurde hauptsächlich anders gemerkt, und zwar	☐ erinnere diese Figur, bzw. meine angewandte Merkstrategie nicht
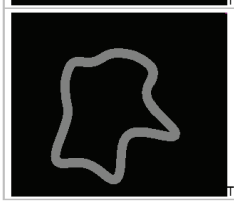 T195	☐ Figur wurde hauptsächlich durch Anzahl & Richtung der Ecken oder ein charakteristisches Merkmal gemerkt (bitte markieren).	☐ Figur wurde hauptsächlich als ..... bezeichnet.	☐ Figur wurde hauptsächlich anders gemerkt, und zwar	☐ erinnere diese Figur, bzw. meine angewandte Merkstrategie nicht

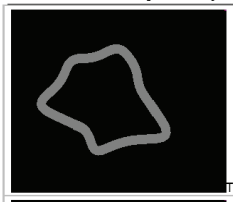 T197	☐ Figur wurde hauptsächlich durch Anzahl & Richtung der Ecken oder ein charakteristisches Merkmal gemerkt (bitte markieren).	☐ Figur wurde hauptsächlich als ..... bezeichnet.	☐ Figur wurde hauptsächlich anders gemerkt, und zwar	☐ erinnere diese Figur, bzw. meine angewandte Merkstrategie nicht
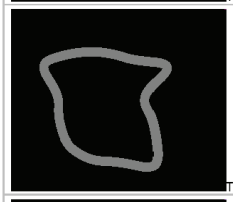 T20	☐ Figur wurde hauptsächlich durch Anzahl & Richtung der Ecken oder ein charakteristisches Merkmal gemerkt (bitte markieren).	☐ Figur wurde hauptsächlich als ..... bezeichnet.	☐ Figur wurde hauptsächlich anders gemerkt, und zwar	☐ erinnere diese Figur, bzw. meine angewandte Merkstrategie nicht
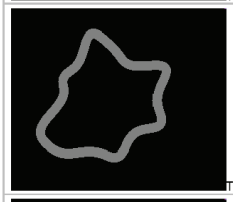 T23	☐ Figur wurde hauptsächlich durch Anzahl & Richtung der Ecken oder ein charakteristisches Merkmal gemerkt (bitte markieren).	☐ Figur wurde hauptsächlich als ..... bezeichnet.	☐ Figur wurde hauptsächlich anders gemerkt, und zwar	☐ erinnere diese Figur, bzw. meine angewandte Merkstrategie nicht
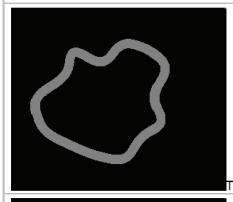 T24	☐ Figur wurde hauptsächlich durch Anzahl & Richtung der Ecken oder ein charakteristisches Merkmal gemerkt (bitte markieren).	☐ Figur wurde hauptsächlich als ..... bezeichnet.	☐ Figur wurde hauptsächlich anders gemerkt, und zwar	☐ erinnere diese Figur, bzw. meine angewandte Merkstrategie nicht
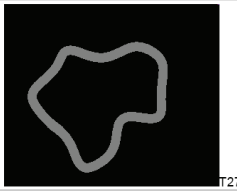 T27	☐ Figur wurde hauptsächlich durch Anzahl & Richtung der Ecken oder ein charakteristisches Merkmal gemerkt (bitte markieren).	☐ Figur wurde hauptsächlich als ..... bezeichnet.	☐ Figur wurde hauptsächlich anders gemerkt, und zwar	☐ erinnere diese Figur, bzw. meine angewandte Merkstrategie nicht
 T28	☐ Figur wurde hauptsächlich durch Anzahl & Richtung der Ecken oder ein charakteristisches Merkmal gemerkt (bitte markieren).	☐ Figur wurde hauptsächlich als ..... bezeichnet.	☐ Figur wurde hauptsächlich anders gemerkt, und zwar	☐ erinnere diese Figur, bzw. meine angewandte Merkstrategie nicht
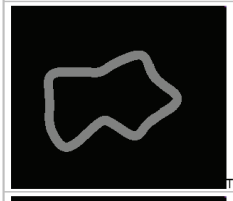 T29	☐ Figur wurde hauptsächlich durch Anzahl & Richtung der Ecken oder ein charakteristisches Merkmal gemerkt (bitte markieren).	☐ Figur wurde hauptsächlich als ..... bezeichnet.	☐ Figur wurde hauptsächlich anders gemerkt, und zwar	☐ erinnere diese Figur, bzw. meine angewandte Merkstrategie nicht
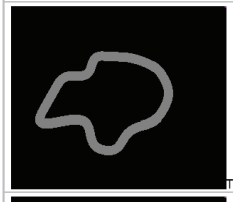 T30	☐ Figur wurde hauptsächlich durch Anzahl & Richtung der Ecken oder ein charakteristisches Merkmal gemerkt (bitte markieren).	☐ Figur wurde hauptsächlich als ..... bezeichnet.	☐ Figur wurde hauptsächlich anders gemerkt, und zwar	☐ erinnere diese Figur, bzw. meine angewandte Merkstrategie nicht
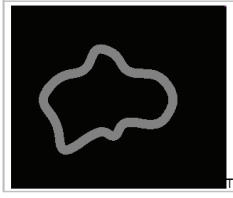 T32	☐ Figur wurde hauptsächlich durch Anzahl & Richtung der Ecken oder ein charakteristisches Merkmal gemerkt (bitte markieren).	☐ Figur wurde hauptsächlich als ..... bezeichnet.	☐ Figur wurde hauptsächlich anders gemerkt, und zwar	☐ erinnere diese Figur, bzw. meine angewandte Merkstrategie nicht

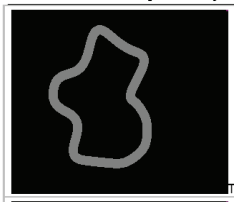 T33	☐ Figur wurde hauptsächlich durch Anzahl & Richtung der Ecken oder ein charakteristisches Merkmal gemerkt (bitte markieren).	☐ Figur wurde hauptsächlich als ..... bezeichnet.	☐ Figur wurde hauptsächlich anders gemerkt, und zwar	☐ erinnere diese Figur, bzw. meine angewandte Merkstrategie nicht
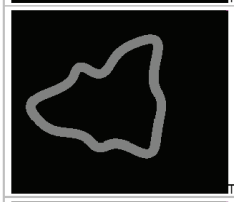 T36	☐ Figur wurde hauptsächlich durch Anzahl & Richtung der Ecken oder ein charakteristisches Merkmal gemerkt (bitte markieren).	☐ Figur wurde hauptsächlich als ..... bezeichnet.	☐ Figur wurde hauptsächlich anders gemerkt, und zwar	☐ erinnere diese Figur, bzw. meine angewandte Merkstrategie nicht
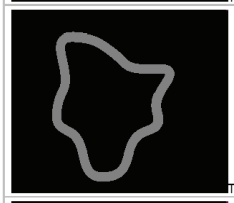 T38	☐ Figur wurde hauptsächlich durch Anzahl & Richtung der Ecken oder ein charakteristisches Merkmal gemerkt (bitte markieren).	☐ Figur wurde hauptsächlich als ..... bezeichnet.	☐ Figur wurde hauptsächlich anders gemerkt, und zwar	☐ erinnere diese Figur, bzw. meine angewandte Merkstrategie nicht
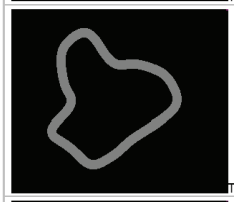 T42	☐ Figur wurde hauptsächlich durch Anzahl & Richtung der Ecken oder ein charakteristisches Merkmal gemerkt (bitte markieren).	☐ Figur wurde hauptsächlich als ..... bezeichnet.	☐ Figur wurde hauptsächlich anders gemerkt, und zwar	☐ erinnere diese Figur, bzw. meine angewandte Merkstrategie nicht
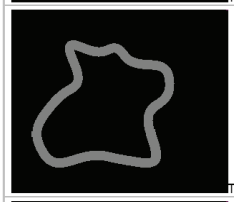 T49	☐ Figur wurde hauptsächlich durch Anzahl & Richtung der Ecken oder ein charakteristisches Merkmal gemerkt (bitte markieren).	☐ Figur wurde hauptsächlich als ..... bezeichnet.	☐ Figur wurde hauptsächlich anders gemerkt, und zwar	☐ erinnere diese Figur, bzw. meine angewandte Merkstrategie nicht
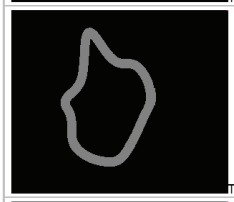 T5	☐ Figur wurde hauptsächlich durch Anzahl & Richtung der Ecken oder ein charakteristisches Merkmal gemerkt (bitte markieren).	☐ Figur wurde hauptsächlich als ..... bezeichnet.	☐ Figur wurde hauptsächlich anders gemerkt, und zwar	☐ erinnere diese Figur, bzw. meine angewandte Merkstrategie nicht
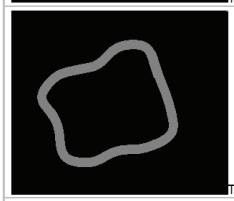 T53	☐ Figur wurde hauptsächlich durch Anzahl & Richtung der Ecken oder ein charakteristisches Merkmal gemerkt (bitte markieren).	☐ Figur wurde hauptsächlich als ..... bezeichnet.	☐ Figur wurde hauptsächlich anders gemerkt, und zwar	☐ erinnere diese Figur, bzw. meine angewandte Merkstrategie nicht
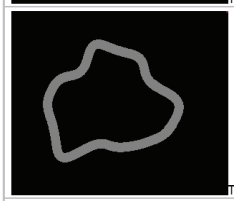 T54	☐ Figur wurde hauptsächlich durch Anzahl & Richtung der Ecken oder ein charakteristisches Merkmal gemerkt (bitte markieren).	☐ Figur wurde hauptsächlich als ..... bezeichnet.	☐ Figur wurde hauptsächlich anders gemerkt, und zwar	☐ erinnere diese Figur, bzw. meine angewandte Merkstrategie nicht
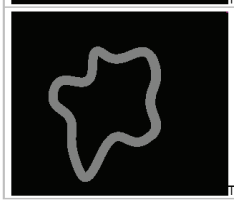 T6	☐ Figur wurde hauptsächlich durch Anzahl & Richtung der Ecken oder ein charakteristisches Merkmal gemerkt (bitte markieren).	☐ Figur wurde hauptsächlich als ..... bezeichnet.	☐ Figur wurde hauptsächlich anders gemerkt, und zwar	☐ erinnere diese Figur, bzw. meine angewandte Merkstrategie nicht

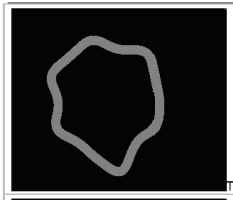 T69	☐ Figur wurde hauptsächlich durch Anzahl & Richtung der Ecken oder ein charakteristisches Merkmal gemerkt (bitte markieren).	☐ Figur wurde hauptsächlich als ..... bezeichnet.	☐ Figur wurde hauptsächlich anders gemerkt, und zwar	☐ erinnere diese Figur, bzw. meine angewandte Merkstrategie nicht
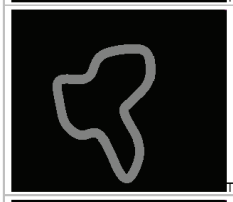 T70	☐ Figur wurde hauptsächlich durch Anzahl & Richtung der Ecken oder ein charakteristisches Merkmal gemerkt (bitte markieren).	☐ Figur wurde hauptsächlich als ..... bezeichnet.	☐ Figur wurde hauptsächlich anders gemerkt, und zwar	☐ erinnere diese Figur, bzw. meine angewandte Merkstrategie nicht
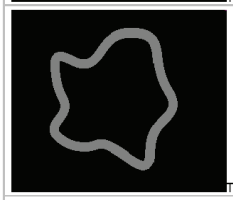 T73	☐ Figur wurde hauptsächlich durch Anzahl & Richtung der Ecken oder ein charakteristisches Merkmal gemerkt (bitte markieren).	☐ Figur wurde hauptsächlich als ..... bezeichnet.	☐ Figur wurde hauptsächlich anders gemerkt, und zwar	☐ erinnere diese Figur, bzw. meine angewandte Merkstrategie nicht
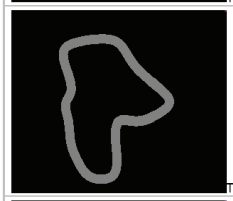 T79	☐ Figur wurde hauptsächlich durch Anzahl & Richtung der Ecken oder ein charakteristisches Merkmal gemerkt (bitte markieren).	☐ Figur wurde hauptsächlich als ..... bezeichnet.	☐ Figur wurde hauptsächlich anders gemerkt, und zwar	☐ erinnere diese Figur, bzw. meine angewandte Merkstrategie nicht
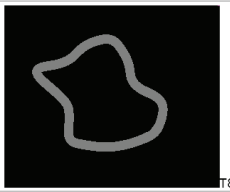 T8	☐ Figur wurde hauptsächlich durch Anzahl & Richtung der Ecken oder ein charakteristisches Merkmal gemerkt (bitte markieren).	☐ Figur wurde hauptsächlich als ..... bezeichnet.	☐ Figur wurde hauptsächlich anders gemerkt, und zwar	☐ erinnere diese Figur, bzw. meine angewandte Merkstrategie nicht
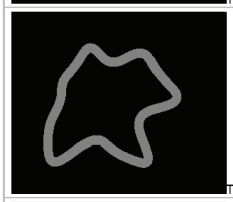 T83	☐ Figur wurde hauptsächlich durch Anzahl & Richtung der Ecken oder ein charakteristisches Merkmal gemerkt (bitte markieren).	☐ Figur wurde hauptsächlich als ..... bezeichnet.	☐ Figur wurde hauptsächlich anders gemerkt, und zwar	☐ erinnere diese Figur, bzw. meine angewandte Merkstrategie nicht
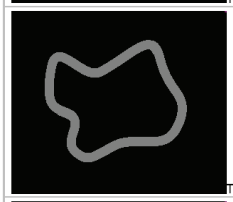 T86	☐ Figur wurde hauptsächlich durch Anzahl & Richtung der Ecken oder ein charakteristisches Merkmal gemerkt (bitte markieren).	☐ Figur wurde hauptsächlich als ..... bezeichnet.	☐ Figur wurde hauptsächlich anders gemerkt, und zwar	☐ erinnere diese Figur, bzw. meine angewandte Merkstrategie nicht
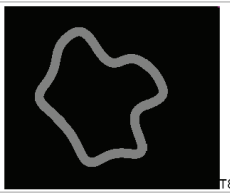 T88	☐ Figur wurde hauptsächlich durch Anzahl & Richtung der Ecken oder ein charakteristisches Merkmal gemerkt (bitte markieren).	☐ Figur wurde hauptsächlich als ..... bezeichnet.	☐ Figur wurde hauptsächlich anders gemerkt, und zwar	☐ erinnere diese Figur, bzw. meine angewandte Merkstrategie nicht
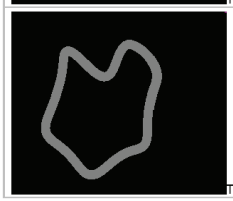 T89	☐ Figur wurde hauptsächlich durch Anzahl & Richtung der Ecken oder ein charakteristisches Merkmal gemerkt (bitte markieren).	☐ Figur wurde hauptsächlich als ..... bezeichnet.	☐ Figur wurde hauptsächlich anders gemerkt, und zwar	☐ erinnere diese Figur, bzw. meine angewandte Merkstrategie nicht

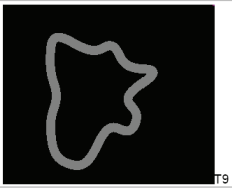 T9	☐ Figur wurde hauptsächlich durch Anzahl & Richtung der Ecken oder ein charakteristisches Merkmal gemerkt (bitte markieren).	☐ Figur wurde hauptsächlich als ..... bezeichnet.	☐ Figur wurde hauptsächlich anders gemerkt, und zwar	☐ erinnere diese Figur, bzw. meine angewandte Merkstrategie nicht
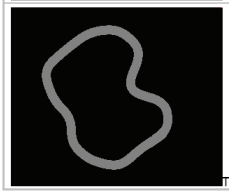 T91	☐ Figur wurde hauptsächlich durch Anzahl & Richtung der Ecken oder ein charakteristisches Merkmal gemerkt (bitte markieren).	☐ Figur wurde hauptsächlich als ..... bezeichnet.	☐ Figur wurde hauptsächlich anders gemerkt, und zwar	☐ erinnere diese Figur, bzw. meine angewandte Merkstrategie nicht

Appendix J: Encoding questionnaire showing all stimuli used in the fMRI session of Experiment 2.

Fragebogen zur Merkstrategie der einzelnen Zielreize [fMRI]
VPN-code: Datum:

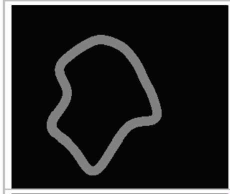	☐ Figur wurde hauptsächlich durch Anzahl & Richtung der Ecken oder ein charakteristisches Merkmal gemerkt (bitte markieren).	☐ Figur wurde hauptsächlich als .... bezeichnet.	☐ Figur wurde hauptsächlich anders gemerkt, und zwar	☐ erinnere diese Figur, bzw. meine angewandte Merkstrategie nicht
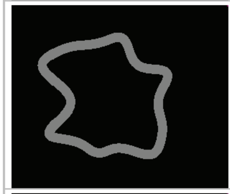	☐ Figur wurde hauptsächlich durch Anzahl & Richtung der Ecken oder ein charakteristisches Merkmal gemerkt (bitte markieren).	☐ Figur wurde hauptsächlich als .... bezeichnet.	☐ Figur wurde hauptsächlich anders gemerkt, und zwar	☐ erinnere diese Figur, bzw. meine angewandte Merkstrategie nicht
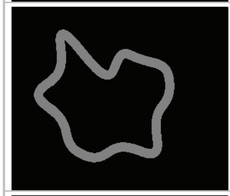	☐ Figur wurde hauptsächlich durch Anzahl & Richtung der Ecken oder ein charakteristisches Merkmal gemerkt (bitte markieren).	☐ Figur wurde hauptsächlich als .... bezeichnet.	☐ Figur wurde hauptsächlich anders gemerkt, und zwar	☐ erinnere diese Figur, bzw. meine angewandte Merkstrategie nicht
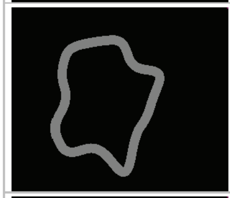	☐ Figur wurde hauptsächlich durch Anzahl & Richtung der Ecken oder ein charakteristisches Merkmal gemerkt (bitte markieren).	☐ Figur wurde hauptsächlich als .... bezeichnet.	☐ Figur wurde hauptsächlich anders gemerkt, und zwar	☐ erinnere diese Figur, bzw. meine angewandte Merkstrategie nicht
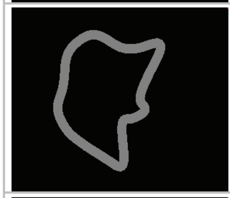	☐ Figur wurde hauptsächlich durch Anzahl & Richtung der Ecken oder ein charakteristisches Merkmal gemerkt (bitte markieren).	☐ Figur wurde hauptsächlich als .... bezeichnet.	☐ Figur wurde hauptsächlich anders gemerkt, und zwar	☐ erinnere diese Figur, bzw. meine angewandte Merkstrategie nicht
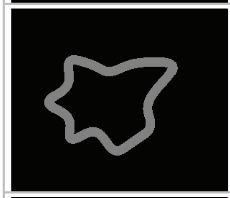	☐ Figur wurde hauptsächlich durch Anzahl & Richtung der Ecken oder ein charakteristisches Merkmal gemerkt (bitte markieren).	☐ Figur wurde hauptsächlich als .... bezeichnet.	☐ Figur wurde hauptsächlich anders gemerkt, und zwar	☐ erinnere diese Figur, bzw. meine angewandte Merkstrategie nicht
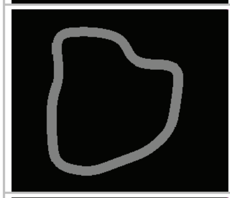	☐ Figur wurde hauptsächlich durch Anzahl & Richtung der Ecken oder ein charakteristisches Merkmal gemerkt (bitte markieren).	☐ Figur wurde hauptsächlich als .... bezeichnet.	☐ Figur wurde hauptsächlich anders gemerkt, und zwar	☐ erinnere diese Figur, bzw. meine angewandte Merkstrategie nicht
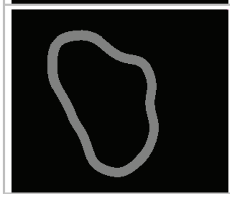	☐ Figur wurde hauptsächlich durch Anzahl & Richtung der Ecken oder ein charakteristisches Merkmal gemerkt (bitte markieren).	☐ Figur wurde hauptsächlich als .... bezeichnet.	☐ Figur wurde hauptsächlich anders gemerkt, und zwar	☐ erinnere diese Figur, bzw. meine angewandte Merkstrategie nicht

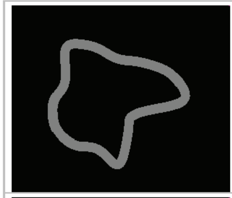		☐ Figur wurde hauptsächlich durch Anzahl & Richtung der Ecken oder ein charakteristisches Merkmal gemerkt (bitte markieren).	☐ Figur wurde hauptsächlich als .... bezeichnet.	☐ Figur wurde hauptsächlich anders gemerkt, und zwar	☐ erinnere diese Figur, bzw. meine angewandte Merkstrategie nicht
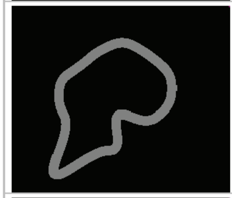		☐ Figur wurde hauptsächlich durch Anzahl & Richtung der Ecken oder ein charakteristisches Merkmal gemerkt (bitte markieren).	☐ Figur wurde hauptsächlich als .... bezeichnet.	☐ Figur wurde hauptsächlich anders gemerkt, und zwar	☐ erinnere diese Figur, bzw. meine angewandte Merkstrategie nicht
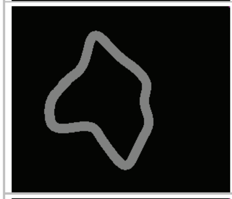		☐ Figur wurde hauptsächlich durch Anzahl & Richtung der Ecken oder ein charakteristisches Merkmal gemerkt (bitte markieren).	☐ Figur wurde hauptsächlich als .... bezeichnet.	☐ Figur wurde hauptsächlich anders gemerkt, und zwar	☐ erinnere diese Figur, bzw. meine angewandte Merkstrategie nicht
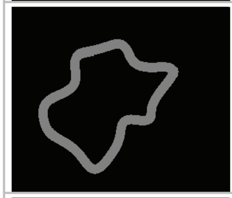		☐ Figur wurde hauptsächlich durch Anzahl & Richtung der Ecken oder ein charakteristisches Merkmal gemerkt (bitte markieren).	☐ Figur wurde hauptsächlich als .... bezeichnet.	☐ Figur wurde hauptsächlich anders gemerkt, und zwar	☐ erinnere diese Figur, bzw. meine angewandte Merkstrategie nicht
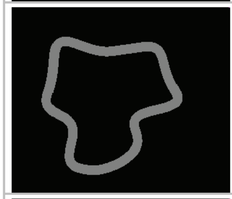		☐ Figur wurde hauptsächlich durch Anzahl & Richtung der Ecken oder ein charakteristisches Merkmal gemerkt (bitte markieren).	☐ Figur wurde hauptsächlich als .... bezeichnet.	☐ Figur wurde hauptsächlich anders gemerkt, und zwar	☐ erinnere diese Figur, bzw. meine angewandte Merkstrategie nicht
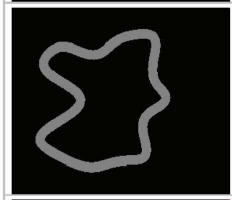		☐ Figur wurde hauptsächlich durch Anzahl & Richtung der Ecken oder ein charakteristisches Merkmal gemerkt (bitte markieren).	☐ Figur wurde hauptsächlich als .... bezeichnet.	☐ Figur wurde hauptsächlich anders gemerkt, und zwar	☐ erinnere diese Figur, bzw. meine angewandte Merkstrategie nicht
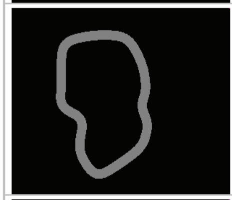		☐ Figur wurde hauptsächlich durch Anzahl & Richtung der Ecken oder ein charakteristisches Merkmal gemerkt (bitte markieren).	☐ Figur wurde hauptsächlich als .... bezeichnet.	☐ Figur wurde hauptsächlich anders gemerkt, und zwar	☐ erinnere diese Figur, bzw. meine angewandte Merkstrategie nicht
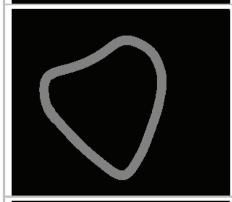		☐ Figur wurde hauptsächlich durch Anzahl & Richtung der Ecken oder ein charakteristisches Merkmal gemerkt (bitte markieren).	☐ Figur wurde hauptsächlich als .... bezeichnet.	☐ Figur wurde hauptsächlich anders gemerkt, und zwar	☐ erinnere diese Figur, bzw. meine angewandte Merkstrategie nicht
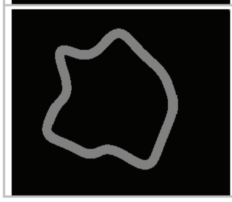		☐ Figur wurde hauptsächlich durch Anzahl & Richtung der Ecken oder ein charakteristisches Merkmal gemerkt (bitte markieren).	☐ Figur wurde hauptsächlich als .... bezeichnet.	☐ Figur wurde hauptsächlich anders gemerkt, und zwar	☐ erinnere diese Figur, bzw. meine angewandte Merkstrategie nicht

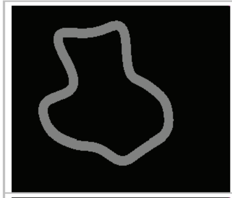	☐ Figur wurde hauptsächlich durch Anzahl & Richtung der Ecken oder ein charakteristisches Merkmal gemerkt (bitte markieren).	☐ Figur wurde hauptsächlich als .... bezeichnet.	☐ Figur wurde hauptsächlich anders gemerkt, und zwar	☐ erinnere diese Figur, bzw. meine angewandte Merkstrategie nicht
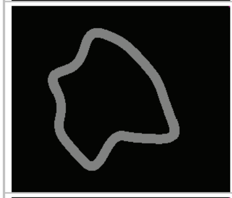	☐ Figur wurde hauptsächlich durch Anzahl & Richtung der Ecken oder ein charakteristisches Merkmal gemerkt (bitte markieren).	☐ Figur wurde hauptsächlich als .... bezeichnet.	☐ Figur wurde hauptsächlich anders gemerkt, und zwar	☐ erinnere diese Figur, bzw. meine angewandte Merkstrategie nicht
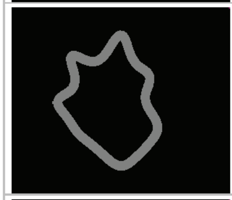	☐ Figur wurde hauptsächlich durch Anzahl & Richtung der Ecken oder ein charakteristisches Merkmal gemerkt (bitte markieren).	☐ Figur wurde hauptsächlich als .... bezeichnet.	☐ Figur wurde hauptsächlich anders gemerkt, und zwar	☐ erinnere diese Figur, bzw. meine angewandte Merkstrategie nicht
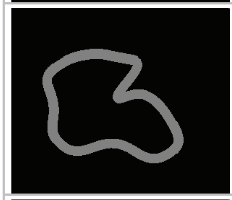	☐ Figur wurde hauptsächlich durch Anzahl & Richtung der Ecken oder ein charakteristisches Merkmal gemerkt (bitte markieren).	☐ Figur wurde hauptsächlich als .... bezeichnet.	☐ Figur wurde hauptsächlich anders gemerkt, und zwar	☐ erinnere diese Figur, bzw. meine angewandte Merkstrategie nicht
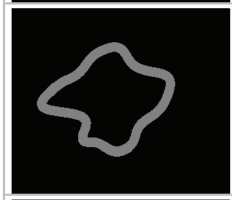	☐ Figur wurde hauptsächlich durch Anzahl & Richtung der Ecken oder ein charakteristisches Merkmal gemerkt (bitte markieren).	☐ Figur wurde hauptsächlich als .... bezeichnet.	☐ Figur wurde hauptsächlich anders gemerkt, und zwar	☐ erinnere diese Figur, bzw. meine angewandte Merkstrategie nicht
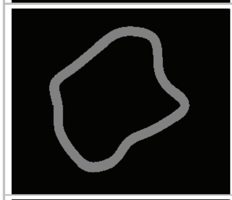	☐ Figur wurde hauptsächlich durch Anzahl & Richtung der Ecken oder ein charakteristisches Merkmal gemerkt (bitte markieren).	☐ Figur wurde hauptsächlich als .... bezeichnet.	☐ Figur wurde hauptsächlich anders gemerkt, und zwar	☐ erinnere diese Figur, bzw. meine angewandte Merkstrategie nicht
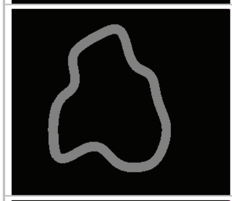	☐ Figur wurde hauptsächlich durch Anzahl & Richtung der Ecken oder ein charakteristisches Merkmal gemerkt (bitte markieren).	☐ Figur wurde hauptsächlich als .... bezeichnet.	☐ Figur wurde hauptsächlich anders gemerkt, und zwar	☐ erinnere diese Figur, bzw. meine angewandte Merkstrategie nicht
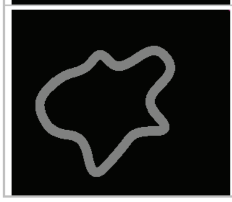	☐ Figur wurde hauptsächlich durch Anzahl & Richtung der Ecken oder ein charakteristisches Merkmal gemerkt (bitte markieren).	☐ Figur wurde hauptsächlich als .... bezeichnet.	☐ Figur wurde hauptsächlich anders gemerkt, und zwar	☐ erinnere diese Figur, bzw. meine angewandte Merkstrategie nicht

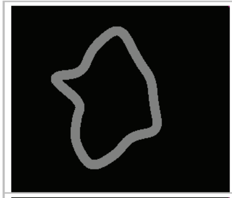	☐ Figur wurde hauptsächlich durch Anzahl & Richtung der Ecken oder ein charakteristisches Merkmal gemerkt (bitte markieren).	☐ Figur wurde hauptsächlich als .... bezeichnet.	☐ Figur wurde hauptsächlich anders gemerkt, und zwar	☐ erinnere diese Figur, bzw. meine angewandte Merkstrategie nicht
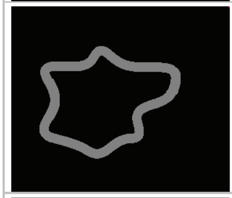	☐ Figur wurde hauptsächlich durch Anzahl & Richtung der Ecken oder ein charakteristisches Merkmal gemerkt (bitte markieren).	☐ Figur wurde hauptsächlich als .... bezeichnet.	☐ Figur wurde hauptsächlich anders gemerkt, und zwar	☐ erinnere diese Figur, bzw. meine angewandte Merkstrategie nicht
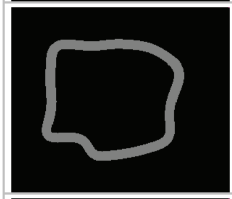	☐ Figur wurde hauptsächlich durch Anzahl & Richtung der Ecken oder ein charakteristisches Merkmal gemerkt (bitte markieren).	☐ Figur wurde hauptsächlich als .... bezeichnet.	☐ Figur wurde hauptsächlich anders gemerkt, und zwar	☐ erinnere diese Figur, bzw. meine angewandte Merkstrategie nicht
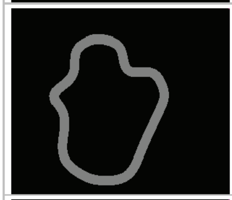	☐ Figur wurde hauptsächlich durch Anzahl & Richtung der Ecken oder ein charakteristisches Merkmal gemerkt (bitte markieren).	☐ Figur wurde hauptsächlich als .... bezeichnet.	☐ Figur wurde hauptsächlich anders gemerkt, und zwar	☐ erinnere diese Figur, bzw. meine angewandte Merkstrategie nicht
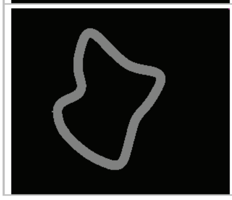	☐ Figur wurde hauptsächlich durch Anzahl & Richtung der Ecken oder ein charakteristisches Merkmal gemerkt (bitte markieren).	☐ Figur wurde hauptsächlich als .... bezeichnet.	☐ Figur wurde hauptsächlich anders gemerkt, und zwar	☐ erinnere diese Figur, bzw. meine angewandte Merkstrategie nicht

Appendix K: number and position of electrode channels which were interpolated with spherical spline interpolation.

participant #	interpolated channels	participant #	interpolated channels
001	FC5	**012**	AF4, T7, T8
002	PO9	**013**	P2, T7, T8
003	TP9, PO9	**014**	T8, T7, PO9, PO10
004	T8, C1	**015**	TP9
006	PO9	**017**	PO4
007	TP9	**018**	FC2, Pz
008	P7, POz, Pz, TP9	**019**	PO9, Oz
011	F5, C1, TP10	**020**	T7, FT8

Appendix L: Source sensitivity images showing source sensitivities for each of the 12 regional sources. The red cross superimposed on each head model indicates the location of the currently used regional source. Scaling: from 0 to 100 percent sensitivity.

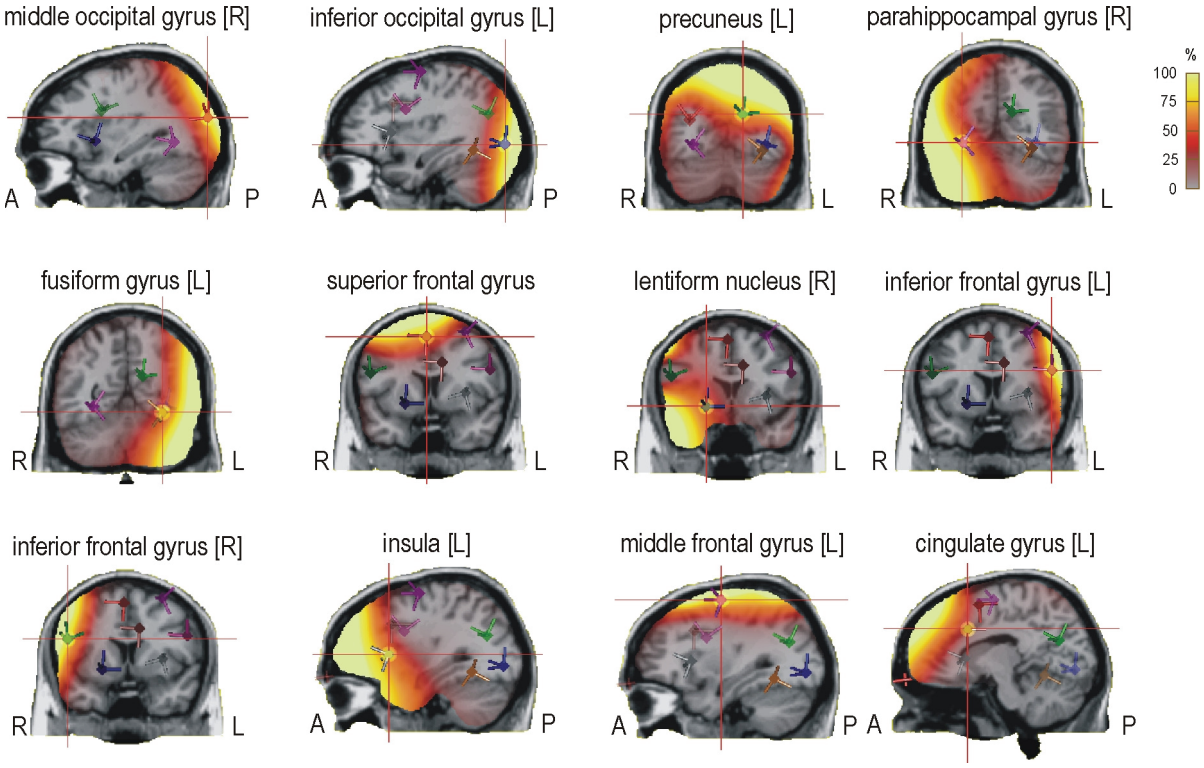

Appendix M: Post-hoc Wilcoxon-tests comparing error rates of the EEG and the fMRI sessions for all memory probe conditions (non-targets: left, targets: right).

non-target conditions: EEG vs. fMRI			target conditions: EEG vs. fMRI		
	z-value	**p-value**		**z-value**	**p-value**
trial position A	-0.5	.64	**trial position A**	-1.2	.24
trial position B	-0.5	.59	**trial position B**	-0.2	.84
trial position C	-0.2	.84	**trial position C**	-0.5	.61

Appendix N: Glass brains showing activation patterns obtained with the contrasts of target trials versus non-target trials (each FDR-corrected, p<.05, k>20); at trial position A (left side) and at trial position B (right side).

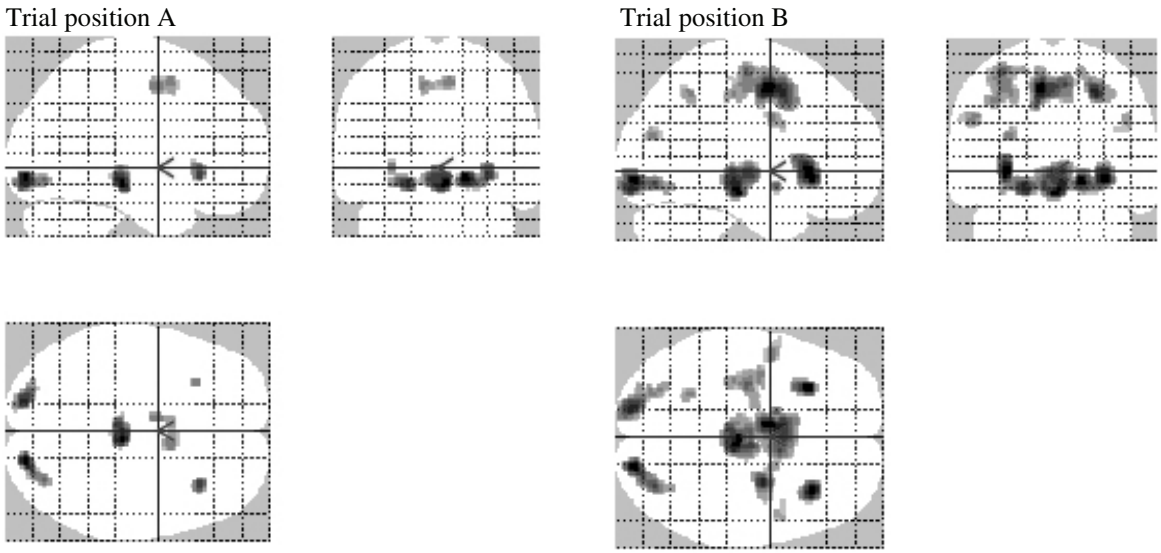

Appendix O: Glass brains showing activation patterns obtained with the conjunction of target trials versus fixation epoch over all delay durations (left side), and the conjunction of non-target trials versus fixation epoch over all delay durations (right side). Both conjunctions are FDR-corrected, p<.05.

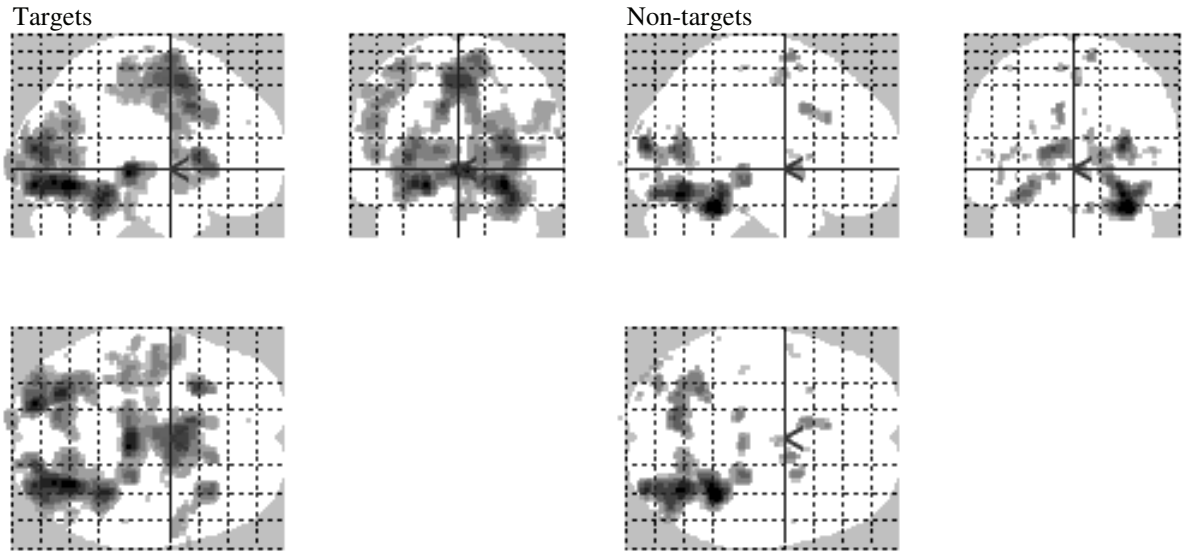

Appendix P: Post-hoc t-tests comparing mean amplitude values (300-700 ms post-stimulus, pooled over both probe types) between the different trial positions at electrode positions Pz (left) and Cz (right). Significant results are indicated with asterisks (* p<.05, ** p<.01).

Pz	**t-value**	**p-value**	**Cz**	**t-value**	**p-value**
trial positions A vs. B	-1.5	=.15	**trial positions A vs. B**	1.7	=.10
trial positions A vs. C	-1.9	=.07	**trial positions A vs. C**	-2.0	=.06
trial positions B vs. C	-0.1	=.94	**trial positions B vs. C**	-3.6	=.002 **

Appendix Q: Descriptive statistics: mean amplitude values (300-700 ms post-stimulus) at electrode positions Pz (left) and Cz (right) separately for all memory probe conditions. A, B and C represent different trial positions.

Pz	mean amplitudes µV (±SD)	Cz	mean amplitudes µV (±SD)
targets at position A	3.13 (±1.5)	**targets at position A**	2.70 (±1.8)
targets at position B	3.26 (±1.9)	**targets at position B**	2.10 (±1.8)
targets at position C	3.23 (±1.5)	**targets at position C**	2.70 (±1.6)
non-targets at position A	2.26 (±1.2)	**non-targets at position A**	1.16 (±1.5)
non-targets at position B	2.68 (±1.2)	**non-targets at position B**	1.27 (±1.4)
non-targets at position C	2.73 (±1.4)	**non-targets at position C**	1.81 (±1.3)

Appendix R: ERPs at the original 64 electrode positions for the target condition (black line), the non-target condition (dashed line) and the difference wave (target trials minus non-target trials, dotted line).

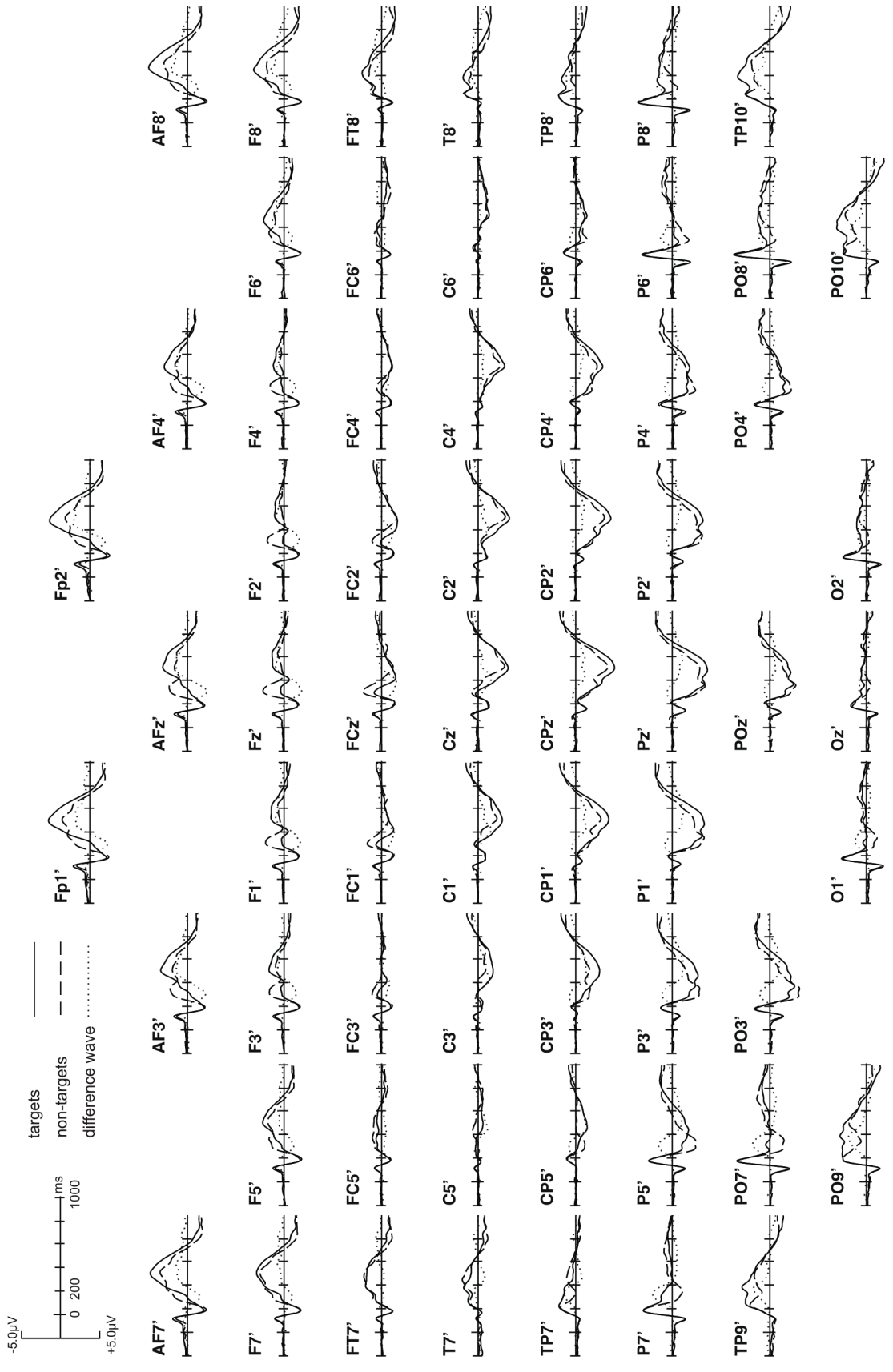

Appendix S: Difference waves (targets minus non-targets) at the original 64 electrode positions separately for stimuli presented at trial position A (black line), trial position B (dashed line) and trial position C (dotted line).

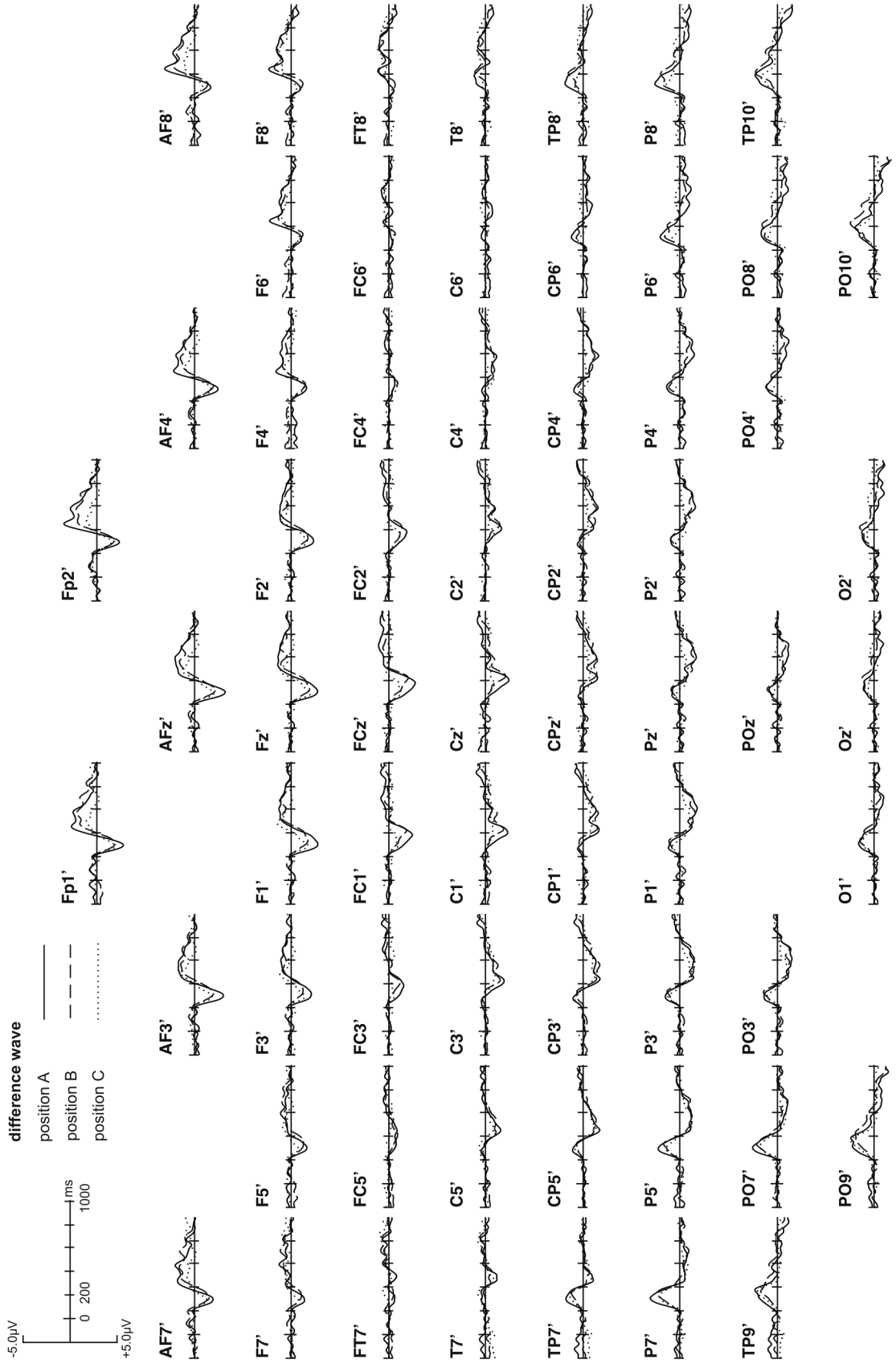

Appendix T: ERPs at the original 64 electrode positions separately for all target conditions (trial position A: yellow; positon B: red; position C: brown) and all non-target conditions (trial position A: turquoise; position B: blue; position C: green).

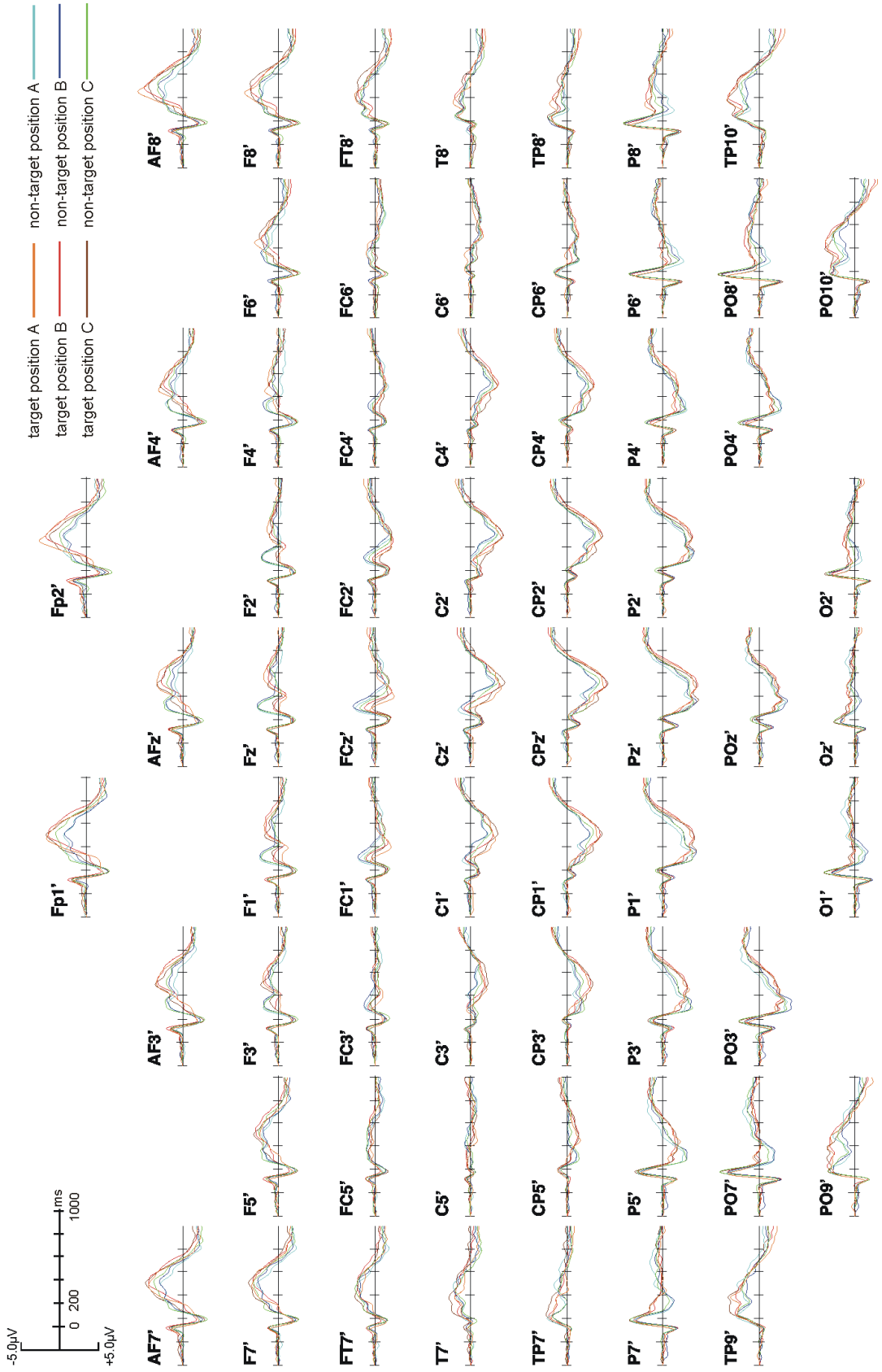

Appendix U: Bootstrap BCa 95%-confidence interval for source activities of each regional source based on the difference source wave (target minus non-target source wave) at trial position A.

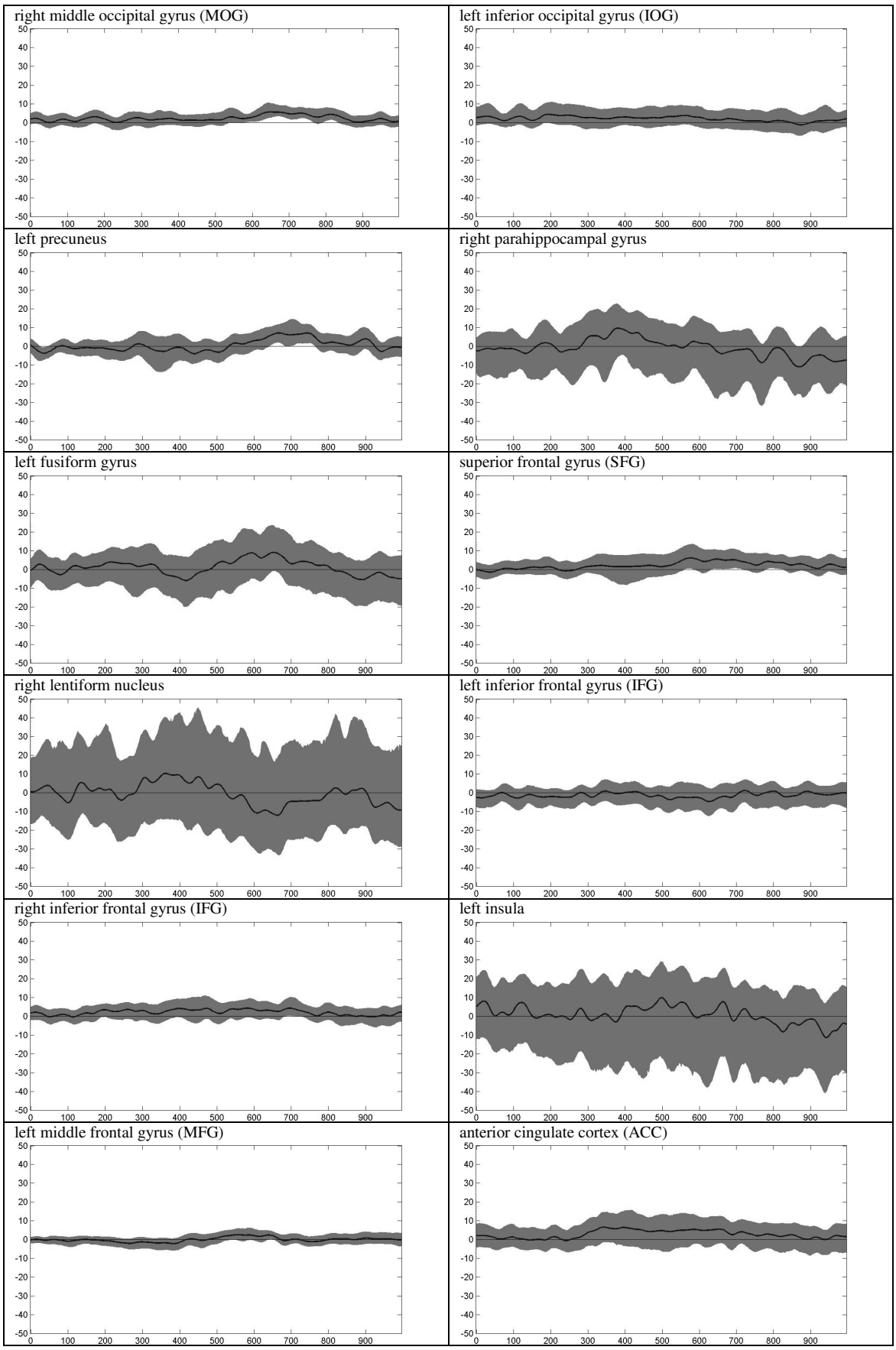

Appendix V: Bootstrap BCa 95%-confidence interval for source activities of each regional source based on the difference source wave (target minus non-target source wave) at trial position B.

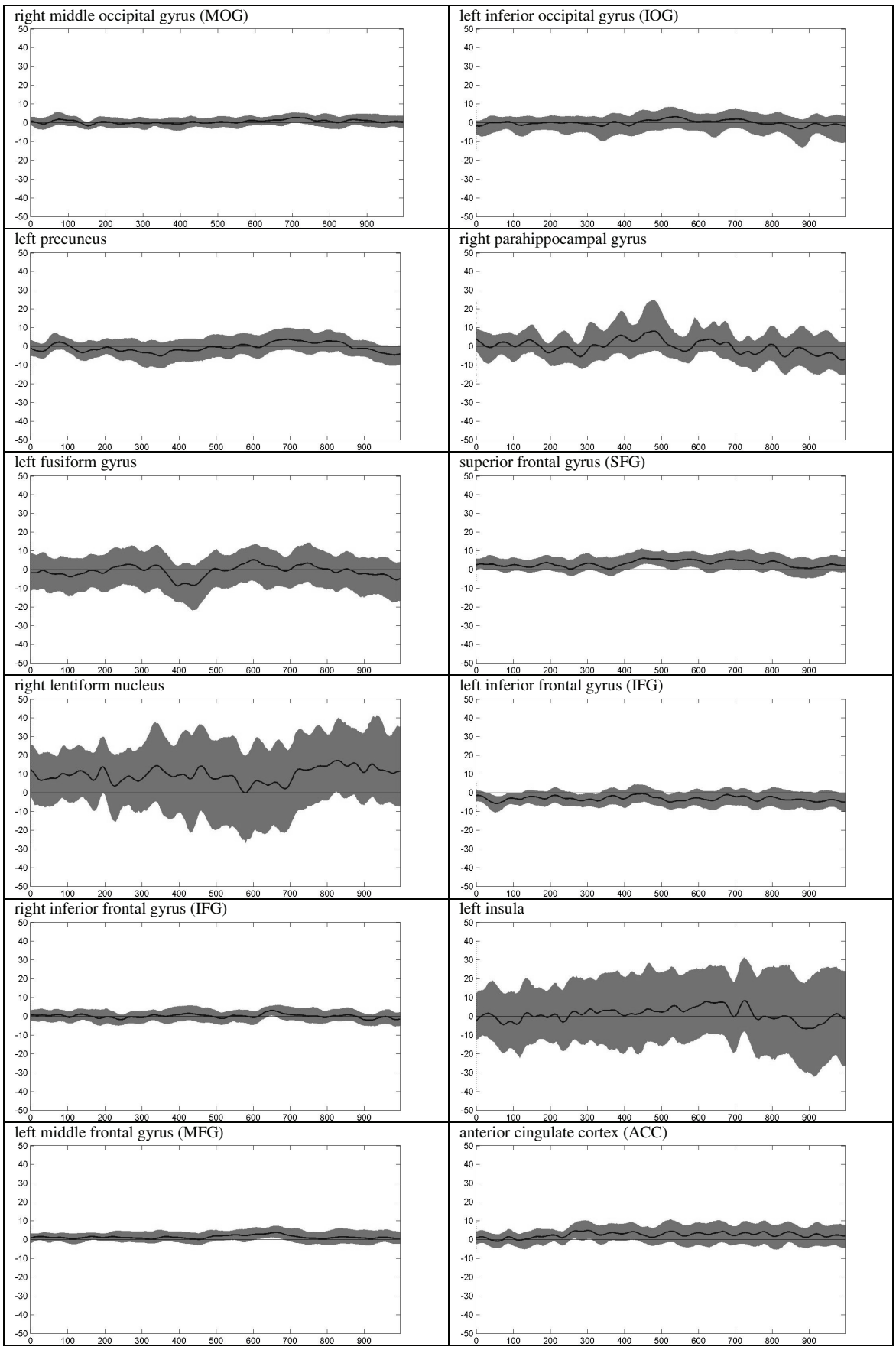

Appendix W: Bootstrap BCa 95%-confidence interval for source activities of each regional source based on the difference source wave (target minus non-target source wave) at trial position C.

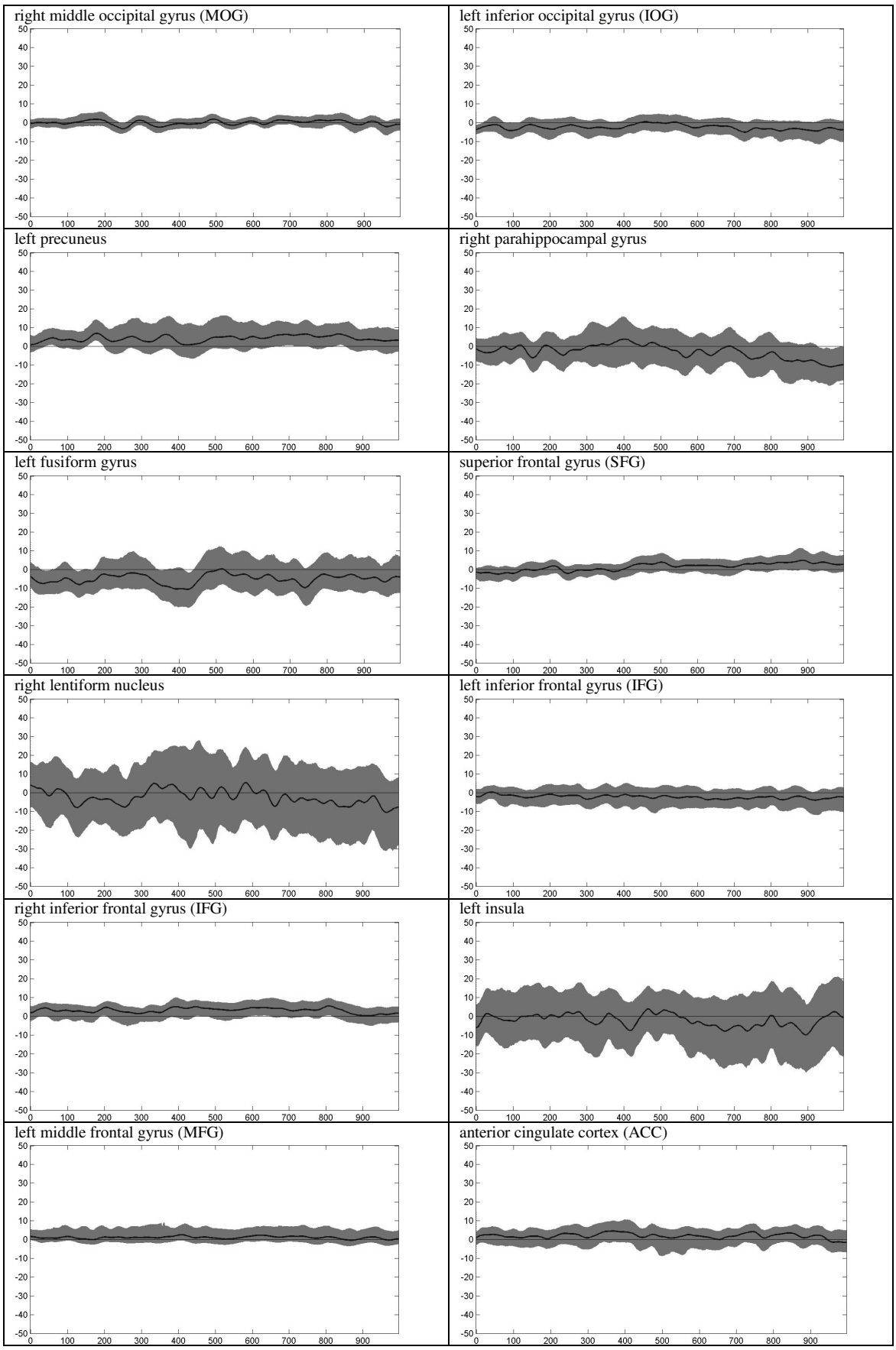

Appendix X: Topographical voltage maps showing source activity of the cingulate regional source (ACC) at 350 ms post-stimulus. A) target condition. B) non-target condition. As different SA models were applied to compute the topographical maps, attention should be paid to the different scaling of both conditions.

A) **B)**